

DEVELOPING A SPATIAL RISK PROFILE: ASSESSING BUILDING VULNERABILITY TO  
EXTREME COASTAL INUNDATION HAZARD

By LAUREN LYN WILLIAMS (MSc)

Dissertation presented for the degree of Doctor of Philosophy  
in the Faculty of Science at Stellenbosch University

Promoter: Dr M. Lück-Vogel

Co-promoter: Dr R. Pharoah



December 2020

## DECLARATION

By submitting this thesis electronically, I declare that the entirety of the work contained therein is my own, original work, that I am the sole author thereof (save to the extent explicitly otherwise stated), that the reproduction and publication thereof by Stellenbosch University will not infringe any third party rights and that I have not previously in its entirety or in part submitted it for obtaining any qualification.

## Publications

Chapter	Nature of contribution	Extent of contribution (%)
2	Components of this chapter were published in a national government guideline document. I was the sole author of the document. Department of Environmental Affairs. 2017. National Guideline Towards the Establishment of Coastal Management Lines, Centre for Environmental Rights, Online: <a href="https://cer.org.za/wp-content/uploads/2009/12/National-guideline-towards-the-establishment-of-coastal-management-lines.pdf">https://cer.org.za/wp-content/uploads/2009/12/National-guideline-towards-the-establishment-of-coastal-management-lines.pdf</a>	L.L. Williams 100%
	Components of this chapter were published as a journal article (Lück-Vogel, Macon and Williams 2018) Lück-Vogel, M., Macon, C., Williams, L.L. 2018. Guidelines for Coastal Lidar. PositionIT, 21 May 2018, EE Publishers. Online: <a href="http://www.ee.co.za/article/guidelines-for-coastal-lidar.html">http://www.ee.co.za/article/guidelines-for-coastal-lidar.html</a>	M Lück-Vogel 60% C Macon 20% L.L Williams 20%
4	This chapter was published as a journal article (Williams and Lück-Vogel 2019). Williams, L.L. & Lück-Vogel, M. 2020. Comparative assessment of the GIS based Bathtub Model and an Enhanced Bathtub Model for coastal inundation. Journal of Coastal Conservation 24, 23. [online]. Available from: <a href="https://doi.org/10.1007/s11852-020-00735-x">https://doi.org/10.1007/s11852-020-00735-x</a>	L.L. Williams 85% M Lück-Vogel 15%
	The model developed in Chapter 4 was published. Williams, L. L. 2019. Coastal Inundation (Enhanced Bathtub Model (eBTM)). Department of Environment, Forestry and Fisheries. DOI: 10.15493/DEFF.10000002.	L.L. Williams 100%
	The toolbox developed in Chapter 4 was published. Williams, L. L. 2019. ArcCoastTools. Department of Environment, Forestry and Fisheries. DOI: 10.15493/DEFF.10000001.	L.L. Williams 100%

Signature of candidate: Declaration with signature in possession of candidate and Supervisor

Signature of supervisor: Declaration with signature in possession of candidate and Supervisor

Date: December 2020

Copyright © 2020 Stellenbosch University

All rights reserved

## SUMMARY

Coastal zones are dynamic spaces where human activities and infrastructure interface directly with natural forces, particularly extreme weather events such as storm surges. Coastal inundation is regarded as one of the most dangerous and destructive natural hazards, and while there are many studies to analyse these events, few provide assessment techniques relevant to the local context.

This research aimed at developing a spatial risk profile for building vulnerability to coastal inundation hazard. GIS was determined to be the most appropriate technology as more sophisticated technologies such as hydrodynamic modelling were found to be limited to specialists, ‘data-hungry’ and computationally expensive. An improved GIS based enhanced Bathhtub Model (eBTM) was thus developed, which is more appropriate to the local coastal inundation context than the widely used simple Bathhtub Model (sBTM). The advantage of the eBTM is that incorporates beach slope and surface roughness and that it instils hydrological connectivity to the coast through embedded cost-distance models. The use of such models thus allows for simplistic hydrodynamic processes such as the water distribution through urban infrastructure to be simulated, the output of which also includes the potential water depth relative to the input elevation model. The model was packaged into a user-friendly Graphical User Interface (GUI) tool and the modelled outputs were further tested and validated against observed data, which supported its applicability.

Strand and Fish Hoek (Cape Town, South Africa) were selected as the study sites for which the inundation levels for three independent scenarios were determined by combining the extreme sea level for a 1-in-100 year storm and two sea level rise scenarios.

The risk assessment component used the eBTM to generate inundation hazard maps for the three defined scenarios and to identify affected buildings. Both the hazard and hazard exposure scores were directly dependent on the eBTM outputs in terms of the inundation limits and water depths respectively. The physical building vulnerability indicators were developed through stakeholder engagements. The assessment was undertaken through the use of desktop technologies and on site building inspections. Weighted indicators were used to determine the vulnerability scores for each individual building. Determining the spatial risk profile was based on the scores from the preceding work to determine the risk status of each individual building in each study site. Again, weightings were applied to highlight the importance of components and to reduce the weight of less robust input factors. Overall, in Fish Hoek, one building was found to be at high risk of experiencing coastal inundation based on the given scenarios and three are at low risk. In Strand the spatial risk profile showed that 71 buildings are at low risk, 86 at moderate risk and 35 at high risk. The identified high

risk buildings can thus be further assessed in terms of methods to reduce their vulnerability and/or hazard exposure.

This study departs from existing regional risk assessment approaches and presents an assessment mechanism that allows the risk components (i.e. hazard, hazard exposure and vulnerability) to be assessed individually, at a locally relevant scale and through their individual assessment frameworks. The eBTM tool and assessment techniques were developed to be transferable to other areas. Furthermore, the eBTM tool enhances the accessibility of GIS based techniques for undertaking localised coastal risk assessments. The maps produced for the individual risk components can thus be used for knowledge transfer, while the final risk maps can be used to inform the management response required relevant to the local context.



## OPSOMMING

Kusgebiede is dinamiese ruimtes waar menslike aktiwiteite en infrastruktuur direk met natuurkragte in aanraking kom, veral uiterste weersomstandighede soos stormstuwings. Kusinundasië word beskou as een van die gevaarlikste en vernietigendste natuurlike gevare, en hoewel daar baie studies is wat hierdie aspekte geanaliseer het, is daar min wat assesseringstegnieke binne die plaaslike konteks verskaf.

Hierdie navorsing het ten doel gehad om 'n ruimtelike risikoprofiel met betrekking tot die kwesbaarheid vir kusinundasië te ontwikkel. Daar is vasgestel dat GIS die geskikste tegnologie was, aangesien meer gevorderde tegnologieë soos hidrodinamiese modellering beperk is tot spesialiste, 'datahonger' is en rekenaarmatig duur is. 'n Verbeterde GIS-gebaseerde verbeterde badmodel (eBTM) is dus ontwikkel, wat meer geskik is binne die plaaslike kusinundasiëkonteks as die eenvoudige badmodel (sBTM) wat algemeen gebruik word. Die voordeel van die eBTM is dat dit die helling van die strand en die oppervlakte-grofheid inkorporeer en dat dit hidrologiese konneksie aan die kus deur middel van ingeboude koste-afstandsmodelle vestig. Die gebruik van sulke modelle maak dit dus moontlik om simboliese hidrodinamiese prosesse soos die verspreiding van water deur stedelike infrastruktuur te simuleer, waarvan die uitset ook die potensiële waterdiepte relatief tot die insethoogte-model insluit. Die model is verpak in 'n gebruikersvriendelike grafiese gebruikers koppelvlak (GUI) instrument en die gemodelleerde uitsette is verder getoets en geverifieer teen waargeneemde data, wat die toepaslikheid daarvan ondersteun.

Strand en Vishoek (Kaapstad, Suid-Afrika) is gekies as die studieterrain waarvoor die inundasiëvlakke vir drie onafhanklike scenarios bepaal is deur die ekstreme seevlak te kombineer vir 'n 1 in 100 jaar storm, asook twee seevlak scenarios.

Die risikobepalingskomponent het die eBTM gebruik om kaarte vir inundasiëgevaar vir die drie gedefinieerde scenarios te genereer en om geboue wat geaffekteer is, te identifiseer. Beide die tellings vir gevaar en blootstelling aan gevaar was direk afhanklik van die eBTM-uitsette met betrekking tot die inundasiëlimiete en waterdieptes onderskeidelik. Die aanwysers vir die kwesbaarheid van die fisiese gebou is ontwikkel deur gesprekke met belanghebbendes. Die beoordeling is onderneem deur gebruik te maak van lessenaartegnologieë en ter plaatse-inspeksies. Geweegde aanwysers is gebruik om die kwesbaarheidstellings vir elke individuele gebou te bepaal. Die bepaling van die ruimtelike risikoprofiel was gebaseer op die tellings van die voorafgaande werk om die risikostatus van elke individuele gebou op elke studieplek te bepaal. Weereens is skalering toegepas om die belangrikheid van komponente te beklemtoon en om die gewig van minder robuuste insetfaktore te verminder. In

Visioek het dit in die algemeen geblyk dat een gebou 'n groot risiko het om kusoervloei te ervaar op grond van die gegewe scenarios, en drie met 'n lae risiko. In Strand het die ruimtelike risikoprofiel getoon dat 71 geboue 'n lae risiko het, 86 'n matige risiko en 35 'n hoë risiko. Die geïdentifiseerde hoërisiko-geboue kan dus verder beoordeel word ten op sigte van metodes om hul kwesbaarheid en / of gevaarblootstelling te verminder.

Hierdie studie wyk af van bestaande streeksrisiko-assesseringsbenaderings en bied 'n assesseringsmeganisme aan wat toelaat dat die risikokomponente (d.w.s. gevaar, blootstelling aan gevaar en kwesbaarheid) individueel beoordeel kan word, op 'n plaaslik relevante skaal en deur hul individuele assesseringsraamwerke. Die eBTM-instrument en assesserings-tegnieke is ontwikkel om na ander gebiede oorgedra te word. Verder verbeter die eBTM-instrument die toeganklikheid van GIS-gebaseerde tegnieke vir die uitvoering van gelokaliseerde assesserings ten opsigte van kusrisiko. Die kaarte wat vir die individuele risikokomponente vervaardig is, kan dus gebruik word vir kennisoordrag, terwyl die finale risikokaarte gebruik kan word om die bestuurs reaksie binne die plaaslike konteks in te lig.

## ACKNOWLEDEMENTS

I sincerely thank:

- Ryan, my husband, and Kayden, my son, for their support, understanding and patience throughout this project.
- My parents, Colleen and Arthur Lewis for their encouragement and support.
- My brother Ryan Lewis and his partner Tanya Ruiters, for their support.
- My supervisors, Dr Melanie Lück-Vogel and Dr Robyn Pharoah for their motivation, guidance and support.
- Dr Andre Theron, Dr Andrew Mather and Dr Christo Rautenbach for their contribution in terms of technical expertise.
- My employer, National Department of Environmental Affairs, for the funding provided and my line managers for allowing me the time and space to conduct my research.
- Photo contributions: Dr Andre Theron, Ms Clare Lindeque, Mr Arthur Lewis, Mrs Colleen Lewis, Mrs Ieptieshaam Bekko, Mr Pierre Roux and Dr Darryl Colenbrander.
- Data Providers: City of Cape Town and the National Department of Environmental Affairs.

**CONTENTS**

<b>DECLARATION</b> .....	<b>i</b>
<b>SUMMARY</b> .....	<b>ii</b>
<b>OPSOMMING</b> .....	<b>iv</b>
<b>ACKNOWLEDEMENTS</b> .....	<b>vi</b>
<b>CONTENTS</b> .....	<b>vii</b>
<b>FIGURES</b> .....	<b>xi</b>
<b>TABLES</b> .....	<b>xiv</b>
<b>ABBREVIATIONS</b> .....	<b>xv</b>
<b>CHAPTER 1: INTRODUCTION</b> .....	<b>1</b>
<b>1.1 BACKGROUND</b> .....	<b>1</b>
<b>1.2 PROBLEM STATEMENT</b> .....	<b>6</b>
<b>1.3 RESEARCH QUESTIONS</b> .....	<b>8</b>
<b>1.4 AIMS AND OBJECTIVES</b> .....	<b>8</b>
<b>1.5 RATIONALE</b> .....	<b>10</b>
<b>1.6 METHODOLOGY AND THESIS STRUCTURE</b> .....	<b>11</b>
<b>1.7 EXCLUSIONS FROM THIS RESEARCH</b> .....	<b>12</b>
<b>CHAPTER 2: LITERATURE REVIEW</b> .....	<b>14</b>
<b>2.1 RISK ASSESSMENT</b> .....	<b>14</b>
<b>2.1.1 Concepts of Risk</b> .....	<b>14</b>
<b>2.1.2 Coastal Hazards</b> .....	<b>17</b>
2.1.2.1 Storm related inundation .....	18
2.1.2.2 Sea Level Rise .....	20
<b>2.1.3 Vulnerability: A Multidimensional Concept</b> .....	<b>21</b>
<b>2.1.4 Capacity to Cope and Resilience</b> .....	<b>22</b>
<b>2.1.5 Coastal Risk Assessment Frameworks</b> .....	<b>23</b>
<b>2.2 ASSESSING COASTAL INUNDATION HAZARD RISK</b> .....	<b>26</b>
<b>2.2.1 Models: To Predict or to Explain/Understand?</b> .....	<b>27</b>
2.2.1.1 Examples of HDm applications .....	29
2.2.1.2 GIS based tools and data models .....	30
2.2.1.3 Geospatial Multi-Criteria Approaches for Assessing Inundation Hazard .....	32
2.2.1.4 Comparative Studies .....	36

2.2.1.5	Hybrid Approaches .....	38
<b>2.3</b>	<b>ASSESSING VULNERABILITY .....</b>	<b>39</b>
<b>2.4</b>	<b>MEASURING RISKS.....</b>	<b>46</b>
<b>2.4.1</b>	<b>International Examples of (Tsunami) Hazard Specific Risk Assessments .....</b>	<b>46</b>
2.4.1.1	Improved Tsunami risk assessment approaches .....	46
2.4.1.2	Lessons learnt in recovering from the tsunami disaster .....	48
<b>2.4.2</b>	<b>The South African Context .....</b>	<b>49</b>
<b>2.4.3</b>	<b>Methods for determining inland flood risk.....</b>	<b>51</b>
<b>2.5</b>	<b>CONCLUSION.....</b>	<b>52</b>
<b>CHAPTER 3:</b>	<b>OVERVIEW OF FALSE BAY AND THE STUDY SITES.....</b>	<b>54</b>
<b>3.1</b>	<b>FISH HOEK .....</b>	<b>56</b>
<b>3.2</b>	<b>STRAND .....</b>	<b>63</b>
<b>CHAPTER 4:</b>	<b>THE DEVELOPMENT AND VALIDATION OF A COASTAL</b>	
<b>INUNDATION MODEL AND TOOL .....</b>	<b>69</b>	
<b>4.1</b>	<b>GUIDING THE MODEL DEVELOPMENT THROUGH STAKEHOLDER</b>	
<b>ENGAGEMENTS .....</b>	<b>69</b>	
<b>4.1.1</b>	<b>Survey and Interview Findings.....</b>	<b>70</b>
<b>4.2</b>	<b>COASTAL INUNDATION MODEL DEVELOPMENT .....</b>	<b>74</b>
<b>4.2.1</b>	<b>Research Assumptions.....</b>	<b>74</b>
<b>4.2.2</b>	<b>Input Data.....</b>	<b>74</b>
4.2.2.1	High resolution topography .....	74
4.2.2.2	Coastline.....	75
4.2.2.3	Inundation water levels .....	75
4.2.2.4	Roughness Coefficient (RC) .....	76
4.2.2.5	Historical Inundation Event and Extent data .....	76
<b>4.2.3</b>	<b>Simple BTM (sBTM) modelling.....</b>	<b>77</b>
<b>4.2.4</b>	<b>Enhanced Bathtub Model (eBTM) modelling .....</b>	<b>77</b>
<b>4.3</b>	<b>eBTM TOOL DEVELOPMENT .....</b>	<b>80</b>
<b>4.4</b>	<b>MODEL TESTING AND VALIDATION .....</b>	<b>82</b>
<b>4.4.1</b>	<b>Test One: Comparing EBTM and SBTM outputs to observed data.....</b>	<b>83</b>
<b>4.4.2</b>	<b>Test Two: The model's response to a DTM vs. a DSM .....</b>	<b>83</b>
<b>4.4.3</b>	<b>Test Three: The model's response to different DSM resolutions .....</b>	<b>83</b>
<b>4.4.4</b>	<b>Test Four: Varying the Roughness Coefficient .....</b>	<b>83</b>
<b>4.5</b>	<b>RESULTS AND DISCUSSION .....</b>	<b>84</b>

4.5.1	Test One: Comparing eBTM and sBTM outputs to observed data .....	84
4.5.2	Test Two: The model's response to a DTM vs. a DSM .....	89
4.5.3	Test Three: The model's response to different DSM resolutions .....	91
4.5.4	Test Four: Varying the roughness coefficient .....	92
4.6	SUB-CONCLUSION .....	94
<b>CHAPTER 5: DETERMINING THE INUNDATION HAZARD AND BUILDING HAZARD EXPOSURE PER SCENARIO AND HAZARD PROBABILITY .....</b>		
<b>97</b>		
5.1	DETERMINING THE INUNDATION HAZARD PER SCENARIO AND HAZARD PROBABILITY .....	97
5.1.1	Producing coastal inundation extent maps .....	97
5.1.1.1	eBTM setup for hazard map development .....	97
5.1.1.2	Results and discussion .....	98
5.1.2	Determining the building hazard probability .....	103
5.1.2.1	Hazard probability scoring .....	103
5.1.2.2	Hazard probability mapping .....	103
5.1.3	Results and discussion .....	104
5.2	ASSESSING BUILDING HAZARD EXPOSURE .....	108
5.2.1	Building hazard exposure assessment .....	108
5.2.2	Results and discussion .....	110
5.2.3	Sub-conclusion .....	113
<b>CHAPTER 6: ASSESSING BUILDING VULNERABILITY .....</b>		
<b>115</b>		
6.1	BUILDING VULNERABILITY ASSESSMENT .....	115
6.1.1	Framework development .....	115
6.1.2	Framework application on study sites .....	118
6.2	RESULTS AND DISCUSSION .....	119
6.2.1	Fish Hoek .....	119
6.2.2	Strand .....	122
6.3	SUB-CONCLUSION .....	124
<b>CHAPTER 7: DEVELOPING A SPATIAL RISK PROFILE FOR BUILDINGS IN THE COASTAL ZONE .....</b>		
<b>126</b>		
7.1	DEVELOPMENT OF A BUILDING INUNDATION RISK FRAMEWORK .....	127
7.1.1	Scaling .....	127
7.1.2	Weighting .....	128

7.1.3	Calculating final building inundation risk scores .....	128
7.2	RESULTS AND DISCUSSION .....	129
7.3	SUB-CONCLUSION .....	133
<b>CHAPTER 8:</b>	<b>CONCLUSIONS .....</b>	<b>134</b>
8.1	RESEARCH PROBLEM .....	134
8.2	AIMS AND OBJECTIVES REVISITED .....	135
8.3	RESEARCH QUESTIONS REVISITED .....	135
8.4	RESEARCH LIMITATIONS.....	136
8.4.1	Dependency on high resolution DEMs.....	136
8.4.2	Outdated data.....	137
8.4.3	Hydrological & hydrodynamic processes not accounted for .....	137
8.4.4	Risk category classes .....	137
8.4.5	Dependence on licenced software .....	138
8.5	RECOMMENDATIONS.....	138
8.5.1	Recommendations for improving the eBTM .....	138
8.5.2	Recommendations for improving the coastal disaster risk assessment process	139
8.6	RESEARCH VALUE AND CONTRIBUTIONS.....	140
8.6.1	Improved GIS based coastal inundation approach .....	140
8.6.2	Framework for building vulnerability developed .....	140
8.6.3	Cross-disciplinary vulnerability and risk assessment.....	141
8.6.4	Providing a method for generating geospatial risk information at levels relevant for local management .....	141
8.6.5	Tool to empower local municipalities to conduct local inundation assessments .....	142
8.7	CONCLUDING REMARKS .....	143
<b>REFERENCES</b>	<b>.....</b>	<b>144</b>
<b>PERSONAL COMMUNICATION</b>	<b>.....</b>	<b>169</b>
<b>APPENDICES</b>	<b>.....</b>	<b>170</b>

## FIGURES

Figure 1.1 Overview of the technical methodology, including the main heading under each chapter (respective chapters are indicated and reflected by the different colour shades).....	11
Figure 2.1 Examples of storm related coastal hazard events experienced in South Africa. A) Storm surge inundation in Victoria Bay, Western Cape; B) Erosion in Ballito, KwaZulu-Natal .....	18
Figure 2.2 Eight-Sided Flood Simulation Approach .....	34
Figure 2.3 A) Waves overtopping the sea wall along the Sea Point Promenade, Cape Town; B) Inundation incurred more than 60 m inland during the August 2008 storm event.....	37
Figure 2.4 Assessment of damage grades to damage cases .....	44
Figure 2.5 Classification of building types into vulnerability classes, including the range of scatter .....	45
Figure 2.6 Risk Assessment scheme for the coast of Oman .....	48
Figure 2.7 Examples of tsunami warning and evacuation signage, Patong Beach, Thailand.....	49
Figure 2.8 Risk categories and components.....	50
Figure 3.1 Study site focus areas (yellow) in relation to the City of Cape Town. Predominant wave direction indicated by red arrows and sheltered areas indicated by orange bars.....	54
Figure 3.2 Locality map of Fish Hoek Beach, A: View of restaurant and southern beach area, B: Revetment, C: End of dune and beginning of gravel parking area, D: Dune, E: Seaside cottages .....	57
Figure 3.3 Central beach region.....	58
Figure 3.4 Restaurant and recreational space at the southern end of the beach.....	58
Figure 3.5 LiDAR derived Digital Surface Model (DSM) of the Fish Hoek study site .....	59
Figure 3.6 Damage caused by previous storm events in Fish Hoek .....	60
Figure 3.7 Sea walls in Fish Hoek A) Palisade sea wall constructed from wooden railway sleepers, 1980; B) Construction of a new (existing) seawall which was completed in 1982 .....	61
Figure 3.8 Existing seawall revetment.....	61
Figure 3.9 Water level in relation to the revetment .....	62
Figure 3.10 Kelp washed ashore indicating the high water mark .....	62
Figure 3.11 Locality map of Strand Beach, A: Small foredune towards Beach Road, B: Greenbelt, C: Wide sandy beach, D: Low sea wall and wide sandy beach, E & F: Wide sandy beach, G: Recently constructed sea wall, H: Narrow beach on rocky shallow cliffs .....	64
Figure 3.12 Northern beach (A) and southern beach (B) showing the landward extent where the high tide reached on a normal day (yellow arrow).....	65
Figure 3.13 LiDAR derived Digital Surface Model of the Strand study site.....	66



Figure 3.14 Inundation in Strand caused by the supermoon in September 2015.....	67
Figure 3.15 Locations of recent storm related inundation events in Strand .....	68
Figure 4.1 Technical skills available in organisations to assess coastal risk .....	72
Figure 4.2 Enhanced Bathtub Model (eBTM) developed for this study. Large numbers correspond to the processing steps described in the text.....	80
Figure 4.3 Model parameters enforced by the GUI .....	81
Figure 4.4 The eBTM GUI tool .....	81
Figure 4.5 The ‘ArcCoastTools’ toolbox developed .....	82
Figure 4.6 Locations of field recordings of the 2008 flood extent (red dots) overlaid with sBTM (blue) and eBTM (yellow) results for (A) Fish Hoek and (B) Strand.....	84
Figure 4.7 Recorded 2008 flood line (red points) compared to the eBTM (yellow) and sBTM (blue) outputs for Strand (A – C) and Fish Hoek (D) .....	86
Figure 4.8 Thoroughfare through the dune in Strand (as per Figure 4.7 A) .....	87
Figure 4.9 eBTM (yellow) and sBTM (blue) results for bridges over rivers in Fish Hoek (top) and Strand (bottom).....	88
Figure 4.10 Comparison between the modelled flood area outputs using a DSM (yellow) and DTM (red) .....	90
Figure 4.11 Results of the eBTM resolution test with (A) 1 m, (B) 5 m and (C) 10 m resolution DSM .....	92
Figure 4.12 eBTM outputs for runs with a RC of 0.5 (orange) and 1 (blue) .....	93
Figure 5.1 Comparison of total inundated area the 3 sea level scenarios for Fish Hoek and Strand.	98
Figure 5.2 eBTM results for Fish Hoek for all three inundation scenarios .....	99
Figure 5.3 eBTM results for Strand for all three inundation scenarios.....	101
Figure 5.4 Building hazard score map of Fish Hoek (numbers in brackets give the total number of buildings per class).....	105
Figure 5.5 Building hazard score map of Strand (numbers in brackets give the total number of buildings per class).....	107
Figure 5.6 Hazard exposure score for buildings in Fish Hoek.....	111
Figure 5.7 Hazard exposure score for buildings in Strand.....	112
Figure 6.1 Summary of categories, indicators and weightings for assessing building vulnerability .....	116
Figure 6.2 Summary of physical building vulnerability indicator scores for Fish Hoek. Zero values are true scores. Data gaps: no data available. ....	120
Figure 6.3 Fish Hoek vulnerability per building.....	121

Figure 6.4 Summary of physical building vulnerability indicator scores for Strand. Zero values are true scores. Data gaps: no data available.....	122
Figure 6.5 Strand: vulnerability per building.....	123
Figure 7.1 Spatial risk profile framework.....	126
Figure 7.2 Spatial Risk Profile of buildings at risk to coastal inundation in Fish Hoek. Numbers in brackets: No. of buildings per class.....	131
Figure 7.3 Spatial Risk Profile for buildings at risk to coastal inundation in Strand. Numbers in brackets: No. of buildings per class.....	132
Figure 8.1 Example of querying risk and vulnerability scores for individual buildings .....	142

**TABLES**

Table 2.1 Expressing risk.....	16
Table 2.2 Summary of proposed assessment levels .....	24
Table 2.3 CRAF Phase Approaches.....	25
Table 2.4 Examples of interactive flood hazard tools.....	32
Table 2.5 Bathtub Model vs. Hydrodynamic model.....	38
Table 2.6 Summary of physical vulnerability assessment techniques .....	41
Table 2.7 Inland flood assessment techniques .....	52
Table 4.1 Summary of survey and interview respondents .....	71
Table 4.2 Combined water levels derived for False Bay relative to LLD under current sea level conditions .....	75
Table 4.3 Water levels for inundation hazard scenarios .....	76
Table 4.4 Summary of the model test 3 results.....	91
Table 5.1 Datasets used for coastal inundation hazard modelling using the eBTM.....	97
Table 5.2 Hazard probability scoring framework .....	103
Table 5.3 Number of buildings per study site affected by the coastal inundation hazard scenarios	104
Table 5.4 Building hazard exposure scoring categories .....	109
Table 6.1 Building vulnerability categories, indicators and scoring.....	117
Table 6.2 Summary of building vulnerability results .....	119
Table 7.1 Rescaled risk component classes and definitions .....	127
Table 7.2 Data summary for mapping risk in Strand and Fish Hoek.....	129
Table 8.1 Revisiting the Objectives .....	135

## **ABBREVIATIONS**

CCT	City of Cape Town
CSIR	Council for Scientific and Industrial Research
DEA	Department for Environmental Affairs
DEM	Digital Elevation Model
DSM	Digital Surface Model
DTM	Digital Terrain Model
eBTM	enhanced Bathtub Model
FEMA	United States' Federal Emergency Management Agency
GIS	Geographic Information Systems
GUI	Graphical User Interface
HDm	Hydrodynamic Modelling
LiDAR	Light Detection and Ranging
RC	Roughness Coefficient
sBTM	simple Bathtub Model
UNDDR	United Nations Office for Disaster Risk Reduction
UNISDR	United Nations International Strategy for Disaster Reduction
WCDMC	Western Cape Disaster Management Centre

## CHAPTER 1: INTRODUCTION

*The world map shows us that most major cities are located by water and many in ocean coastal zones. Coastal zones have historically been a natural place for human settlements as they typically offer ready access to water and fertile soil. Coastal zones have never ceased to attract people, and urban expansion in recent years has become quite rapid. As we admire the rising skyscrapers of coastal cities and celebrate the prosperity that comes with them, recent studies are sending some alarming messages – coastal cities are facing serious risks.*

(UNU-IDHP 2015: 4)

### 1.1 BACKGROUND

Globally, coastal zones provide important economic and social opportunities including recreational spaces, consumable resources, transport facilities, tourism and economic activities. In South Africa, the contribution of coastal resources to the Gross Domestic Product in 2009 was estimated to be in the order of R57 billion (Turpie & Wilson 2011). Direct benefits derived from coastal resources are estimated to contribute approximately 35% to South Africa's annual Gross Domestic Product (GDP), as well as an additional 28% of the GDP derived from coastal resources indirectly (South Africa 2014). Through Operation Phakisa<sup>1</sup>, a Presidential initiative to unlock economic potential of South Africa's oceans, the value of the coast is set to increase dramatically.

Coastal zones are dynamic spaces where human activities and infrastructure are exposed to and respond in various ways to natural forces, climate change and extreme weather events such as storm surges (Appelquist, Balstrøm & Kirsten 2016; Pfaff et al. 2019; South Africa 2019; Williams & Lück-Vogel 2020). In this context, coastal environments present many challenges with regards to human habitation, which society has largely ignored (Appelquist, Balstrøm & Kirsten 2016; South Africa 2019). Coastal flooding is regarded as one of the most dangerous, harmful and destructive natural hazards (Douben 2006; Williams & Lück-Vogel 2020). However, coastal developments continue to proliferate in the absence of adequate spatially explicit assessments indicating risk at local level, particularly in developing countries where data and technical expertise are limited (Appelquist, Balstrøm & Kirsten 2016).

The demand for reliable data and information is becoming increasingly important, particularly those pertaining to global environmental risks such as climate change (Doukakis 2005; Eurostat 2018; IPCC

---

<sup>1</sup> <http://www.operationphakisa.gov.za>

(Intergovernmental Panel on Climate Change) 2019). Most studies focused primarily on the mechanics of these environmental changes themselves, with little attention to the ecosystems and societies that these changes might endanger (Armenakis et al. 2017; Doukakis 2005). However, questions regarding the vulnerability of social and natural systems have emerged as a focus of policy-driven assessments of global environmental risks in various forums e.g. in the IPCC, the World Economic Forum, and the World Food Forum, amongst others (Doukakis 2005; IPCC 2019; IPCC 2014).

The IPCC's Fifth Assessment Report (2014) states that the Global Mean Sea Level Rise is projected to be 0.28 to 0.98m by 2100, although, considering regional variation and local factors, localised sea level rise can be higher than the projected Global Mean Sea Level Rise (Wong et al. 2014). This implies that not just for currently low-lying areas which are directly affected by the effects of sea level rise, but also for some areas that are currently not within the bounds of high tides and severe storm surges, further coping strategies adequate for at least another 100 years need to be put in place (Cartwright 2011). The previous projections suggested by the IPCC have however been challenged by Krabill et al. (2004), Rignot & Kanagaratnam (2006), Velicogna & Wahr (2006), Hansen (2007) and Tol, Klein & Nicholls (2008), amongst others, who claim that the IPCC's projected levels are too conservative. Their research highlights the accelerated rate of sea level rise and shifts the focus from thermal expansion of the oceans (which accounted for two-thirds of the rise experienced over the 20<sup>th</sup> century) to the less understood potential for non-linear, rapid melting of the Greenland and West Antarctic Ice Sheets (Nicholls et al. 2008). While there is debate and uncertainty around the rate of climate change induced sea level rise, it is undisputed that sea levels are indeed rising (Cartwright 2011). The rate of sea level rise is increasing, and due to the latent heat of water, the sea will continue to rise for at least a century after the atmospheric temperatures have stopped warming (Cartwright 2011).

Sea level rise will have both direct and indirect effects on the world's population, the majority of which already resides in coastal areas. Approximately 60% of the world's 39 metropolises with populations exceeding 5 million people are located within 100 km of the coastline, including 12 of the world's 16 cities with populations greater than 10 million (IPCC 2007). Currently, in South Africa approximately 31% of developments within 100 m of the coast are threatened by sea level rise (South Africa 2019).

Observations reveal that South Africa's coastline is dominated by affluent residential areas (South Africa 2019), tourism properties (e.g. hotels, guest houses) and commercial developments (e.g. shopping malls, restaurants) and public spaces (e.g. promenades, parks). Coastal areas are directly

exposed to the effects of atmospheric, climatological and hydrological processes, where the impacts of these processes are causing increasing damage and costly recovery (Kim, Arrowsmith & Handmer 2004). Goshen (2011) states that in the light of rising sea levels coupled with the increased frequency and intensity of storms originating at sea, accompanied by an increase in wave heights, South Africa's coastline can expect to experience:

- increased exposure to more intense and more frequent extreme events;
- increased risk of damage by storm surges and consequently increased flooding, with greater extent and frequency;
- increased saltwater intrusion and raised groundwater tables;
- greater tidal ranges;
- increased coastal erosion;
- more frequent destruction of coastal property and infrastructure; and
- periodic destruction or negative disruption of the coastal biosphere and environment.

These anticipated changes in turn, are likely to have an impact on the receiving environment, increasing the exposure of populations, properties, economic activities, public services etc. to potential disasters (van Westen 2013). Since the 1970s focus has shifted from analysing the physical hazards to include components of people's vulnerability (Armaş & Gavriş 2013; O'Keefe, Westgate & Wisner 1976), which includes a combination of factors that determine the degree to which an individual's life, livelihood, property and other assets are put at risk (Wisner et al. 2003). Villagrán de León (2006) states that the basic components of vulnerability can broadly be classified as human, physical, socio-economic, environmental, functional and administrative and are therefore dependent on several related factors including but not limited to the population characteristics, degree of poverty, livelihoods, building types and their strength (structural vulnerability).

Kron (2012) states that great natural events are not avoidable, but great disasters are. **Disaster risk arises when hazards interact with physical, social, economic and environmental vulnerabilities** of societies, communities or systems (UNISDR 2004; van Westen 2013). Thus, disasters are not only the product of chance, but also result from the interaction between political, financial, social, technical and natural circumstances (Kron 2013). While effective mitigation measures can be implemented and in many cases are important to protect people and property, it should be acknowledged that they will never guarantee full protection. Society thus must be aware of this in order to properly manage risk (Kron 2013). Current spatial development plans in South Africa are increasingly placing emphasis on sustainability and the prevention or mitigation of natural disasters at both regional and local level,

taking progressive processes (e.g. sea level rise) as well as sudden impact events (e.g. storm surges) into account (Cova, 1999). The assessment and knowledge of risk is therefore an essential component of a people-centred early warning system and has a significant impact with regards to disaster reduction (Strunz et al. 2011).

Disaster risk management, as well as plans and policies should be based on a holistic understanding of disaster risk. This includes hazard characteristics, dimensions of vulnerability, exposure to hazards, preparedness and capacity to cope with impacts (UNISDR 2015).

Disaster risk assessments provide the foundation for planning an effective disaster risk reduction programme (South Africa 2005). The purpose of these assessments is to identify relevant hazards, assess the conditions of vulnerability including the impact the hazard would have on livelihoods and determine the needs to improve the preparedness and capacity to cope with hazard impacts (South Africa 2005). Therefore a comprehensive disaster risk assessment methodology should be investigated and applied. Vulnerability is considered the most complicated component of a risk assessment due to the wide range of interpretations, multi-dimensionality, dynamic nature and site and scale dependencies. It can be assessed using both quantitative and qualitative methods, which then further differentiate between physical vulnerability (primarily following engineering approaches) and other more socially focused components e.g. income (van Westen 2013).

Geographic information systems (GIS) and remote sensing techniques have been used widely for understanding coastal processes and mitigating coastal zone hazards and risks (Ajai 2012; Desai et al. 1991; Navalgund et al. 1998; Nayak 1996; Nayak, Sarangai & Rajawat 2001; Rajawat et al. 2005; Rajawat & Nayak 2000; Rajawat & Nayak 2004), although Gesch (2009) states that most maps of potential inundation have been based on outdated coarse elevation data, resulting in crude representations that add minimal value to decision making processes.

Assessing potential risk also involves an assessment of the receiving environment in the form of vulnerability maps which are essential for effective management and planning, particularly for those involved in impact mitigation and managing the costs to both communities and ecosystems (Brock & Purkis 2009). Traditionally, 'vulnerability' referred to people (Wisner et al. 2003) and vulnerability assessments were undertaken through the analysis of disasters where vulnerable conditions were deducted from the losses and damages experienced (Villagrán de León 2006). However, 'vulnerability' is increasingly being recognised as a multi-dimensional and trans-disciplinary concept covering inherent social, economic, physical, political, engineering and ecological aspects and dimensions (Cutter et al. 2008; Polsky, Neff & Yarnal 2007; Sumaryono 2010).



The seismic community has a familiar saying coined by the inventor of the Richter scale, Charles Richter, who stated that earthquakes don't kill people, but buildings do, because most deaths and physical losses result from buildings or other man-made structures collapsing during or after an earthquake (Sumaryono 2010; UNISDR 2004). This statement purposefully directs focus to the receiving environment i.e. the structural integrity of buildings to withstand natural hazards and the role of infrastructure during and after the initial hazard impact. For example, buildings that can withstand hazard impacts can also be used as areas of safety or for vertical evacuation (if appropriate) when the hazard threat is imminent (Sumaryono 2010).

Undoubtedly, physical building vulnerability assessments are most meaningful when conducted at a local scale. Authors have employed various methods such as surveys (Papathoma & Dominey-Howes 2003) and developing indices and indicators where structural vulnerability is assessed based on the construction materials for walls, floors and roofs, considering their susceptibility to failure (Hahn, Villagrán de León & Hidajat 2003). While there are limitations to these methods, such as the applicability of the survey or index to be used to assess other areas, these approaches allow for the identification of specific vulnerable elements, thus providing direct information regarding the state of vulnerability of a process, system or sector (Villagrán de León 2006).

Both qualitative and quantitative risk assessment methods have been used to assess risk, with quantification techniques primarily following one of two (successfully adopted) approaches, namely quantification based on qualitative description/ranking techniques (e.g. community surveys) and quantification based on detailed analysis of specific physical parameters e.g. wave height (Hettiarachchi et al. 2015).

Risk is produced by a hazard interacting with pre-existing vulnerability (Hettiarachchi et al. 2015; UNISDR 2004; Villagrán de León 2006). It is often represented as:

$$\textit{Risk} = \textit{Hazard} * \textit{Vulnerability}$$

Equation 1.1 Risk equation

In this equation, risk represents the probability of harmful consequences or expected losses, including death, injuries, properties, livelihoods, disruption of economic activity or affected environments that arise from the interactions between a natural or human induced hazard and vulnerable conditions (Hettiarachchi et al. 2015). Generally the hazard is a singular and specific event such as a tsunami, while vulnerability is more multi-dimensional, referring to the physical receiving environment and/or human dimensions (such as preparedness, ability to recover etc.), in relation to that singular hazard.

## 1.2 PROBLEM STATEMENT

Coastal hazards have varying impacts ranging from physical, to environmental, economic and social dimensions (Boateng 2010). Many international studies have been undertaken to measure how coastal processes impact the coastal space and there are many examples of practical implementation regarding the use of models to determine risk (Burbidge et al. 2008; Gesch 2009; Hammar-Klose & Thieler 2001; Lui, Sherman & Gu 2007; amongst others). However, it is also evident that there are many studies relating to large-scale events, while localised events such as storm surges tend to be less prominent in literature even though they can cause extensive localised damage. In light of rising sea levels and the more direct localised impacts of flooding from coastal storm surges on coastal developments, there is a need for improved methods for determining the risk to coastal developments at a local level and by local decision makers. Hazard modelling techniques need to be accessible, repeatable and locally relevant in order to determine the elements at risk. In turn, once the elements at risk are identified, they should be assessed to determine their vulnerability in the context of the hazard.

In South Africa's risk assessment context there are gaps both in literature as well as in practical implementation of existing models to assist in determining risk. Mather, Stretch & Garland (2011) developed the most recent theoretical model to determine extreme wave run-up on natural beaches, based on international best practice, applicable to the South African context. However, the model is based on Hydrodynamic modelling (HDm) techniques, relying on datasets that are either too expensive for assessing large areas or do not exist for particular regions. In addition, these models are data-driven and the outputs are reflective of single scenario inputs i.e. specific wind speeds, wind direction, water level etc. They are generally only utilised by specialists and are computationally expensive to run. These types of models, while being insightful and innovative, are largely unfeasible in terms of practical implementation in environments with limited resources, and implementable solutions are often not forthcoming. Conversely, available GIS based models such as the simple Bathtub Model (sBTM) statically raise water levels, resulting in areas that are hydrologically disconnected from the coast shown to be inundated and not considering the influence of topography, thus usually overestimating flood risk areas.

Adequate base data are often unavailable or captured at inappropriate scales and therefore do not readily allow for localised hazard and vulnerability analysis. For analysing coastal processes such as inundation, Light Detection and Ranging (LiDAR) data are much preferred due to their high resolution and precision but are still expensive to acquire in South Africa. This contrasts significantly with many developed countries where LiDAR is more readily available and seemingly has become

the standard base dataset for inundation hazard analysis e.g. in the context of Hurricane Katrina (2005), Hurricane Sandy (2012) and the Louisiana flooding (2016).

In the international context, physical vulnerability of buildings is relatively well studied in areas where buildings are frequently impacted by hazards through the development of fragility curves and damage indices. However, in the South African context, and considering that coastal infrastructure is regularly damaged by coastal processes, there has not been meaningful advancement in developing methods to assess the physical vulnerability. Building standards in South Africa do not address the potential impact of natural hazards on buildings, resulting in the inappropriate placement and construction of buildings that suffer damage on almost an annual basis (Sowman, Scott & Sutherland 2016).

In short, the challenges associated with addressing coastal risk can be summarised as follows:

- i. capacity to develop and/or run appropriate coastal (GIS and/or HDm) models in South Africa is limited;
- ii. high resolution topographic data e.g. LiDAR is required in order to assess land-sea interactions such as coastal inundation, however, currently LiDAR datasets do not exist for the entire South African coastline. Where LiDAR does exist, it is often a single acquisition date i.e. no additional surveys have been conducted and therefore the topography is representative of the date it was captured and might be outdated;
- iii. locally relevant and technologically accessible (GIS and/or HDm based) coastal inundation models do not exist:
  - HDm is computationally expensive, relying on varying datasets such as tidal, atmospheric, topography data etc. to simulate complex systems and interactions. This has resulted in HDm only being utilised for specific local applications with focused research questions such as designing sea walls;
  - operational oceanographic models which are based on HDm models and are used for forecasting events, do not currently exist at adequate resolutions to consider localised impacts. In addition, capacity is needed to run these types of models on an operational basis;
  - existing GIS based models, while relatively easy to apply, are often inappropriate in the coastal space. A typical example is the simple bathtub model (sBTM), which is commonly used to depict both temporary coastal inundation and permanent sea level rise;
- iv. no assessments have been undertaken to assess the exposure and vulnerability of buildings to extreme coastal inundation events; and

- v. spatial risk profiles which incorporate both coastal hazards and building vulnerability do not currently exist.

The problems that this thesis project aimed to address are the lack of easily applicable coastal flood models, the lack of standards for building vulnerability assessments and subsequently the lack of spatial risk profiles incorporating coastal flood hazard and building vulnerability.

### **1.3 RESEARCH QUESTIONS**

The overarching research questions that will be addressed in this study are:

- i. How can a GIS based coastal inundation model be developed that is more accurate than the existing sBTM, but simpler and quicker to apply than HDm to assess coastal flood hazard on a local level?
- ii. How can buildings be categorized according to their exposure and vulnerability to coastal inundation?
- iii. How can, based on i and ii, a spatial risk profile relating to coastal inundation and building vulnerability be developed using GIS?

### **1.4 AIMS AND OBJECTIVES**

This study aims to develop and test a GIS based methodology for developing a spatial risk profile for physical building vulnerability to extreme coastal inundation scenarios for two test sites in False Bay, South Africa. The spatial risk profile will be derived from a GIS based hazard modelling component and physical building vulnerability assessment.

The following objectives have been set:

1. Review of literature on GIS and HDm based inundation models, building vulnerability assessments and risk quantification to inform the study based on international best practice;
2. Select appropriate study sites, based on data availability and accessibility;
3. Data collation;
4. Stakeholder engagements;
5. Develop an inundation model to determine the areas within the selected study sites that will be affected by coastal inundation scenarios;

6. Test the coastal inundation model's response to changes in the input parameters and demonstrate the model's appropriateness for determining coastal inundation
7. Determine the vulnerability of buildings potentially exposed to the coastal inundation hazard through the analysis of available data, spatial analysis techniques and field studies;
8. Quantify the coastal inundation hazard, hazard exposure and building vulnerability; and
9. Develop a spatial risk profile illustrating a risk gradient of individual buildings to coastal inundation hazard.

## 1.5 RATIONALE

*Our current disaster risk assessments are conducted at a district municipality or metro level, so localised hazards are often lost in the end results. Coastal processes are particularly challenging because the modelling requires expertise that is not readily available or accessible. For risk assessments and planning purposes, we need a methodology that is easily repeatable using available data and technology to communicate areas potentially exposed to particular hazards and similarly, a method to assess the vulnerability of the receiving environment.*

(Rylands 2016, Pers com)

Due to the numerous vectors of global change, including coastal urbanization, exploitation of coastal resources and climate change, the threat to sensitive coastal environments is increasing and developments are potentially becoming unsustainable and threatening public safety (South Africa 2014).

Coastal managers are constantly faced with the complexities of human interactions with the coastal space. Records prior to the year 2000 suggested that the South African coast would experience waves of up to 7 m every year, with waves exceeding 10 m occurring roughly every 20 years. On 16 May 1984 an extreme storm hit Cape Town producing waves exceeding 11 m. A similar storm occurred in September 2001 (Brundrit 2009). Since then, Cape Town has seen storms of similar magnitude in 2001, 2002, 2008, 2014 and 2016.

Currently, there is little evidence that planning and regulatory processes incorporate risk aspects, including the dangers associated with rising sea levels and coastal flooding. Meanwhile, due to the influence of climate change, infrastructure such as roads and buildings are being increasingly subjected to the onslaught of coastal processes, resulting in high costs relating to recovery (repair or replacement of damaged assets) from these events (Hammar-Klose & Thieler 2001). The need for local scale infrastructure assessments and information to guide mitigation and/or response actions is thus becoming even more important. This need is being addressed in this research.

The aims and objectives of this research were achieved primarily through a co-development approach, involving stakeholders (who are actively involved in coastal and risk management) in both the inundation model and vulnerability indicator development. The inundation model determined the inundation limits for selected water level (hazard) scenarios and subsequently identified individual exposed buildings. These buildings were assessed in terms of their vulnerability to coastal inundation hazard using the developed vulnerability indicators. Considering the inundation hazard, building hazard exposure and building vulnerability, a final building spatial risk profile was produced. The methods employed demonstrate a practical framework for determining localised risk to buildings to

coastal inundation hazard. Bringing together a physical flood risk assessment and a building vulnerability assessment is a new and important contribution to coastal flood risk management.

## 1.6 METHODOLOGY AND THESIS STRUCTURE

This research made use of various methodologies including interviews, surveys, on-site building vulnerability assessments and GIS based spatial analysis. The methodology is aligned with the three research questions phrased above (Section 1.3). An overview thereof is presented in Figure 1.1, whereby research question 1 is addressed through Chapters 4 and 5.1, question 2 is addressed in Section 5.2 and Chapter 6 and research question 3 is addressed in Chapter 7:

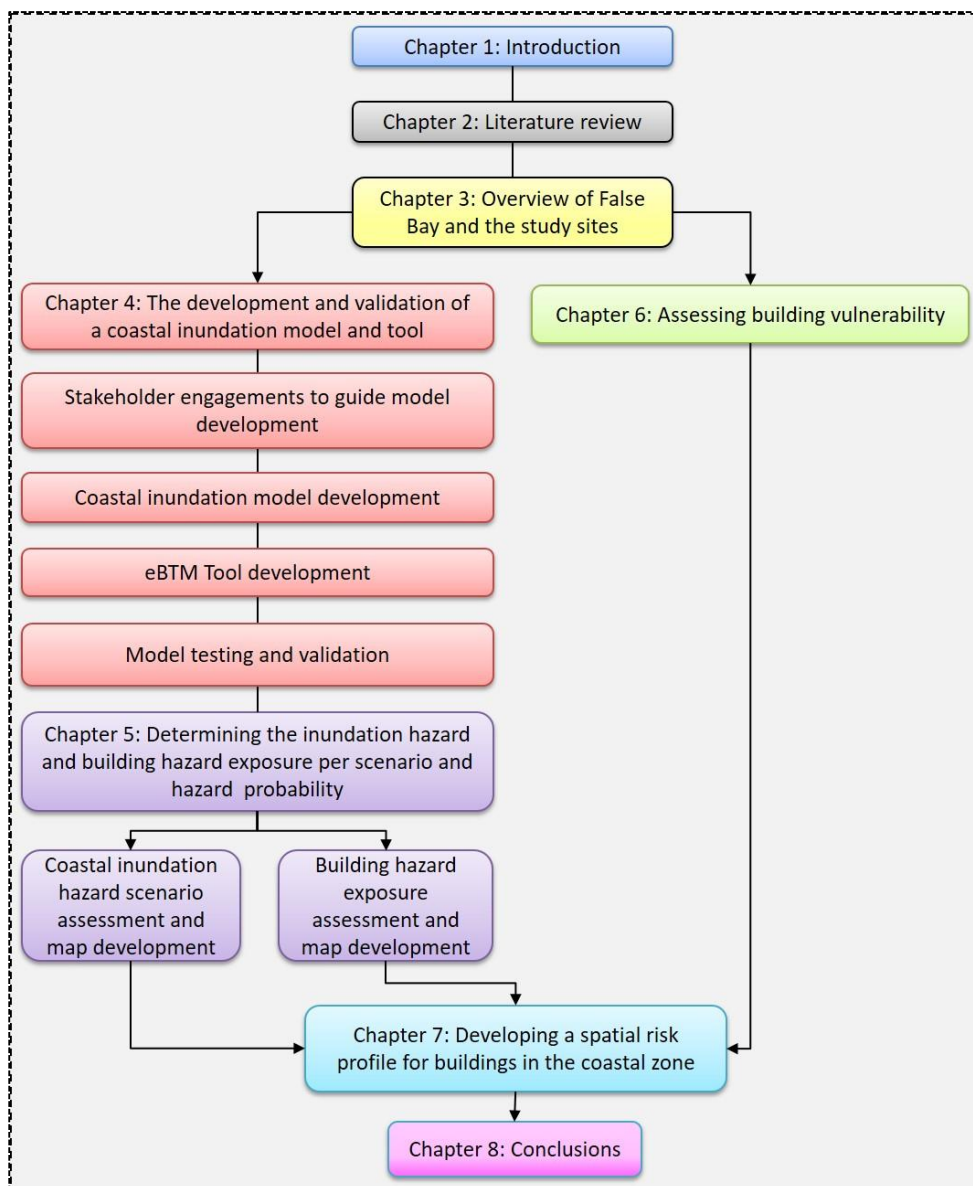


Figure 1.1 Overview of the technical methodology, including the main heading under each chapter (respective chapters are indicated and reflected by the different colour shades)

The flood hazard assessment involved a survey and interviews as well as the technical development of the model. Further, in order to determine the available capacity within institutions to utilise the model and to understand the assessment techniques currently being used, written surveys were disseminated to coastal practitioners to gather this information. The outcomes of the surveys and interviews and an extensive literature review on methods to model coastal inundation were used to inform the development of the GIS based inundation hazard model.

The model was validated by testing its response to varying parameters, including surface roughness, raster resolution and the response to a Digital Terrain Model (DTM) vs. a Digital Surface Model (DSM), and was also assessed against data that were captured during an actual storm event to compare the model outputs vs. reality. Once the model was validated, coastal inundation maps were generated for three scenarios per study site and hazard probability scores were applied to each building.

The vulnerability component focused on a physical building vulnerability assessment, based on field work for investigating building characteristics and features as well as examining damage histories for buildings. The consultation with disaster management officials informed the vulnerability indicators and weightings and subsequently, a building vulnerability index was developed. The output of this component assigned a hazard exposure score and a physical vulnerability score to each building, both presented as maps.

The spatial data outputs for flood hazard and building vulnerability were used as the primary input for the development of a GIS-based spatial risk profile relating to coastal inundation and building vulnerability. The quantified results were represented as spatial risk profile maps.

## **1.7 EXCLUSIONS FROM THIS RESEARCH**

This research involves the development of a GIS based enhanced Bathtub Model (eBTM), which is presented in the form of a tool with a user-friendly Graphical User Interface (GUI). Hydrodynamic modelling will not be used as part of this research; it is however discussed and recognised as an appropriate localised inundation modelling technique when specific physical parameters (e.g. wind speed) are provided.

Guided by the vulnerability indicators and through agreement with stakeholders and experts, only buildings will be used in the building vulnerability assessment and all other infrastructure types e.g. pipelines and roads are excluded.



The most recent available LiDAR data for the study areas were acquired in 2014, and therefore do not include recent developments in the coastal space, such as the sea wall constructed in Strand post 2014.

The influence of drainage infrastructure on inundation was not considered as the model cannot accommodate subterranean data.

The potential role rivers can play in coastal inundation processes was excluded, too, as the model does not cater for such additional water sources.

## CHAPTER 2: LITERATURE REVIEW

This section provides an overview of the existing approaches to (coastal) disaster risk assessments and the components that make up ‘risk’ i.e. hazard, vulnerability, capacity to cope and resilience. In addition, holistic disaster risk assessment approaches will be reviewed, including those undertaken in the South African disaster risk assessment context. Considering that one of the aims of this study is to develop a GIS based coastal inundation model, relevant modelling processes and their applications will also form part of this literature review.

### 2.1 RISK ASSESSMENT

Risk assessment is one of the fundamental tools in planning, improving and implementing effective disaster risk reduction responses, policies and programmes (Aitsi-Selmi et al. 2016; Hettiarachchi et al. 2015; South Africa 2005). It is critical to identify and understand risk in order to effectively manage it (Hettiarachchi et al. 2015). The risk assessment process aims to identify hazards and vulnerabilities within a defined area and examine the probability and outcomes of potential disasters (South Africa 2005). Ultimately, the availability and reliability of hazard, exposure and vulnerability data, at the appropriate spatial scales, determines the overall quality of the risk assessment (Aitsi-Selmi et al. 2016).

#### 2.1.1 Concepts of Risk

The coastal zones comprise of natural ecosystems, the built environment and communities, all of which are exposed to a variety of hazards arising from natural processes as well as human induced activities. The assessment and management of coastal risk plays an important role in nature conservation, protection of the built environment and safety of human lives (Hettiarachchi et al. 2015) and future planning. The United Nations Office for Disaster Risk Reduction (UNDRR; formerly: United Nations International Strategy for Disaster Reduction, UNISDR) states that regardless of how risk is represented, the end result should be the same, whereby:

“**Risk** should represent the probability of harmful consequences, or expected losses (deaths, injury, property, livelihoods, economic activity disrupted or environmental damage) resulting from the interactions between natural or human-induced hazards and vulnerable conditions” (UNISDR 2004:16).

**Hazards** are defined as a process, a phenomenon or human activity that may cause loss of life, injury or other health impacts, property damage, social and economic disruption or environmental

degradation (UNISDR 2017). For assessment purposes, natural hazards are often classified according to their origin e.g. geophysical, meteorological, hydrological, climatological, biological, extra-terrestrial and technological (Guha-Sapir, Hoyois & Below 2015). These classifications should however be considered as subjective and arbitrary as a single hazard may have different origins e.g. coastal erosion may be induced by long term sediment movement caused by wave action, an episodic event such as a storm surge or as a result of human activity such as inappropriate planning and/or development. Subsequently, hazards have a multitude of characteristics that need to be understood in order to inform planning and reduce potential damage (van Westen & Greiving 2017). Hazards can be assessed by their probability, predictability, frequency, magnitude (size) and intensity (van Westen & Greiving 2017). Historical data are frequently used to understand the magnitude-frequency relationship for hazard events. Intensity in terms of coastal inundation may be measured in terms of the water height or velocity (van Westen & Greiving 2017).

Hazard events may be harmful to people, property, infrastructure, economy, environment and/or activities, termed ‘elements-at-risk’ (van Westen & Greiving 2017). These elements have a certain level of vulnerability which can be defined independently. In the context of people, vulnerability can be changeable and unpredictable, particularly when confronting a hazard and can therefore even be considered a behavioural response (Lewis 2019). Birkmann (2006) and van Westen & Greiving (2017) describe aspects of vulnerability, including physical, social, economic and environmental conditions. According to the UNDRR, **vulnerability generally describes the *characteristics and conditions determined by physical, social, economic and environmental factors or processes which increase the susceptibility of an individual, a community, assets or systems to the impacts of hazards*** (UNISDR 2017). Relevant to this thesis, physical vulnerability on its own can be defined as the degree of potential damage to a building that is exposed to the coastal inundation hazard, considering the intensity of the hazard.

Exposure and vulnerability are intrinsically linked as **exposure is defined as *the situation of people, infrastructure, housing, production capacities and other tangible human assets located in hazard-prone areas*** (UNISDR 2017). Increases in either vulnerability or exposure or both will result in an increase in risk (Terry & Goff 2012, cited in (Aitsi-Selmi et al. 2016), particularly in the human context where people are able to (rapidly) change both their states of vulnerability and degree of exposure, making ‘human’ risk a more fluid rather than static concept (Lewis 2019).

A **disaster** is defined as a serious disruption of the functioning of a community or a society at any scale due to hazardous events interacting with conditions of exposure, vulnerability and capacity, leading to one or more of the following: human, material, economic and environmental losses and

impacts (UNISDR 2017). It occurs when a hazard event manifests and is combined with the pre-existing vulnerability of people, infrastructure, services or systems as well as the inability of the affected society to cope using their existing resources (Villagrán de León 2006).

Various methods have been used to quantify risk. The most commonly used is the UNISDR's (2004) equation, with authors presenting various adaptations (Table 2.1).

Table 2.1 Expressing risk

Equation	Notes
$Risk = Hazard * Vulnerability$ (UNISDR 2004)	Risk is presented by combining hazard and vulnerability
$Risk = Hazard * Vulnerability - Coping Capacity$ (Villagrán de León 2006)	Coping Capacity can include both physical resources as well as awareness, training and education initiatives.
$Risk = Hazard * Vulnerability * Deficiency in Preparedness$ (Villagrán de León, 2001, cited in Villagrán de León 2006)	Deficiencies include the lack of emergency committees, plans and early warning systems. It is commonly identified as the inverse of capacity.
$Total Risk = (\sum elements at risk) * Hazard * Vulnerability$ (Alexander 2000)	The total risk is comprised of the sum of predicted casualties, damages and losses.
$Risk = Hazard * Exposure * Vulnerability$ (Dilley et al. 2005)	Exposure refers to people or infrastructure that would be negatively affected by an individual hazard.
$Risk = Hazard + Exposure + Vulnerability - Coping Capacities$ (Hahn, Villagrán de León & Hidajat 2003)	Exposure indicates what is at stake if a hazard event takes place. In this instance it considers the magnitude rather than actual economic values.
$Risk = Hazard * Vulnerability * Amount of elements - at - risk$ (van Westen & Greiving 2017)	'Elements-at-risk' is used interchangeably with 'exposure' as per Dilley et al. (2005)

Adapted from: Villagrán de León (2006: 9-10)

Capacity broadly reflects the manner in which people, communities or organisations have and utilise available resources, abilities and knowledge to cope with adverse conditions that could lead to disasters. Increasing the coping capacity of communities usually builds resilience to withstand hazard impacts (Alexander 2012). Capacity can include both physical resources as well as awareness, training and education initiatives (Hettiarachchi et al. 2015) and generally involves management of resources before, during and after a disaster event (Villagrán de León 2006).

Inadequate preparedness refers to the pre-existing conditions that prevent a community, institution or society from timeously and effectively responding to a hazard and thereby minimizing its impact, particularly the loss of human life (Villagrán de León 2006). Hettiarachchi et al. (2015) further argue that deficiency in preparedness can be used to represent certain measures that, if absent, could reduce the loss of human life and/or property during the time of the event. Such deficiencies include the lack of emergency committees, plans and early warning systems (Villagrán de León 2006). It is commonly identified as the inverse of capacity (Hettiarachchi et al. 2015).

Hettiarachchi et al. (2015) state that it is possible to quantify risk in terms of monetary loss e.g. the cost to replace infrastructure. However, measuring capacity and preparedness introduces a human dimension e.g. the physical ability of people to evacuate an area. These human dimensions introduce challenges in terms of measurability as people have different physical capabilities such as some being more physically fit than others, thereby making it difficult to adopt direct quantification techniques (Hettiarachchi et al. 2015).

The equations used to express risk (Table 2.1) are widely accepted, and recent evidence suggests that globally, overall risk has increased (Aitsi-Selmi et al. 2016). The severity of disaster impacts is strongly dependent on both exposure and vulnerability (Terry & Goff 2012, cited in Aitsi-Selmi et al. 2016) and consequently the increase in exposure of people and assets has resulted in increased vulnerability (Aitsi-Selmi et al. 2016). More focus is thus needed on these components of risk (Aitsi-Selmi et al. 2016).

### **2.1.2 Coastal Hazards**

Natural hazards are natural processes that cannot be influenced e.g. wind speeds, earthquake magnitude, storm surge height etc. For effectively managing coastal hazards, approaches are required to minimize coastal risk as well as to meet the demands of growing populations and pressures in the coastal zones within existing legislative frameworks (Rollason, Fisk & Haines 2010). This was reiterated in March 2013 in Durban, South Africa, where START (Global Change System for Analysis and Research Training) and partners convened for a four-day scoping workshop on “Cities at Risk: Africa” to assess the knowledge and capacity needs regarding vulnerability, capacity and risk in urban areas, and knowledge sharing regarding climate change and adaptation. The key conclusions of the workshop (START 2013) are:

- good governance contributes to enhancing resilience by promoting integrated action on climate change by all stakeholders;
- there is a strong need for ‘climate translators’ presenting scientific knowledge in formats that are more accessible to urban planners, governments and the public;
- urban poverty needs to be addressed in the context of community and infrastructure vulnerability; and
- additional work is needed in bridging the data, information and knowledge gaps on climate change impacts, vulnerability and exposure of African cities. It was observed that in many African cities even basic data relating to the then Millennium Development Goals are unavailable.

Hazards (physical events) have a spatio-temporal aspect, occurring at a specific time, in a specific area at a given intensity (UNISDR 2004; van Westen 2013). The primary aim of a hazard assessment

is to identify the hazard itself, the affected areas and create ‘zones’ with respect to the severity/magnitude (e.g. low, medium, high) and frequencies (van Westen 2013). Rollason, Fisk & Haines (2010) summarise this process in stating that managing coastal hazards will be incomplete if the likelihood and consequence are not described. This can be conducted both quantitatively and qualitatively and it is important to not provide a ‘false sense of confidence’. Cowell et al. (2006) and Cutter & Gall (2015) argue that the hazard profile must be regarded as a best estimate due to the possible limitation of data, variable and/or limited climate data, assumptions produced in models, limitations in the various methodologies and uncertainties driven by climate change. Declaring these uncertainties also creates a culture of transparency (Aitsi-Selmi et al. 2016; Rollason, Fisk & Haines 2010); for example, a series of hazard lines that provides more than one probability or likelihood will provide better guidance for coastal managers when planning for coastal hazards.

#### 2.1.2.1 Storm related inundation

By nature, coasts are affected by many natural perils and in many cases constitute the boundary between continental plates, making them more prone to earthquakes and volcanic eruptions (Kron 2013). However, coastal hazards are usually associated with meteorological events, the most common being storm surges that have triggered amongst the most costly and deadly disasters in the past decade (Kron 2013). Severe storms such as tropical and extratropical cyclones can generate storm surges over coastal seas, the severity of which is determined by a number of factors including the storm track, regional bathymetry, nearshore hydrodynamics and wave contributions (Wong et al. 2014). Examples of storm related coastal hazard events experienced in South Africa are provided in Figure 2.1.



Source: A) Western Cape Government (2008); B) eThekweni Municipality (2006)

Figure 2.1 Examples of storm related coastal hazard events experienced in South Africa. A) Storm surge inundation in Victoria Bay, Western Cape; B) Erosion in Ballito, KwaZulu-Natal

Climate change has drastic direct effects on coastal settlements including the loss of dry land due to erosion and/or submergence, damage emanating from extreme events such as wind-driven storms,

storm surges, coastal inundation, but also heat waves and droughts (Wong et al. 2014). It is important to recognize that climate change does not only include changes in mean climate, but also in weather extremes which can be characterized by singular or a combination of events, by observing changes in the mean, variance, or shape of probability distributions (Spencer et al. 2017).

The effects of climate change can also impact on infrastructure in terms of energy usage, water availability and loss of cultural heritage (Wong et al. 2014). In terms of coastal flood risk, the IPCC's Fifth Assessment report projects that the global population residing near the coast and exposed to the 1 in 100 year coastal inundation projections is set to increase from 270 million people in 2010, to 350 million people in 2050 due to an increase in available economic opportunities e.g. ocean's economy initiatives (Jongman, Ward & Aerts 2012).

The interaction between ocean processes such as wave run-up and the terrestrial space including coastal infrastructure, has received much attention in empirical studies particularly with regards to nearshore processes (e.g. Mather, Stretch & Garland 2011b; Nielsen & Hanslow 1991; Rautenbach et al. 2020; Viavattene et al. 2018; Williams & Lück-Vogel 2020; amongst others). However, increasing interest is being placed on the coastal space with regard to the effects of climate change, i.e. more frequent and severe storms resulting in inundation and erosion etc. and the impacts of these hazards on society and economic activities. Developments are generally long-lived and development rights are permanently granted to property owners and thus the effects of coastal processes should be considered carefully in order to guide land-use planning (The State of Queensland 2013).

Storms surges are primarily influenced by atmospheric conditions, occurring when low barometric pressure and strong onshore winds coincide to produce higher tide levels. As the barometric pressure decreases, creating a low pressure over the ocean, the water level rises by approximately 1 cm for every 1 mbar (Rautenbach et al. 2020; Viles & Spencer 1995). The higher sea levels are energised through the transfer of energy contributed by strong onshore winds (Viles & Spencer 1995). Along the coast, this interaction often results in large scale sediment movement (erosion and accretion) and inundation events and subsequent damage to coastal properties, developments and infrastructure.

The inundation hazard impact is dependent on a variety of factors including the run-up distribution, water levels, substrate and beach morphology and topography (Mather, Stretch & Garland 2011b; Nielsen & Hanslow 1991). Modelling run-up is a complex process, dependent on a variety of input parameters (Mather, Stretch & Garland 2011b), some of which are unknown and highly variable e.g. bore speed prior to wave collapse and the influence of backwash from previous run-up (Nielsen & Hanslow 1991). However, many different approaches have been used in many different contexts such



as disaster management, coastal management, academia, environmental monitoring etc. Most flood/inundation maps in existence are not representations of actual floods, but rather forecasts of potential flooding (Jones 2004).

Inundation modelling has been addressed in different ways such as the use of GIS, remote sensing and numerical modelling, or combinations of various technologies (Neumann & Ahrendt 2013). All these methods are aimed at the ability to predict future water levels and the inundation extent resulting from a particular trigger such as meteorological and tidal conditions (Bates et al. 2005). Didier et al. (2015) state that the maximum inland inundation extent is determined by a combination of the astronomical tide, barometric pressure and wind-induced surge, however this information is not always available at the required local or regional scales. This emphasises that inundation modelling still has many associated uncertainties, particularly in the light of climate change and expected sea level rise (Neumann & Ahrendt 2013).

#### 2.1.2.2 Sea Level Rise

The major factors contributing to global mean sea level rise (sea level relative to fixed points on land) include the thermal expansion as the ocean temperatures increase, and meltwater from glaciers, icecaps and ice sheets of Greenland and Antarctica (Wong et al. 2014). Less commonly, human activity contributes directly to relative sea level rise such as land subsidence induced by excessive groundwater or fossil fuel (oil and gas) abstraction (Church et al. 2013). Assessing coastal impacts, vulnerability and adaptations should therefore ideally consider global mean sea level rise, regional variations and non-climate related changes to sea level (Wong et al. 2014).

Regional sea level rise is important when considering coastal impacts at the local scale as it is often the driver of coastal processes and hazard events such as inundation, erosion and accretion (Wong et al., 2014). While global sea level rise factors do play a role in regional sea level rise, regional variations in the rate of sea level rise are primarily governed by ocean circulation patterns and annual and decadal variability (Wong et al. 2014).

In the South African context, Mather (2007) states that there is agreement between long-term global records when compared with 30 years of South African tidal gauge records. This implies that the South African coastline's local rate of sea level rise is within the range of global trends. However, Mather, Garland & Stretch (2009) state that sea level rise recorded along the south-western coast of South Africa is less than the sea level rise experienced on the more northwest and eastern coastlines. The linear trend recorded between 1957 to 1991 in Simons Bay (Cape Town) is  $1.1 \pm 0.2$  mm/annum, which is significantly less than the recorded global rate of 1.8 mm/annum for the period 1961 to 2003.



### 2.1.3 Vulnerability: A Multidimensional Concept

*Vulnerability is the most elusive component of the hazard-vulnerability-coping capacity-risk (losses)-recovery cycle. It needs to be defined as 'vulnerability of what', 'vulnerability to what' at 'what scale' to mention but the most important aspects.*

(Villagrán de León 2006: 5)

Assessing vulnerability has recently become an urgent and significant topic, particularly in climate change and disaster risk studies (Aitsi-Selmi et al. 2016; Cho & Chang 2017). Initially 'vulnerability' was used in engineering disciplines as an approach to describe the physical fragility or strength of a structure to resist physical forces exerted by ground motion, water and air (wind) (Birkmann 2007; UNISDR 2004). Later it was introduced by O'Keefe, Westgate & Wisner (1976) in a social framework to investigate the role of socio-economic factors preventing people from optimally responding to and recovering from extreme natural disasters and their associated effects (Armaş & Gavriş 2013). The concept of vulnerability has thus evolved into an analytical tool for evaluating susceptibility to harm, powerlessness, and marginality in social and physical systems. It is also used as a tool for enhancing human well-being through risk mitigation and reduction techniques (Adger 2006).

In addition to its multi-dimensionality, 'vulnerability' is also trans-disciplinary, covering social, economic, physical, political, engineering and ecological aspects and dimensions (Cho & Chang 2017; Cutter et al. 2008; Polsky, Neff & Yarnal 2007; Sumaryono 2010). However, the lack of standardization has created confusion between practitioners in terms of the application (Aitsi-Selmi et al. 2016; Villagrán de León 2006). Today, the term 'vulnerability' is more commonly associated with people rather than buildings, economies, hazardous conditions or hazard prone areas (Wisner et al. 2003), which adds further confusion, as vulnerability itself does not exist in isolation (Cho & Chang 2017).

There is extensive literature discussing the concept of 'vulnerability' (Adger 2006; Cannon 2008; Füssel 2007; Villagrán de León 2006; Wisner et al. 2003; amongst others) all of which identify the uncertainty/lack of clarity and associated confusion in the use of the word. In particular, vulnerability is often used interchangeably with poverty, deprivation, marginalization and other connotations of victimhood and usually is 'discovered' after a damaging event has occurred (Cannon 2008). More recently, 'vulnerability' has also been described as a fluid construct that is both a changeable and unpredictable human behavioural response when people are faced with a hazard (Lewis 2019). In light of these differences, the UNDDR (Exposure and Vulnerability (Working Group 2)) provided

recommendations towards promoting a common understanding of exposure and vulnerability (Aitsi-Selmi et al. 2016; UNISDR ) 2016).

Cannon (2008) provides a breakdown of five interrelated components that define vulnerability by capturing the aspects at risk from natural hazards:

- i. livelihood strength and resilience which are determined by the amount and quality of assets owned and accessible to the person, particularly those that enable productivity and income-generation for self-sustenance, including employment opportunities;
- ii. wellbeing and base-line status which is derived from the strength of an individual's livelihood;
- iii. self-protection which is indicated by the willingness and capability of individuals to build a home that is safe from prevalent hazards, which is based on their wellbeing and the ability to afford the required safety features;
- iv. social protection which focuses on the types of protection against the hazard that cannot be implemented by the individual, e.g. the implementation of building codes through government institutions, which society needs to conform to; and
- v. governance in terms of the willingness of authorities to properly manage resources for the betterment of society.

#### **2.1.4 Capacity to Cope and Resilience**

While vulnerability is generally defined as the predisposition of something to be affected, some authors have also included factors such as the lack of coping capacity and/or resilience as the primary influencer of vulnerability (Villagrán de León 2006).

Coping capacity refers to interventions undertaken prior, during and post hazard events which reduce vulnerability, including implementation of mechanisms to contain the event once it has manifested itself (Villagrán de León 2006). These interventions include the combination of the strengths and resources available within a community to reduce the level of risk via various means including institutional, physical, social or economic as well as skilled personnel or collective attributes such as strong leadership and good management (South Africa 2005).

Resilience refers to the ability of a system, element or community to resist or absorb the impact of a natural or social event (Villagrán de León 2006). Mechanisms of resistance can include the ability to adapt, by resisting or changing in order to achieve and maintain an acceptable level of functioning

and structure (South Africa 2005). Often achieving these states is largely dependent on the social system's ability to self-organise and increase its capacity by taking lessons from past experiences for better protection from future potential events and improved disaster risk reduction measures (South Africa 2005). In this context, resilience and vulnerability are reciprocal, i.e. more vulnerable systems should be less resilient and less vulnerable systems are more resilient (Villagrán de León 2006). However there is ongoing debate regarding the linkages between vulnerability and resilience, which have largely been kept separate by conceptual constructs (Miller et al. 2010).

### **2.1.5 Coastal Risk Assessment Frameworks**

Birkmann (2007) states that risk can be represented in many different ways and is therefore dependent on the objectives of the risk assessment. A risk assessment framework is designed to explore the potential impact on a particular value (social, economic, environmental, infrastructure etc.) from a threatening process (hazard), through a systematic and defensible approach (Elrick & Travers 2009; Rollason, Fisk & Haines 2010). Ultimately frameworks are designed to guide disaster risk reduction efforts for specific known hazards and primarily comprise of the following steps (South Africa 2005):

- identification and analysis of potential hazards;
- assessment of the conditions of vulnerability that increase the chance of loss for elements at risk;
- determining the level of risk for different situations and conditions; and
- setting priorities for action.

Various generic risk assessments have also been applied to the coastal context (e.g. South Africa 2005), with some authors having adapted or devised frameworks specifically for the coast (e.g. Elrick and Travers 2009; Rollason, Fisk & Haines 2010; Sharples, Attwater & Carley 2008 amongst others). The methods used for conducting (coastal) risk assessments vary depending on the nature and type of risk being assessed (South Africa 2005). Literature reveals many differing approaches to coastal risk assessments, however Sharples, Attwater & Carley (2008) suggest that they should be viewed rather as complimentary methods. They further discuss a proposed conceptual framework following a “Three Pass Approach”, reflecting the different scales of assessments. These are summarized in Table 2.2:

Table 2.2 Summary of proposed assessment levels

Level	Scale	Purpose
<b>First Pass</b>	Regional Sensitivity Assessment	Identifies areas potentially sensitive to physical processes
<b>Second Pass</b>	Regional Exposure Assessment	Identifies the magnitude and variability of the processes or the energies driving the hazards e.g. sea level rise, tidal processes, wave climate, storm climate etc.
<b>Third Pass</b>	Site Specific Assessment	Identification of coastal sites potentially at risk as a result of the preceding assessments, and production of a detailed model of how the coast is likely to respond to the specific hazards.

Source: Sharples, Attwater & Carley (2008: 4-6)

With reference to Table 2.2, the third pass would be costly, time consuming and impractical to conduct at national/regional level as it would involve the incorporation of local variable factors into a national/regional assessment, hence the approach of first identifying (and prioritizing) areas potentially at risk at a regional scale, prior to conducting the site specific analysis (Sharples, Attwater & Carley 2008). This provides a logical interrelation between assessments (Sharples, Attwater & Carley 2008), particularly when considering characteristics of both the spatial and non-spatial components (van Westen, Castellanos & Kuriakose 2008).

Recently, research efforts have taken a more ‘sector-based’ approach, recognizing that different environments experience risk differently. Viavattene et al. (2018) developed a Coastal Risk Assessment Framework (CRAF) through a 2 phase approach:

- Phase 1, a GIS-based index approach (or “screening approach”) designed to characterise the spatial distribution of hazards at the regional level to identify hotspots; and
- Phase 2, integrated modelling to further interrogate the hotspots by increasing the spatial resolution and utilizing more sophisticated analyses. This is particularly significant because coastal hazards are almost always experienced as localised events.

Stakeholders are actively engaged in both phases. The respective analyses proposed by Viavattene et al. (2018) for undertaking the various CRAF phases are presented in Table 2.3 below:

Table 2.3 CRAF Phase Approaches

	<b>CRAF Phase 1: GIS index based approach</b>	<b>CRAF Phase 2: Integrated Modelling Approach</b>
Assessment area	Entire regional coast (~ 100 km)	3 – 4 potential hotspots within the regional coastal boundary
Hazard pathway assessment model	Simple (empirical) model	1D, process based, multi-hazard
Hazard pathway assessment scale	Uniform hazard pathway per sector (~ 1 km)	Multiple hazard pathway computations per sector (up to 100 transects per km, given the computational constraints)
Hazard mode (inundation extent)	Simple bathtub/overwash extent model	2D inundation model
Computation of hazard probability	Response approach (in the case of absence of long time series, event approach)	
Receptor and vulnerability information	Exposure only (receptor types and associated ranking values)	Receptor and vulnerability data at individual or aggregated (neighbourhood) scale
Calculation of impact	Exposure indicators	Indicators of direct and indirect impacts and multi criteria analysis
Outcomes	Coastal index per sector – potential hotspots	Regional score per hotspot using a multi criteria analysis – select hotspots for detailed risk assessment

Source: Viavattene et al. (2018: 3)

The Phase 1 GIS-based approach (large scale coastal index) calculates coastal risk by combining several indicators into a single index which allows for the entire coastline to be rapidly assessed. Involvement of stakeholders with the relevant expertise and neutrality informed the index based approach which incorporated various impact indicators such as risk to life, financial recovery, household displacement etc. (Viavattene et al. 2018). The indicators, ranking and the formulae used to combine variables are not standardised to allow the relative flexibility to choose indicators best suited to the respective coastal environments (Viavattene et al. 2018). Unlike other methods (including the approach adopted in South African Risk Assessments) that allow multiple hazards and vulnerabilities to be considered and amalgamated into a single index, the CRAF considers each hazard individually. This level of analysis uses more regionally appropriate modelling techniques such as the GIS based sBTM, which considers static sea level rise, excluding other dynamics such as atmospheric and oceanographic influence.

CRAF Phase 2 undertakes hotspot impact assessment and multi-criteria analysis, where the scale of the analysis is more localised and each identified hotspot is ‘independent’ i.e. the hazard impact at one hotspot is independent from the hazard impact at another hotspot, regardless whether the hazard originates from the same source e.g. a storm surge (Viavattene et al. 2018). In this context, the hazard impacts are assessed for each hotspot and then further inter-compared from a regional perspective. The simple empirical models that were used in Phase 1 are replaced by more sophisticated modelling

techniques that can accommodate localised conditions e.g. sBTM is replaced by localised HDm (Viavattene et al. 2018).

While many risk assessment frameworks exist (e.g. Elrick & Travers 2009; Rollason, Fisk & Haines 2010; Sharples, Attwater & Carley 2008; South Africa 2005 amongst others), risk mapping highlights the importance of the spatial aspects of risk assessments and subsequently the importance of having spatially explicit information (van Westen & Greiving 2017). GIS has therefore been identified as an important tool in analysing risk (van Westen & Greiving 2017).

## **2.2 ASSESSING COASTAL INUNDATION HAZARD RISK**

Hazard data are often the most difficult to acquire or generate as different modelling approaches are applicable to different hazards e.g. erosion, inundation etc. and therefore it is important that hazard scenarios are well defined (van Westen & Greiving 2017).

The European Union (EU) Directive 2007/60/CE regarding the assessment and risk management of floods, known as the “EU Flood Directive”, states that each member of the EU must:

- i. assess the flooding risk level;
- ii. create risk charts; and
- iii. take adequate measures in order to mitigate the risk where needed.

This directive is explicitly applicable to coastal and estuarine areas (Marujo-Silva 2011). Subsequently, the Horizon 2020 EU research framework is investing substantially in improving the understanding of risk posed to the European population and economy by climate-induced hazards (Perini et al. 2016).

An inundation assessment usually comprises two primary components, namely the assessment of extreme waters levels and inundation modelling and mapping (The State of Queensland 2013). The latter can be approached in various ways, the most common being the geospatial (GIS) based assessment and the lesser used HDm approach. Both are explained in more detail in the following section.

The objective of conducting an inundation assessment is to determine the extent and severity of a potential inundation scenario (e.g. storm surge) for a defined area. It should be noted however, that to date, there is no standardized scale available to categorise flooding and/or inundation severity. In general, floods are qualitatively assessed as ‘minor, moderate or major’. The United States’ Federal

Emergency Management Agency (FEMA) (2016) however, provides guidance for mapping and analysing “shallow” flooding, which is defined as “an average depth limited to 3.0 feet or less where no defined channel exists.” (FEMA 2016: 1).

The reliability of inundation models greatly relies on the vertical accuracy and precision of the digital elevation model which forms a key input dataset in this process (Gesch 2009). Subsequently, LiDAR technology has become a popular and precise means of obtaining accurate high resolution surface data. LiDAR is a remote sensing technology that uses a pulsed laser to measure variable distances (ranges) to the surface. Based on the information derived from the light pulses’ return, precise, three-dimensional information regarding the Earth’s surface characteristics can be derived (NOAA 2012). The level of accuracy achieved by LiDAR technology provides the means to most confident identification of low-lying regions susceptible to sea level rise inundation, storm surge or tsunamis. International literature suggests that LiDAR, often coupled with passive optical imaging, is being used in a variety of coastal scientific studies assessing for instance landslides along sea cliffs, subsidence causing coastal land loss and the topographic monitoring of active volcanoes in continental margins (Brock & Purkis 2009).

Currently in South Africa the acquisition of LiDAR data is still expensive, thus repetition is low and bathymetric LiDAR is unavailable. Lück-Vogel, Macon & Williams (2018) provide guidance on coastal LiDAR acquisition in the South African context, outlining the preferred specifications that will allow for the data to be used in multiple contexts. It is expected that in the near future, LiDAR and high-resolution stereo imagery acquisition using Unmanned Aerial Vehicles (UAVs) will present a potential solution for cheaper, quick, small scale topographic data generation for coastal inundation hazard risk assessments.

### **2.2.1 Models: To Predict or to Explain/Understand?**

*...it becomes pertinent to investigate the possibilities of predictive procedures autonomous of those used for explanation*

(Helmer & Rescher 1959: 33)

Models are simplified versions of reality (Neumann & Ahrendt 2013). The advantage of environmental modelling is a numerically precise hypothesis that can be quantified and evaluated, allowing for observations to be explained and forecasts to be made (Neumann & Ahrendt 2013). They allow for the quantification of results, comparisons between alternative theories, describe effects of complex factors (e.g. random variable input) and explain how underlying processes contribute to the observed results. Furthermore they allow for the extrapolation of results to other situations such as



predicting future events and ultimately translate science into more self-explanatory formats e.g. graphic visualisation (Neumann & Ahrendt 2013).

In the coastal context, there are two primary techniques for determining coastal inundation, namely using GIS based sBTM or HDm. The GIS based sBTM is arguably the most commonly used model to depict inundation (Ajai 2012; Desai et al. 1991; Eckert et al. 2012; Frazier et al. 2010; Kleinosky, Yarnal & Fisher 2007; Navalgund et al. 1998; Nayak 1996; Nayak, Sarangai & Rajawat 2001; Rajawat et al. 2005; Rajawat & Nayak 2000; Rajawat & Nayak 2004). The method excludes other physical processes such as wind push and can be described as an **explanatory model** (Shmueli 2010). An explanatory model aims to test causal hypotheses against a theoretical construct, here for instance, the potential amount of land lost based on varying sea level rise scenarios (Shmueli 2010).

Conversely, HDms enforce the laws of physics and consider multiple parameters which are used to generate various scenarios describing the flow of water (Woodruff, Vitro & BenDor 2018). HDm therefore predicts the outcome of a single event based on multiple parameters and is therefore called **predictive modelling** (Shmueli 2010). Parameters include factors that could influence flow direction and velocity such as wind speed and direction, bottom friction, barriers and tides (Woodruff, Vitro & BenDor 2018). One of the main challenges of HDm is selecting representative storm conditions as changes to the input conditions will affect the results (Corbella & Stretch 2012; Salecker et al. 2011; Villatoro et al. 2014, cited in Perini et al. 2016). Another challenge is the requirement of specialised software, powerful computers and expert knowledge to set up and run these models.

Shmueli (2010) summarises that explanatory modelling focusses on minimising bias, with the goal of obtaining the most accurate representation of the underlying theory i.e. quantifying the causal effect to obtain the 'average' record. However, predictive modelling aims to minimise the combination of bias and estimation variation, which also occasionally sacrifices theoretical accuracy for improved empirical precision i.e. to predict new individual observations (Shmueli 2010).

Nock (2014) identified that there is currently a general inability to integrate GIS and numerical modelling as numerical modelling primarily exists in complex programming languages and formats and algorithms to convert between numerical models and GIS formats are not commonly available yet. This poses a great challenge as it restricts the ability to exchange model predictions. While the existing GIS based approach largely results in an sBTM model being utilised, the multiple available numerical models do not conform to a structured methodology to predict coastal inundation. Furthermore, there is a growing demand for systems with the purpose of communicating coastal inundation model outputs to non-technical end users (Nock 2014).



### 2.2.1.1 Examples of HDm applications

In contrast to geospatial approaches, hydrodynamic modelling is a more specialized field, more applicable in the engineering contexts. Hydrodynamic models are powerful tools used to calculate the wave climate and most commonly used in ocean and coastal engineering projects such as designing ports and coastal structures, construction and management of offshore structures and naval operations (Thomas & Dwarakish 2015).

Earlier numerical wave prediction models used coarse grids that were suitable for deep water regions, while modelling coastal regions required higher resolution grids due to the varying bathymetry, resulting in the development of improved models such as the third generation numerical model MIKE21 and the third generation spectral wave model Simulating Waves Nearshore (SWAN) (Thomas & Dwarakish 2015).

The application of numerical wave modelling extends beyond coastal engineering with its realized potential as a risk reduction tool particularly in storm and cyclone prone areas. In India, wave forecasting is conducted by the Indian National Centre for Ocean Information Service (INCOIS) which uses the MIKE21 model for operational forecasting and the ability to inform communities by issuing early storm warning. This approach drastically reduced the number of casualties in 2013, when cyclone Thane impacted the Indian coastline (Balakrishnan Nair et al. 2013).

Research pertaining to renewable energy is also benefitting from the potential of numerical wave models and their ability to calculate wave energy potential. A South African study used the SWAN model to identify the spatial distribution of wave power off South Africa's most energetic coasts (Joubert & van Niekerk 2013).

Wave model accuracy has also become an area of interest to researchers, particularly regarding the inclusion of wind data as wind induced waves are amongst the most important topics in ocean and coastal engineering. Strauss, Mirferendesk & Tomlinson (2007) compared the MIKE21 and SWAN models and found that the outputs produced by SWAN are more sensitive to the inclusion of wind data, while the inclusion of wind data in MIKE21 increases the simulation period. Overall, the inclusion of wind data in both models resulted in an overestimation of wave attenuation. Sharifi, Ezam & Karami Khaniki (2012) compared MIKE21 with WAVEWATCH III, with the outputs of both models further compared with available satellite altimeter measurements of significant wave heights. The results showed that WAVEWATCH III produced more reliable results predicting wave characteristics in deep water, while in shallow water MIKE21's results were more consistent with the

measurements taken from the altimeter. A major limitation in this study was the level of accuracy of the wind data and therefore inaccuracies in the wind data led to inaccuracies in the model outputs.

Numerical wave models are powerful tools for calculating wave climate and assists in overcoming the challenges of predicting waves (Thomas & Dwarakish 2015). However, HDm has a high computational cost. In many instances, this is resolved by reducing the Digital Elevation Model (DEM) resolution and subsequently reducing the accuracy of the model outputs (Gesch 2009; Perini et al. 2016).

#### 2.2.1.2 GIS based tools and data models

While the sBTM is not provided in the form of a tool, this simple GIS based approach is widely used and accepted (Ajai 2012; Brundrit 2009; Fitchett et al. 2016; Rodriguez 2010, amongst others). In the sBTM approach, all areas occurring below a specified height are being classified as “flooded”. This method simply raises the water surface or performs linear supposition by delineating a contour based on the selected ‘water raising’ value, like a bathtub or single value water surface (NOAA 2012). More recently, the applicability of the sBTM has been criticised due to its inability to incorporate the effects of wind and wave characteristics (Didier et al. 2015). The sBTM does not take bottom composition and friction etc. into account either, however this has not discouraged its use. Further, the common use of a DTM (instead of a DSM) as key input data layer has resulted in criticism of the sBTM’s poor predictive power (Gallien, Sanders & Flick 2014; Poulter & Halpin 2008). Attempts have been made at refining the method to address topographical uncertainties by reclassifying DEMs to the scenario heights (Klein & Nicholls 1999; Neumann & Ahrendt 2013; Rodriguez 2010) as well as implementing additional parameters such as friction (Li, Grady & Peterson 2014) and beach slope (Perini et al. 2016).

The Hydrological Engineering Centre of the US Army Corps of Engineers produced the River Analysis System (HEC-RAS<sup>2</sup>) which performs 1D and 2D hydraulic calculations for natural and constructed channels (US Army Corps of Engineers 2018). While HEC-GeoRAS was developed in conjunction with ESRI as a plugin to import and export products between HEC-RAS and ArcMap’s GIS environment (Els 2011), it is a tool applicable to river systems rather than coastal applications.

---

<sup>2</sup> <http://www.hec.usace.army.mil/software/hec-ras/>

ArcHydro<sup>3</sup> operates in ESRI's ArcGIS environment, comprising of a set of data models and tools to delineate and characterise watersheds (ESRI 2018). Similar to HEC-RAS, this tool is applicable to river systems rather than coastal applications.

The ArcGIS ArcMarine Data Model<sup>4</sup> is a community driven initiative to improve the integration of ocean data in a geodatabase, considering the need for 3D space and time components. Currently the data model is limited to 2.5D, but includes 'placeholders' which are intended to represent the fluidity of ocean data and processes (Nock 2014). While the data model has been developed to be primarily incorporated into ArcGIS version 9, there are some newer versions available for use in ArcGIS 10 and extensive examples of the model being applied in MIKE Marine GIS (Nock 2014). The application of the data model has allowed calculations of wave climate, transfer of wave climate from the offshore to the nearshore and to view waves from a 2D model. However, the model does not allow for the generation of inland coastal inundation extents (Nock 2014).

Given the limitation of the ArcMarine Data Model excluding coastal inundation, Nock (2014) developed the ArcFLOOD Data Model which allows for improved analysis, assessment and mitigation of potential coastal inundation risk. The rationale for developing the data model was the distinct lack of GIS data modelling for coastal inundation. The schema developed was an extension of the ArcMarine Data Model to include coastal inundation and thereby provided the linkage between numerical flood modelling, flood risk assessment and information technology. Nock (2014) utilised XBeach as the model to propagate coastal inundation and reprogrammed the open source environment for the outputs to be exchanged with GIS systems. Essentially the data model still requires the user to be competent with numerical modelling as it is only the outputs that are further analysed in a GIS environment.

Despite its limitations, sBTM, or derivatives thereof, is widely used in the international context, providing online interactive tools for users to "drown their town" by implementing varying levels of static sea level rise. On inspection of the tools, efforts have been made to remove the system's inherent false-positive flood results in low-lying areas that are not hydrologically connected to the coast. All tools state that a LiDAR derived elevation model is utilised where available. In addition, each

---

<sup>3</sup> <http://resources.arcgis.com/en/communities/hydro/01vn0000000s000000.htm>

<sup>4</sup> <https://dusk.geo.orst.edu/djl/arcgis/>

interactive viewer bears a disclaimer regarding its use and exempting the creator from liability. Examples of interactive viewers are listed in Table 2.4.

Table 2.4 Examples of interactive flood hazard tools

Country / Region	Tool	Link
South Africa	OCIMS Coastal Flood Hazard Decision Support Tool	<a href="https://www.ocims.gov.za/coastal-flood-hazard/">https://www.ocims.gov.za/coastal-flood-hazard/</a>
Australia	Coastal Risk Viewer	<a href="http://www.coastalrisk.com.au/">http://www.coastalrisk.com.au /</a>
United States of America	NOAA Sea Level Rise Viewer	<a href="https://coast.noaa.gov/slr/">https://coast.noaa.gov/slr/</a>
	NOAA Coastal Flood Exposure Mapper	<a href="https://www.coast.noaa.gov/floodexposure/#/map">https://www.coast.noaa.gov/floodexposure/#/map</a>
Global Maps	Climate Central's Global Maps	<a href="http://choices.climatecentral.org">http://choices.climatecentral.org</a>

### 2.2.1.3 Geospatial Multi-Criteria Approaches for Assessing Inundation Hazard

GIS and remote sensing techniques have been widely used in understanding coastal processes and mitigating coastal zone hazards (Ajai 2012; Desai et al. 1991; Hsu et al. 2017; Navalgund et al. 1998; Nayak 1996; Nayak, Sarangai & Rajawat 2001; Perini et al. 2016; Rajawat et al. 2005; Rajawat & Nayak 2000; Rajawat & Nayak 2004; Rodriguez 2010, amongst others). The benefit of using GIS and remote sensing is that they are fairly accessible analysis tools. The visual results/products are also able to be more effectively communicated to the broader public (Graham et al. 2011).

Hammar-Klose & Thieler (2001) utilized a simple classification considering tidal range, wave height, coastal slope, shoreline erosion rates, geomorphology and historical rates of relative sea level rise. The method combines the coastal system's susceptibility to change with its natural ability to adapt to changing environmental conditions, resulting in a relative measure of the system's natural vulnerability to the effects of sea level rise (Klein & Nicholls 1999). The input data were utilised in their original state and horizontal resolution, which was then sampled to a 3-minute grid cell. A dataset for each risk variable is then linked to each grid point. The resultant coastal vulnerability index (CVI) allows the variable to be related in a quantifiable manner that expresses the relative coastal vulnerability to physical changes as a result of sea level rise (Hammar-Klose & Thieler 2001). A limitation of this study is that the CVI values apply specifically to the U.S. Pacific coast, U.S. Atlantic coast and the Gulf of Mexico coast and the results are not directly comparable between the different coastal segments. Additional data from other studies were also incorporated, thus the values used in the CVI only reflect the relative vulnerability along each respective coast.

The study conducted by Ajai (2012) focused on a more holistic approach that considered sea level rise, coastal elevations, shoreline changes and historic flooding in order to predict the areas likely to be affected by future flooding events on selected study sites in Dahej, Paradip and Nellore in India. While Hammar-Klose & Thieler (2001) concluded their study by using GIS to create a spatial

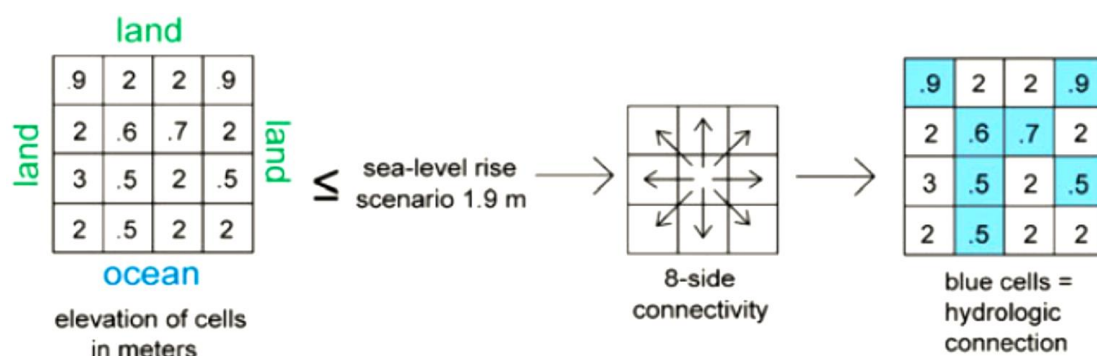
visualization of their results, Ajai (2012) conducted a coastal hazard assessment for India's 7500 km coastline based on individual coastal characteristic and flooding events, where the physical response of coastal environments to water level and shoreline changes over a times series was analysed using GIS. The study included sensitive ecosystems such as beaches, mudflats, mangroves, coastal reefs, wetlands etc., as well as areas of high population densities, which pose a major concern in relation to coastal processes and climate change. The anticipated sea level rise of 0.48 – 1.0 m by 2100 was used based on international acceptance (Ajai 2012). The final vulnerability line was demarcated using GIS by taking the union of the shore displacement line and the flood line (whichever is the most landward). The benefit of this method is that it incorporates the coastal response to the change in flood height with time (Ajai 2012). However, the Water Layer tool used to produce the inundation results is no different to the commonly used sBTM.

Rodriguez (2010) attempted to refine the sBTM by reclassifying a Shuttle Radar Topography Mission (SRTM) DEM to the sea level rise scenario height similar to the methodology employed by Klein & Nicholls (1999), however providing much more detail. The methodology uses a global climate change sea level rise estimation of 0.6 m by 2100.

More recent refinements of the sBTM, improving on its applicability to coastal areas were published by Li, Grady & Peterson (2014) and Perini et al. (2016). Li, Grady & Peterson (2014) developed a model in ESRI's ArcGIS Model Builder to determine inundation based on sea level rise (i.e. permanent inundation), using the Cost-Distance<sup>5</sup> tool in the Spatial Analyst toolbox to instil the hydrological connectivity to the coast. Other studies (Cooper et al. 2013; Gesch 2009; Henman & Poulter 2008; Marcy et al. 2011; Poulter & Halpin 2008) utilised the 8-sided approach (Figure 2.2) to instil hydrological connectivity directly in the LiDAR based raster layer, where only adjacent grid cells with an elevation less than the input sea level rise scenario are identified as hydrologically connected (and prone to flooding).

---

<sup>5</sup> <http://desktop.arcgis.com/en/arcmap/10.3/tools/spatial-analyst-toolbox/cost-distance.htm>



Source: Cooper et al. (2013: 555)

Figure 2.2 Eight-Sided Flood Simulation Approach

Li, Grady & Peterson (2014) used two raster layers, one representing the ocean (or the source) and another representing the land, or what they refer to as the 'friction surface'. The friction surface was essentially a DEM where a value of 1 was assigned to cells occurring below or equal to the specified sea level height (inundation height), as per the sBTM method. The cost-distance was then applied to only reflect the cells where the elevation was less than the specified inundation height. The final output is a raster where only the cells that are hydrologically connected to the coast are represented (Li, Grady & Peterson 2014).

Similar to the work undertaken by Li, Grady & Peterson (2014), Perini et al. (2016) developed an improved method, also utilising ESRI's Cost-Distance tool to incorporate hydrological connectivity to the coast, but also incorporating the beach slope into a model that can be applied in the regional context. The input surface was a LiDAR derived 2 m resolution DTM. The model was compiled in ESRI's ArcGIS Model Builder. The output binary raster grid comprised of water pathways indicating paths that either avoided or favoured inland water movement, rather than paths defined in terms of Euclidean distance (Sekovski et al. 2015). In addition, a cotangent of 0.002 was introduced to provide the representative land slope which the water would travel along in order to result in inundation. The static cotangent value is specific to the study site and was also accommodated in the model using the raster calculator (Perini et al. 2016). The resulting model outputs were shown to improve on those obtained from the basic sBTM, despite the noted limitations of excluding other physical processes/components. A secondary success is that the model offers a good trade-off between the sBTM and HDm, as it eliminates overestimation of the former and unlike HDm, it can be implemented over a large area at a meaningful resolution using relatively limited computational power (Perini et al. 2016).

Considering the work conducted by both Li, Grady & Peterson (2014) and Perini et al. (2016), Hejazi, Ghavami & Aslani (2017) concluded through an additional study that the effect of roughness (described by Li, Grady & Peterson (2014) as the friction surface) depends on both roughness and

the beach slope. The wave runup over a rough slope caused a reduction in runup height when compared to the runup on smooth slopes (Hejazi, Ghavami & Aslani 2017). The effect of roughness also increased as the beach slope became more gradual (Hejazi, Ghavami & Aslani 2017).

In the South African context, the sBTM is more commonly used. Fitchett et al. (2016) focused on the impact of sea level rise and climate change on the tourism sector in Cape St. Francis and St. Francis Bay in the Eastern Cape, South Africa. Their geospatial analysis made use of the sBTM, based on and the freely available ASTER Global DEM with a 90 m resolution, noting that it does not take wind, tides or waves into account. The raster calculator available in ESRI's ArcGIS software was used to calculate the area affected by the projected sea level rise for the years 2050 and 2100, using the projected sea level rise scenarios of 0.4 m and 1.6 m respectively (Fitchett, Grant & Hoogendoorn 2016).

The study revealed that with static sea level rise, there would be a considerable reduction in beach area as well as an impact on infrastructure in low lying areas. The impact on infrastructure will be exacerbated in the event of a storm surge, which would further threaten tourism opportunities which were already impacted by severe storm surges that occurred in 1996 and 2007 (Fitchett, Grant & Hoogendoorn 2016). The authors acknowledged that due to the limitations of the sBTM and the coarse resolution of the DEM, the analysis likely underestimated the flooding potential of the region.

A more intricate example of using the sBTM exists for the City of Cape Town (CCT) which conducted a series of studies in 2008 to 2009 (Brundrit 2009; Cartwright, Brundrit & Fairhurst 2008b), focusing on the impact of Global Climate Change in the context of a sea level rise risk assessment through the development of a GIS based inundation model. The information gathered through this study was intended to inform future planning, preparedness and risk mitigation (Brundrit 2009).

More recently, South Africa's national Department of Environmental Affairs (DEA) has embarked on undertaking a National Coastal Assessment (NCA) which commenced in 2017, recognising the need for locally relevant data. Flooding and erosion were the only physical hazards addressed in the study which also excluded climate change considerations. The parameters used to determine flood hazard risk were limited to the elevation above sea level and the distance to the coast, with both indices being rated on a 1 – 5 scale (CSIR 2018). A flood hazard index was generated as the average between the elevation risk and distance risk to the coast (CSIR 2018). Subsequently in February 2019 the project was extended to include climate change scenarios, however no results were available in



time to include in this review. The NCA identifies the number and type of buildings at risk to flooding (and other hazards), based on point locations of buildings, but not the vulnerability of these buildings.

The methodologies discussed illustrate the potential for risk management through the advancement of technology and the integration of information i.e. GIS and Remote Sensing combined with other datasets (Haq et al. 2012). However, the availability of more accurate data (e.g. LiDAR) and advanced (spatial) analysis tools, will contribute significantly to the advancement in flood modelling methodologies.

#### 2.2.1.4 Comparative Studies

As indicated in the sections above, HDm and sBTM both have their advantages and disadvantages. The HDm, depending on the amount and quality of physical input parameters used, probably displays flood behaviour more realistically. However, it is based on specific user defined scenarios and is computationally intense and requires expert knowledge for the model set-up and executing. The sBTM in contrast, is easier, quicker and can be executed by average GIS operators. In order to quantify the actual differences in performance, Neumann & Ahrendt (2013) conducted a comparative study between the sBTM and HDm.

They used a storm named Daisy as the basic hydro-meteorological event, representing a common storm with average storm wind velocities and water level heights, for the south western Baltic area. The following scenarios were considered:

- i. Daisy as a stand-alone event with a maximum water level of 1.21 m;
- ii. Daisy + 0.33 m as the lowest predicted sea level rise for the Baltic; and
- iii. Daisy + 1.25 m as the highest predicted sea level rise for the Baltic.

The sBTM assumed that the complete area under a certain level would be inundated, which was further corrected for hydrological connectivity. The HDm considered three components, namely the DEM, input data and the physics, which calculated the behaviour of the DEM and input data relative to each other (Neumann & Ahrendt 2013). The results of the comparison demonstrated that when no sea level rise is considered, there is a tolerable fit between both models, however at higher water levels, the sBTM distinctly overestimates the level of inundation compared to the Mike21 HDm used in the study (Neumann & Ahrendt 2013).

Similarly, Gallien, Sanders & Flick (2014) tested the static sBTM method compared to HDm modelling based on a storm that occurred in 2011 causing inundation by overtopping coastal barriers



in Newport Beach, California. The sBTM was run twice, using the tide elevation and wave height respectively, however neither was successful in predicting the experienced inundation. Considering that the inundation was incurred due to the overtopping of coastal barriers, the HDm produced significantly improved results. Overtopping as a direct consequence of compounding was driven by strong winds.

Gallien, Sanders & Flick (2014) concluded that the choice between static (sBTM) and HDm models largely depends on the project goals. Static methods are useful to communicate risk and raise awareness. They also adequately demonstrate impacts of rising sea levels under normal weather conditions. HDm methods are useful for predicting episodic events such as storm surge scenarios or wave overtopping. Users are cautioned that while HDm considers other input parameters, they must be carefully defined as they all affect the model outputs.

The message conveyed by Gallien, Sanders & Flick (2014) is echoed by the interviews with technical experts (further discussed in Section 4.1) in that both sBTM and HDm are useful and serve their respective purposes. An example was provided related to remodelling a big storm that occurred in August 2008, to determine the effectiveness of a sea wall using HDm. The HDm used different parameters and all outputs suggested that the sea wall was high enough to prevent an inundation event. However, during the storm, the compounding waves and high wind speeds resulted in overtopping and subsequent inundation. In this real life scenario, the sBTM was useful as it revealed areas where the water was likely to pool as the topography created a situation whereby water flowed inland (Figure 2.3).

A



B



Source: A) Jacaranda FM (2017); B) Visual Buzz SA (2017)

Figure 2.3 A) Waves overtopping the sea wall along the Sea Point Promenade, Cape Town; B) Inundation incurred more than 60 m inland during the August 2008 storm event

The differences between GIS based sBTM and HDm approaches are summarised in Table 2.5:

Table 2.5 Bathtub Model vs. Hydrodynamic model

Considerations	GIS based BTM	Hydrodynamic modelling
Data inputs	Only requires topography data	Requires a variety of datasets to introduce physical tidal and atmospheric forcing
Planning application	Generalised, based on static, user defined water levels	Scenario based, taking user defined physical processes and factors into account
Physical processes	Not taken into account	Are taken into account to construct the scenario. User defined. Includes wind speed and direction, tidal constituents, water density, bottom roughness etc.
Grids	Input datasets are raster grids with defined and consistent resolutions, usually DEMs or DSMs	Grids user defined, normally starting with a coarse resolution in the offshore areas, decreasing as it approaches the coast to accommodate localised coastal behaviour
Defining the study site	Can be undertaken over a large area i.e. wherever topography data is available	Grids need to be created to define the study area
Model calibration	Not required	Required
Computational requirements	Does not require high computing power	Computationally expensive
Computational time	Relatively fast to process and produce results	Highly dependent on the grid resolution and data inputs
Outputs	Static	Dynamic time series, whereby time slices can be exported
Broad considerations for users	Understanding that external forcing e.g. tidal and atmospheric are not taken into account	The parameters need to suit the research question e.g. if the aim is to model coastal inundation based on a storm surge then ideally representative storm event parameters most closely associated with the study site should be used

### 2.2.1.5 Hybrid Approaches

Hybrid approaches make use of two or more models to determine the impacts of natural hazards, which may produce improved results when compared to a single model (Nandi et al. 2016; Tehrany, Pradhan & Jebur 2014). Currently, while there are many successful models that have been applied in the terrestrial flooding context e.g. univariate models (Sivakumar 2001), multivariate models (Rozos, Bathrellos & Skillodimou 2010, cited in Nandi et al. 2016) and artificial neural networks (Kia et al. 2011, cited in Nandi et al. 2016), only a few approaches and examples exist in terms of coastal applications.

In order to develop a localised coastal inundation mapping approach, Didier et al. (2015) utilized a wave runup empirical model, validated against field surveys that took place during and immediately after the storm that occurred on 6 December 2010 in Maria (Quebec, Canada). The inundation limits were identified using the assumption that the inundation resulted from a combination of astronomical tide, storm surge and wave runup. Wave runup was estimated using the formula proposed by Stockdon et al. (2007) which also required a beach morphology assessment. The assessment was conducted using a mobile terrestrial LiDAR system and the cross-shore profiles generated in ESRI's ArcMap (Didier et al. 2015). In addition, relative sea level rise resulting from regional glacio-isostatic adjustment and eustatic contributions were included in the study to account for future coastal

inundation levels. The sea level rise trend was obtained using linear regression in line with previous work conducted by Boon (2012).

Using these integrated approaches, the modelled results largely concur with the post-storm field measurements, despite the empirical model not accounting for physical processes occurring in the surf zone or the time varying beach morphology (Didier et al. 2015). This supported the notion that using extreme water levels alone, as often done when mapping potential coastal inundation, is insufficient.

### 2.3 ASSESSING VULNERABILITY

*Unlike in maths and physics where elements are explicitly defined, for example, force is the product of mass and acceleration, where we can measure each one of those elements and they have a standardised unit of measurement, vulnerability is more complex. There are no standardised units nor is there one single accepted formula, never mind having a singular definition. The concept of vulnerability extends to different scales such as the vulnerability of an individual compared to the vulnerability of a community. Quantifying vulnerability therefore needs to occur through consultation and agreement.*

(Villagrán de León 2016, Pers com)

Vulnerability can be assessed using two primary approaches, namely understanding the vulnerability of a system to adverse effects, and human ecology which considers who is vulnerable and why (Füssel 2005, cited in Armaş & Gavriş 2013). It involves the systemization and evaluation of households, livelihoods, a group of people, community, province, country, sector or a system in relation to different types of hazards (Villagrán de León 2006).

Assessing vulnerability requires reliable information regarding the population and assets exposed to the hazard in question, including the distribution of people, location and function of critical infrastructures and the location and types of buildings (Aitsi-Selmi et al. 2016; Strunz et al. 2011). Once vulnerabilities have been systemized and evaluated, mechanisms can be put in place to reduce these vulnerabilities and minimize impacts (Villagrán de León 2006).

As previously stated, literature reveals many notions of vulnerability, however methods of vulnerability assessment are limited, without any standardisation (Aitsi-Selmi et al. 2016; Villagrán de León 2006). Villagrán de León (2016, Pers com) stated that measuring vulnerability means measuring the estimated potential loss and damage of people and assets from a defined hazard occurrence. This could include injury and loss of life, damage and loss of building and infrastructure, economic loss or environmental loss. While statistical information such as census data (which relate directly to people) are useful, they are normally aggregated to administrative units and do not provide

spatially explicit population distribution descriptions that consider factors such as day occupancy vs. night occupancy (Aitsi-Selmi et al. 2016; Lewis 2019; Strunz et al. 2011). Therefore, the data are not useful in the context of assessing vulnerability associated with the location of buildings, building features and the populations making use of those buildings (Aitsi-Selmi et al. 2016; UNISDR 2016).

Traditionally, vulnerability assessments were undertaken through the analysis of disasters where vulnerable conditions were identified from the losses and damages experienced (Villagrán de León 2006). It was also assessed relative to the overall methodology used e.g. social sciences would undertake a more consultative approach focusing on people and their socio-economic circumstances within society, while emphasizing the value of equity, justice and human rights (Cho & Chang 2017). Conversely, applied physical sciences would focus extensively on the causes and ability to predict hazards, quantifying physical vulnerability in terms of the degree of exposure and the fragility of the exposed element in relation to the hazard (Cho & Chang 2017). More recently however, there has been a growing interest in trying to quantify vulnerability as a planning tool (Adger 2006; Sumaryono 2010; Villagrán de León 2006; Weis et al. 2016; Wisner et al. 2003, amongst others), moving away from checklists of ‘vulnerable groups’ to being more concerned with the ‘vulnerable situations’ that people move into and out of over time (Lewis 2019; Wisner et al. 2003). This further underscores that vulnerability needs to be understood as a comprehensive concept that includes aspects of exposure, sensitivity and adaptive capacity (Cutter et al. 2008, cited in Cho & Chang 2017; Lewis 2019; Polsky, Neff & Yarnal 2007; Weis et al. 2016). Assessing vulnerability thus needs to capture both direct physical impacts (exposure and susceptibility) and indirect impacts (socio-economic fragility and lack of resilience) (Birkmann et al. 2006, cited in Cho & Chang 2017).

Ultimately, the multi-dimensionality of vulnerability makes it difficult to assess, as the definition of vulnerability is still evolving as the understanding of hazards improves. However, the varied approaches have all contributed to a better understanding of the impacts of climate change and provided baseline data for more detailed and precise analyses. In addition, the interdependencies amongst different disciplines such as climate change and disaster management are becoming more evident (Lal et al. 2012; Weis et al. 2016). In particular, flood modelling and mapping has become more widespread and interdisciplinary due to more expert collaborations, assisting planners and decision makers to better understand the complexities by combining spatio-temporal data (Ouma & Tateishi 2014, cited in Cho & Chang 2017).

Physical vulnerability is primarily approached through applied sciences (Cho & Chang 2017). In the context of building vulnerability, structural engineers have been assessing vulnerability through the analysis of building material and construction techniques to inform mechanisms to reduce

vulnerability (Villagrán de León 2006). Other techniques define buildings as ‘elements-at-risk’, with vulnerability indicators relating to their location, use, material and occupancy (e.g. daytime vs. night-time) (van Westen & Greiving 2017). The classification and distribution of buildings is important in both the hazard and vulnerability assessments. For hazard assessments the influence of buildings plays an important role in fine scale analyses, while in vulnerability assessments, the building design, construction materials, height and purpose are all important in identifying the hazard resilience and potential use of the structure for vertical evacuation (Strunz et al. 2011). Papathoma-Köhle et al. (2017) provide an overview of the primary physical vulnerability assessment techniques that are currently utilised (Table 2.6). Assessing the damage resulting from inundation events is an important but insufficiently documented and investigated task (Schwarz & Maiwald 2008). Undoubtedly, building vulnerability assessments are most meaningful when conducted at a local scale and many authors use surveys to develop indices and indicators based on different factors. While there are limitations to these methods, they allow for the identification of specific vulnerable elements, thus providing direct information regarding the state of vulnerability of a process, system or sector (Villagrán de León 2006). Notably, only a few focus specifically on buildings (Sumaryono 2010). Remote sensing techniques, such as those utilised by Strunz et al. (2011) and Sumaryono (2010) are useful as a ‘first estimation’ to identify which structures are highly exposed, however more in depth modelling/analysis or further integration with other methods is required to obtain more insightful results which accommodate the influence of road systems, built infrastructure, existing waterbodies etc. (Birkmann et al. 2006). These spatial technologies (including GIS) are currently being promoted as cost-effective and reliable techniques to improve on existing data collection and assessment processes in the risk assessment context (Aitsi-Selmi et al. 2016; UNISDR 2016).

Table 2.6 Summary of physical vulnerability assessment techniques

Method	Advantages	Shortcomings
Vulnerability matrices	Qualitative method, no need for ex-ante data or detailed information	Results may not be translated into monetary loss. Assessment of damage under specific intensities or process characteristics is objective.
Vulnerability curves	The method is quantitative and may "translate" an event into monetary cost. Vulnerability curves may be used for the assessment of costs for future scenarios.	Important characteristics of the natural process (e.g. velocity, duration, direction etc.) as well as the element at risk (number of floors, construction material) are ignored. Highly-demanding in ex-post information. A large number of affected buildings are required. Vulnerability curves cannot be transferred to areas with different housing types.
Vulnerability indicators	Characteristics of the element at risk are taken into consideration. Results may be the basis for the adoption of local adaptation measures and simple vulnerability reduction actions.	Some indicators consider only the characteristics of buildings and not the potential intensity of the process on the buildings, resulting in a relative vulnerability index. Moreover, the amount and detail of the data required is high, leading to time consuming field surveys since most of the data are not available at the local scale. Last but not least, the results are not expressed in monetary damage making the method less attractive for practitioners.

Source: Papathoma-Köhle et al. (2017: 276)

Currently the most widely used index-based method for assessing building vulnerability to tsunami is the Papathoma Tsunami Vulnerability Assessment (PTVA), originally developed in 2003. Prior to the 2004 Indian Ocean Tsunami, it was the only building vulnerability assessment tool available (Papathoma & Dominey-Howes 2003). The most recent revision to the model resulted in the development of PTVA-4 through consultations with authors of scientific literature from 2005 – 2015 in the field of building vulnerability to tsunamis. The PTVA-4 was compared to its predecessor, PTVA-3, using a cohort of 2000 buildings and hydrodynamic modelling, whereas PTVA-3 used the GIS-based sBTM (Dall’Osso et al. 2016). The results of the comparison showed that the PTVA-4 was more sensitive to variations in the tsunami demand parameter, building attributes and their surroundings. In addition, the extensive consultative process resulted in the PTVA-4 model being applicable in areas where no tsunami vulnerability curves have been developed yet (Dall’Osso et al. 2016).

The PTVA-4 model incorporates many idealized structural attributes in determining the overall building vulnerability, allowing the differences between different buildings to be determined at a fine scale e.g. building A is more/less vulnerable than building B, rather than trying to predict the absolute response a building will have to a given tsunami flow depth (Dall’Osso et al. 2016). The attributes considered for the PTVA-4 model are:

- number of floors;
- building material;
- ground floor hydrodynamics;
- foundation type;
- shape and orientation of the building footprint;
- proximity to movable objects;
- preservation conditions;
- building row;
- presence of sea walls;
- natural barriers;
- wall around the building;
- exposure (water depth at the location of the building); and
- water intrusion.













Voulgaris & Murayama (2014) further expanded on the PTVA-4 by incorporating population demographics, specifically the number of building inhabitants per residential dwelling, while Izquierdo, Fritis & Abad (2018) further validated the model using 2015 post-tsunami data from Chile.

Considering additional vulnerability components, Villagrán de León (2006) developed a procedure to assess four different types of vulnerability relating to the housing sector at a local level, namely: physical/structural, functional, social and economic value. Each type of vulnerability was measured using hazard specific parameters directly related to the type of vulnerability in question i.e. the parameters were rated based on their relevance to each individual hazard. The parameters were also weighted according to importance e.g. the structural integrity of walls played a more important role during an earthquake than the integrity of windows. The benefit of the procedure is that it is applicable to multiple hazards, that it recognizes that certain structures are more important than others rather than having equal weighting and that the assessment is aimed at individual households but can also be aggregated to community, municipal, provincial or national level. At present the approach has been successfully applied in rural communities of Guatemala, focusing on earthquakes, landslides and volcanic eruptions.

Similar to Villagrán de León (2006), Schwarz & Maiwald (2008) tested a systematic procedure for assessing flood damage, based on that developed to analyse the risk of earthquakes. The study aimed to establish a new set of damage functions and to validate the existing GIS-based approach by comparing the predicted building damage with actual observed damage or loss. The study focused on basic components of the flood damage and loss prediction model (taken from Schwarz & Maiwald 2008):

- i. harmonization of damage descriptions and assignment of repeatedly observed effects;
- ii. refining the damage grades;
- iii. correlating flood impact parameters and damage grades;
- iv. defining ranges of vulnerability classes for the predominant building types;
- v. correlating damage grades and inundation levels; and
- vi. correlating damage grades and the specific energy heights.

D <sub>i</sub>	Damage		Description	Drawing	Example
	Structural	Non-structural			
D1	no	slight	only penetration and pollution		
D2	no to slight	moderate	slight cracks in supporting elements impressed doors and windows contamination replacement of extension elements		
D3	moderate	heavy	major cracks and / or deformations in supporting walls and slabs settlements replacement of non supporting elements		
D4	heavy	very heavy	structural collapse of supporting walls, slabs replacement of supporting elements		
D5	very heavy	very heavy	collapse of the building or of major parts of the building demolition of building required		

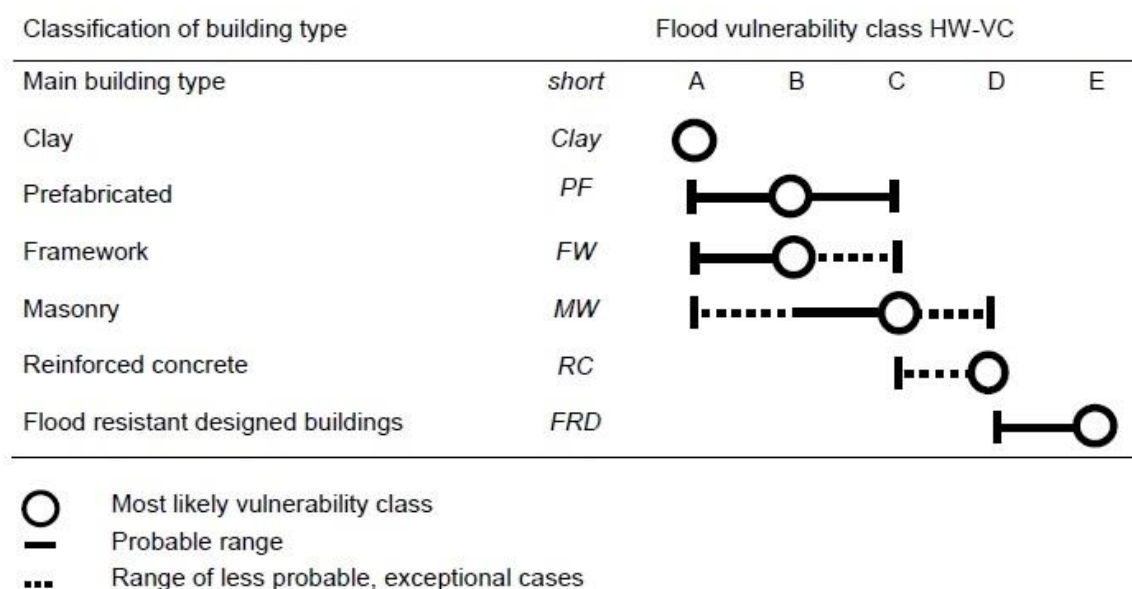
Source: Schwarz & Maiwald (2008: 3)

Figure 2.4 Assessment of damage grades to damage cases

In order to develop a generalized scheme of damage interpretation (as per i and ii above), documented field survey damage assessments were assessed to identify typical damage patterns and the repeatedly observed effects were used as the indicators for the damage grade definitions (Figure 2.4).

Focusing on structural damage resulting from inundation impact (as per iv above), vulnerability classes were determined for the different building material types. In this context, vulnerability was defined as a measure for the resistance of a building against comparable impact conditions. Ultimately, five flood vulnerability classes were identified, decreasing in vulnerability as the categories progressed i.e. a flood vulnerability class 'A' refers to a structure that would be highly vulnerable to an inundation event, while a class 'E' refers to a flood resistant designed building (Figure 2.5). These classifications can be related back to the damage grades defined in Figure 2.4.





Source: Schwarz & Maiwald (2008: 5)

Figure 2.5 Classification of building types into vulnerability classes, including the range of scatter

An additional approach to assessing vulnerability is through the development of indicators and implementing weightings (Papathoma-Köhle et al. 2019). The benefit of this method is that it does not rely on large amounts of empirical data. Applying indicators and weightings is not a standardised approach and therefore allows flexibility and customisation to best suit the relevant area (Viavattene et al. 2018). As such, this method has been repeatedly used for planning and decision making purposes, particularly where data relating to the respective hazards are unavailable (Papathoma-Köhle et al. 2017). The limitation of this method however is due to the fact that because data is limited or in some cases does not exist, it needs to be acquired through extensive fieldwork exercises which may be time consuming (Papathoma-Köhle et al. 2019).

In the broader risk context, elements that are exposed to hazards are not all equally susceptible. In the physical context this implies that elements (such as buildings) may be located adjacent to each other, but differ in terms of their physical vulnerability due to their dimensions, materials, orientation etc. (Papathoma-Köhle et al. 2019). Hence the importance of having well defined indicators to assess the factors contributing to individual vulnerability. A review of 104 studies using indices revealed that most (44) utilised equally weighted indicators, 13 used weights defined by the authors, 19 used participatory methods and 28 used statistical methods for defining weights (Papathoma-Köhle et al. 2019). Papathoma-Köhle et al. (2019) demonstrated that two identical methods using different weighting techniques produced different results and may lead to different mitigation actions. Hence, given its direct impact on decision making, the weighting of indicators should be relevant to the local context.

## 2.4 MEASURING RISKS

*Natural hazards such as earthquakes or tsunamis cannot be controlled, but may be forecasted. However, disaster risk can be reduced by minimising vulnerability or exposure to hazards. The disaster risk reduction is therefore a good example on how science can be utilised for safety of society.*

(Satake 2014: 9)

Risk Assessments are conducted to determine the degree of risk that communities face and subsequently to identify measures needed to reduce the risks. These interventions include structural and non-structural measures aimed at reducing the exposure to the hazard, reducing vulnerability, increasing preparedness and increasing coping capacity (Hettiarachchi et al. 2015). Hahn, Villagrán De León & Hidajat (2003) argue that without undertaking hazard assessments, exposure measures and vulnerability studies, communities will be unaware of their unique vulnerabilities and how they may be affected during a hazard event.

Notably, the 2004 Indian Ocean tsunami has led to a dramatic advancement of tsunami and earthquake sciences, including modelling techniques (Satake 2014). This in turn has improved applications of disaster risk reduction, such as real-time estimations of earthquake and tsunami source parameters and the implementation of early warning systems (Satake 2014). Specifically in those countries that were affected by the 2004 Indian Ocean tsunami, Early Warning Systems were prioritised in order to initiate evacuation protocols (Suppasri et al. 2015). With tsunamis being a special and particularly well documented case of coastal inundation, the following section presents the huge advances for tsunami hazard risk assessments and mitigation in more detail.

### 2.4.1 International Examples of (Tsunami) Hazard Specific Risk Assessments

#### 2.4.1.1 Improved Tsunami risk assessment approaches

The Indian Ocean tsunami of 2004 was one of the biggest tsunamis ever recorded, affecting most Asian countries that bordered the Indian Ocean (Suppasri et al. 2015). The tsunami event was devastating in terms of the high number of fatalities, infrastructure and economic loss and impacted a large area. The media exposure that the event received catalysed international partnerships and studies relating to tsunami hazard modelling, post-tsunami impacts, aspects of recovery, vulnerability studies, awareness campaigns and development and improvements to early warning systems (Burbidge et al. 2008; Dias, Dissanayake & Chandratilake 2006; Dias, Yapa & Peiris 2009; Hettiarachchi et al. 2015; Nanayakkara & Dias 2016, amongst others).

These studies and collaborations culminated in improved approaches to undertaking risk assessments, including integrating the analyses of hazards, vulnerability and preparedness involving either

qualitative or quantitative descriptions of indicators and encompassing social, physical, economic and environmental aspects (Strunz et al. 2011). Specifically, the advancements in technological approaches to hazard assessments are well documented (Borrero et al. 2006; Hettiarachchi et al. 2008; Martínez Sánchez 2015; Sieh et al. 2008; Suppasri et al. 2015).

Subsequent to the 2004 tsunami, Indonesia, Sri Lanka and Oman (amongst other Indian Ocean countries) undertook improved risk assessments in order to prepare for future potential events. GIS and HD proved to be key technologies in generating the final tsunami risk maps.

In both Indonesia and Sri Lanka, the hazard assessment processes focused on the determination of hazard zones and the related probability of being hit by a tsunami. In Indonesia, GIS techniques were used as a first pass approach, using a mapping scale of 1:100 000 to determine where tsunami generated inundation limits were likely to occur based on sBTM techniques, and distance to the coast (Strunz et al. 2011). This was proceeded by HDm to calculate the inland tsunami propagation (Strunz et al. 2011). The numerical models were used to simulate real scenarios, and the impacts on the land were then further analysed. In some cases, the worst case scenario was selected as the basis for the subsequent detailed local level assessment (Borrero et al. 2006; Sieh et al. 2008, cited in Strunz et al. 2011).

In Oman, numerical modelling was used to model various probable and credible scenarios which based on key parameters<sup>6</sup> that could be stored in GIS format to simplify and illustrate the risk to policy decision makers (Martínez Sánchez 2015). In Sri Lanka, only HDm was used and the modelled outputs were compared to field measurements, where available (Hettiarachchi et al. 2008).

The vulnerability assessments undertaken in all countries focused on human and infrastructure dimensions (Martínez Sánchez 2015). In Oman, the human dimensions considered intrinsic local population characteristics that made them more susceptible to the impact of tsunami hazard such as age, disabilities, literacy and total number of exposed persons. The infrastructure dimension primarily assessed the usage of buildings and critical facilities (Martínez Sánchez 2015). In Sri Lanka, the vulnerability assessment was based on consultation with relevant experts and focused separately on structural, economic, human, social, cultural and psychological vulnerability. For improving the GIS database, the structural aspects were captured and subsequently the design guidelines for tsunami

---

<sup>6</sup> Inundation height relative to mean sea level, distribution of inundation levels, velocity of propagating waves, currents, run-up and inundation volume (where applicable).

resilient infrastructure were developed, based on the structural damage assessment (Hettiarachchi et al. 2008).

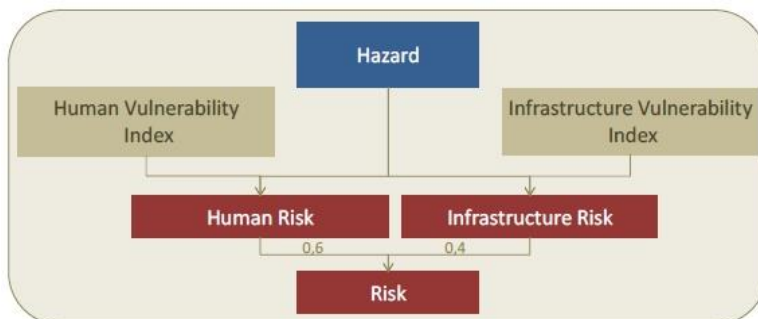
For both Indonesia and Oman, the final risk assessment outputs comprised of maps that reflected the (tsunami) hazard (hazard probability and hazard zones), exposure map (population and critical facilities), response map (evacuation time) and risk map (aggregated tsunami risk) (Martínez Sánchez 2015; Strunz et al. 2011), while the Indonesian risk map was developed by combining the outputs of the hazard and vulnerability assessments by adopting the following equation:

$$\begin{aligned} \text{Risk (probability of loss of life)} \\ &= \text{Hazard (probability of being hit by a tsunami)} \\ &* \text{Vulnerability (probability of reaching safe areas in time)} \end{aligned}$$

Source: Strunz et al. (2011: 74)

Equation 2.1 Assessing tsunami risk

Similarly, the Oman final risk maps were generated by applying factors to both the hazard and vulnerability assessments to calculate risk (Figure 2.6). Maps were produced reflecting the spatial outputs in both hard copy format and as an online interactive map viewing application (Martínez Sánchez 2015).



Source: Martínez Sánchez (2015: 9)

Figure 2.6 Risk Assessment scheme for the coast of Oman

#### 2.4.1.2 Lessons learnt in recovering from the tsunami disaster

In the aftermath of the 2004 Indian Ocean Tsunami, affected countries undertook various approaches to ensure that the potential loss of life was minimised should another event occur. In this context, large amounts of data were generated through collaborative studies and gathered through fieldwork, particularly in the affected areas (e.g. Indonesia, Thailand and Sri Lanka). The common starting point for many areas was scenario modelling, which was used to inform evacuation and mitigation plans. These studies further prompted examining vulnerability at various levels (Wijetunge 2018, Pers com).

A



B



C



D



Source: A – B) A Lewis (2019); C – D) C Lewis (2019)

Figure 2.7 Examples of tsunami warning and evacuation signage, Patong Beach, Thailand

From an academic perspective, there were significant advances in probabilistic hazard modelling techniques, emanating from national and international partnerships, which were catalysed by the lack of technical expertise in the affected regions (Suppasri et al. 2015). However, challenges were identified in implementing recommendations, specifically in the development of policies to create resilient communities through urban planning. In Thailand and the Maldives, whose economies are both centred around (coastal) tourism, there have been no significant changes in terms of land use planning. However, early warning systems, vertical evacuation structures and evacuation signage (Figure 2.7) have been implemented (Suppasri et al. 2015).

#### 2.4.2 The South African Context

In South Africa, the National Disaster Management Framework provides broad guidance on undertaking disaster risk assessments (South Africa 2005). In the Western Cape, the Department of Local Government published a guideline for conducting comprehensive disaster risk assessments (Province of the Western Cape 2012a). This has resulted in a relatively standardised approach (see Province of the Western Cape 2013a; Province of the Western Cape 2013b; Province of the Western Cape 2012b), which is beneficial in terms of understanding the holistic status quo of potential disaster risk in the province. For the Western Cape and Eastern Cape provinces, two primary approaches are used to assess disaster risk, namely an index based approach (relative risk prioritisation; example



provided in Appendix A1.1) and a GIS based approach (example provided in Appendix A1.2), both of which are reflected in the final versions of the respective Disaster Risk Assessment documents.

The relative risk prioritisation process relies on stakeholder engagements requiring the participants to provide a rating for each of the identified hazards based on scoring criteria. In the Western Cape, the individual hazards are assessed independently to produce a hazard rating, vulnerability rating, capacity rating and a relative risk rating per hazard. The final relative risk rating is then categorised into classes i.e. low, moderate, high, and extremely high, and called the ‘Relative Risk Priority’ (i.e. a score relative to the hazard). The components making up each category for the Western Cape disaster risk assessments are as follows:



Source: Williams (2013:10)

Figure 2.8 Risk categories and components

The Eastern Cape approach differs slightly in that consultation is seemingly limited to specialists rather than the public. Their disaster risk assessments also use the available census data as vulnerability indicators (Province of the Eastern Cape 2010). The Nelson Mandela Bay Municipality (NMBM) assesses each vulnerability indicator independently, without achieving an overall vulnerability index (Province of the Eastern Cape 2010). A similar approach is used to determine the hazard factors (Province of the Eastern Cape 2010). This contrasts with the techniques used in the Western Cape where final overall ratings are achieved (Province of the Western Cape 2012b).

The index based process is followed by a GIS based desktop exercise to map hazards, vulnerabilities and capacity (example provided in Appendix A1.2, Figure A.1 A - C). However, only the Western Cape attempts to spatially reflect areas at risk (example provided in Appendix A1.2, Figure A.1 D). For both approaches each category score is equally weighted to calculate the risk score using the following equation:

$$\text{Relative Risk Rating} = \text{Hazard Rating} * \text{Vulnerability Rating} / \text{Capacity Rating}$$

Equation 2.2 Risk equation used for relative risk prioritization in the Western Cape (Source: Province of the Western Cape 2013a; Province of the Western Cape 2013b; Province of the Western Cape 2012b)

The two approaches, namely the relative risk prioritization and the GIS mapping are intended to be complimentary, however there is a clear disconnect (Province of the Eastern Cape 2010; Province of the Western Cape 2013a; Province of the Western Cape 2013b; Province of the Western Cape 2012b). The short-coming of the GIS mapping is that the scale at which data are displayed is inadequate in representing localised hazards such as storm surge. Seemingly, hazards for which there are no GIS data readily available are not mapped, however it is acknowledged that coastal management (risk) lines<sup>7</sup> were produced for the Western Cape in 2017 - although they do not form part of the provincial disaster risk assessments. Conversely, the relative risk prioritisation captures and scores all hazards, regardless as to whether data is available or not and therefore their locations of occurrence are unknown.

While this section focuses on the disaster risk management approach, it is also important to acknowledge that other studies have been undertaken within the Western Cape that focus on sea level rise specifically (e.g. Province of the Western Cape 2010a; Province of the Western Cape 2010b; Province of the Western Cape 2010c).

### **2.4.3 Methods for determining inland flood risk**

Estimating areas at risk to coastal inundation hazard requires that multiple factors are considered. In this context, it is important to consider the work that has been conducted with regards to inland flood modelling as certain aspects can be customised to be applicable to coastal inundation. Recent examples of flood risk assessment methods are summarised in Table 2.7.

---

<sup>7</sup> In terms of the Integrated Coastal Management Act (Act No. 24 of 2008), section 25

Table 2.7 Inland flood assessment techniques

Methodology	Author(s)
A multi-criteria decision analysis algorithm was developed for flood risk assessments in Vietnam. Hazard and vulnerability indicators were defined and used as inputs into the Analytical Hierarchy Process (AHP) to define the indicator weights. Risk was calculated as $Risk = Flood\ Hazard * Flood\ Vulnerability$ .	Dang, Babel & Luong 2011
GIS and remote sensing was used as a hybrid approach to flood modelling in Sri Lanka. Flooding was simulated using hydrologic and hydraulic modelling and census data was used to determine vulnerability. The flood risk was determined using the equation $Risk = Hazard * Vulnerability$ .	Samarasinghea et al. 2010
Rainfall intensity was determined using GIS and the placement of wireless sensor networks. The rainfall intensity was used to determine flood risk.	Ahmad et al. 2013
Statistical analyses have been derived to determine flood related vulnerabilities and fragility relationships. These probabilistic approaches use data obtained from previous events, modelled outputs or hazard severity assumptions to determine flood risk.	Pregolato, Galasso & Parisi 2015
Principal Components Analysis (PCA) and Logistic Regression (LR) was used to determine flood hazard in Jamaica.	Nandi et al. 2016
Supervised classifications were used in China to determine flood risk.	Wang et al. 2015
Random forest decision trees using binary rules (i.e. flooded vs. non-flooded areas) were undertaken using unmanned aerial vehicle imagery.	Feng et al. 2015
GIS based spatial analytics and the inclusion of social factors were used to assess flood risk in Canada.	Armenakis et al. 2017

## 2.5 CONCLUSION

There is no standardised method for assessing risk, and all scoring mechanisms to quantify risk are subjective (Aitsi-Selmi et al. 2016; UNISDR 2016). Various risk assessment frameworks exist (e.g. Elrick & Travers 2009; Rollason, Fisk & Haines 2010; Sharples, Attwater & Carley 2008; South Africa 2005; Viavattene et al. 2018; van Westen 2013, amongst others), but need to be adapted to suit the context of the study area, hence they should be flexible/adaptable. A risk assessment needs to be robust enough to inform decision making processes. While a regional risk assessment may be useful to provide context and identify hotspots (e.g. Sharples, Attwater & Carley 2008; Viavattene et al. 2018), further assessments must be undertaken within these identified hotspots to evaluate the identified hazards at a local scale and consider what could be potentially impacted and how they would be impacted (vulnerabilities).

Considering physical building vulnerability assessments, the building design, construction materials, height and purpose are important parameters in identifying the hazard resilience and assessing the potential of the structure for vertical evacuation (Strunz et al. 2011). While these physical elements are valuable, it is useful to include social aspects regarding the building such as building use, peak occupancy, number of people, children vs. adults vs. elderly people etc. (Aitsi-Selmi et al. 2016; Lewis 2019; Strunz et al. 2011; van Westen & Greiving 2017; Villagrán de León 2018, Pers com). In addition, this would provide context regarding expected losses, whether social and/or economic (Villagrán de León 2006). This highlights the value in considering a cross-disciplinary approach that assesses building vulnerability in the context of both physical and social and economic factors.

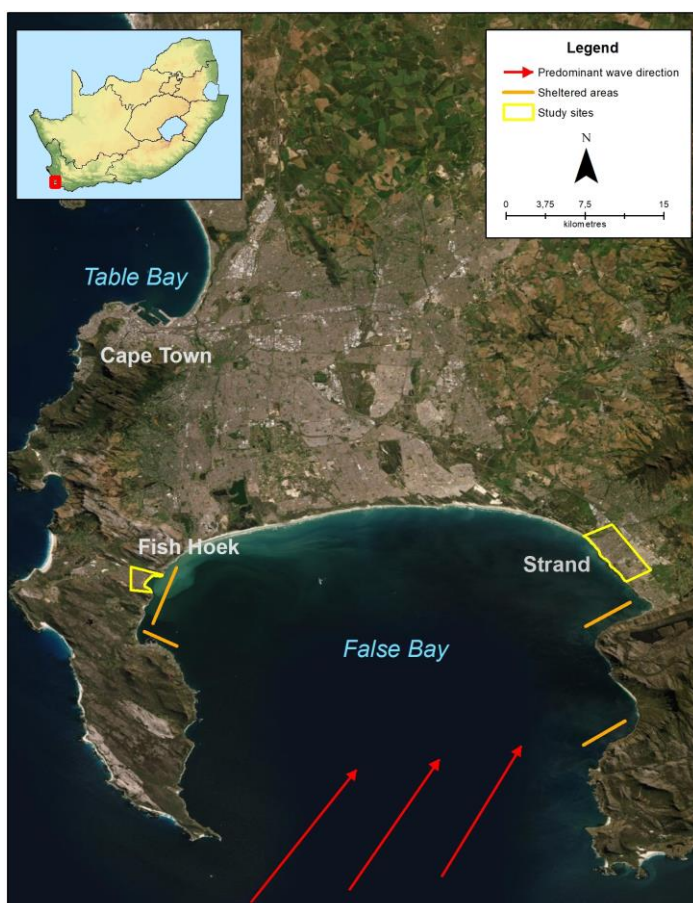


However, this approach would also require ‘vulnerability’ to be clearly defined in the respective contexts to avoid confusion.

### CHAPTER 3: OVERVIEW OF FALSE BAY AND THE STUDY SITES

False Bay is located in the south-western tip of the Western Cape Province in the City of Cape Town (CCT) in South Africa. It is characterised by long sandy beaches with intermittent rocky shores. The northern sandy beaches of False Bay have a gently sloping bottom topography, while the east and west facing coasts have steep sloping contours to cliffs and pocket beaches (Brundrit 2009; Pfaff et al. 2019). Waves enter False Bay from the south-west, resulting in the western shore north of Cape Point (including Fish Hoek) being more sheltered from wave impact, while most other areas (including Strand) are more exposed (Figure 3.1) (Brundrit 2009; Pfaff et al. 2019).

False Bay experiences a Mediterranean climate, with hot, dry summer months (December – February) and cold, rainy winters (June – August). The summer months are characterised by strong south-easterly winds, and winter months are dominated by north-westerly winds. Storm surges frequently occur during the winter months (Pfaff et al. 2019) and, particularly when coupled with spring tides, cause damage to coastal infrastructure and sand movement (Bekko 2018, Pers com).



Source: Adapted from Brundrit (2009: 15)

Figure 3.1 Study site focus areas (yellow) in relation to the City of Cape Town. Predominant wave direction indicated by red arrows and sheltered areas indicated by orange bars

The north-eastern and north-western areas of False Bay are characterised by dense formal urban development, while the northern central area and the steep eastern and western shores are largely undeveloped or show nodes of intense informal development.

The effects of climate change within False Bay can be observed through shoreline regression and damage/loss of coastal infrastructure (Pfaff et al. 2019). Cartwright, Brundrit & Fairhurst (2008a) identify the areas within the CCT vulnerable to sea level rise and an increase in frequency and intensity of storm events as Sea Point Promenade and Woodbridge Island (Milnerton) located on the Atlantic seaboard, as well as Fish Hoek, Strand and Harbour Island (Gordon's Bay) in False Bay. For the purpose of this study, Strand and Fish Hoek were selected as the focus areas, with Strand being located on the eastern shore and Fish Hoek on the west (Figure 3.1). Other factors that influenced the selection of these areas as study sites, are the availability of data, both being located in False Bay and thus being subjected to similar oceanographic and atmospheric conditions and both sites comprising of sandy beaches, dunes and coastal developments. However, they receive different impact from the prevalent south-westerly swell direction.

Climate change studies suggest that the region will experience more intense and frequent storms and increased storm energy (e.g. Brundrit 2009). Hughes (1992) presents a detailed study regarding the impacts of sea level rise on the False Bay coastline, noting that the erosion sustained by a 1 m increase in the sea level accompanied by an increase in storm events will have a detrimental effect to the entire area, with the potential to disrupt lifestyles and livelihoods in developed areas.

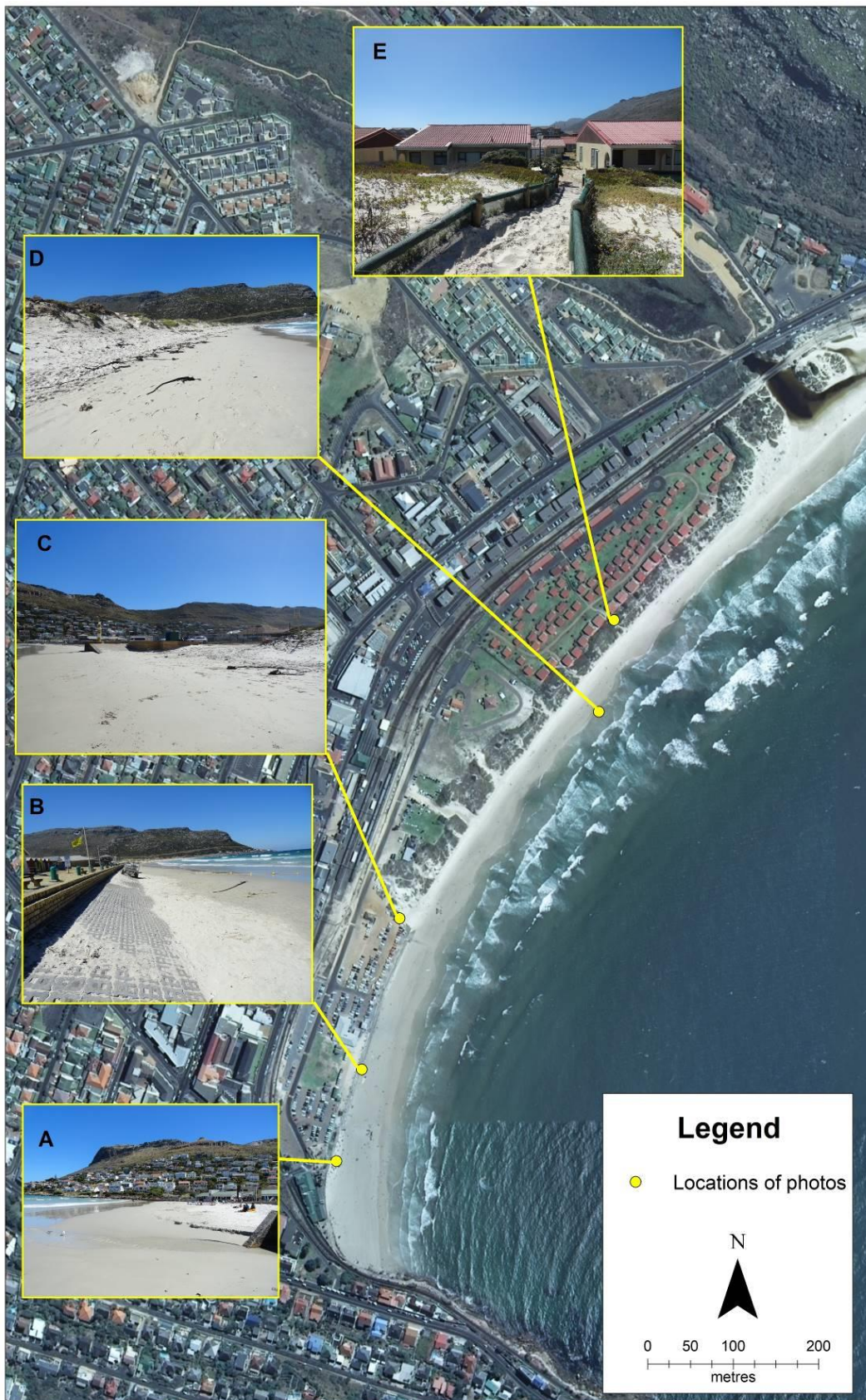
In low-lying areas, such as Strand, 1 m sea level rise will result in a lowering of the beach profile, with the possibility of sandy beach being completely lost in some areas. In Fish Hoek, the loss of beach will be manageable but car parks and adjacent infrastructure may be severely affected. Additionally, the raised groundwater-table resulting from sea level rise is expected to cause serious engineering problems (Hughes 1992).

The greatest impact of these natural events will be felt by developments in close proximity to the coast, thus promoting the need for coastal protection either in the form of managed retreat or adaptive/protective intervention (CCT 2012b). Developments occurring along the coast will increasingly rely on the protection provided by the remaining dunes, failing which alternative protection mechanisms will be required, most likely in the form of hard or soft engineering approaches to reduce the exposure to coastal hazards (CCT 2012a). The following section describe both study sites and experienced damage from coastal hazards in more detail.

### 3.1 FISH HOEK

The study site in Fish Hoek includes the entire area seaward of Main Road, to the beach. The length of the beach is approximately 1.3 km, and the maximum distance from coastal waters inland is approximately 0.26 km. Fish Hoek's beach is approximately 1.3 km long with the Silvermine River mouth demarcating the northern end. The entry point to Fish Hoek Beach is via a railway crossing located in the southern area which is more intensely used for recreation (Figure 3.2 A and Figure 3.4). The back beach extending northwards is highly modified, comprising of a restaurant, parking areas, a lifeguard tower and benches. The more intensely used part of the beach is bordered by a revetment (Figure 3.2 B), which serves to lessen sand movement. A low seawall is located at the top of the revetment, both of which extend northwards and terminate in the central region where the dune system begins. Further north, adjacent to the beginning of the dune, a second parking area also provides a slipway for boat launching (Figure 3.2 C, Figure 3.2 D and Figure 3.3). The Seaside Cottages development is located in the northern beach area behind the existing dune system, with access paths leading from the development through the dunes to the beach (Figure 3.2 E). The development comprises of many single storey structures without any visible flood protection. According to the CCT (2012b), the development occurs seaward of the Coastal Urban Edge and should not have been used for urban development.





Source of A-E: Author (2017)

Figure 3.2 Locality map of Fish Hoek Beach, A: View of restaurant and southern beach area, B: Revetment, C: End of dune and beginning of gravel parking area, D: Dune, E: Seaside cottages





Source: Author (2017)

Figure 3.3 Central beach region



Source: Author (2017)

Figure 3.4 Restaurant and recreational space at the southern end of the beach

The study site is generally low-lying with the majority of the area occurring below 3 m above mean sea level (Figure 3.5). The dune running from the northern to the central region of the study site peaks at approximately 7 m above mean sea level, with most of the dune being approximately 6 m high. The majority of the area behind the dune is low-lying, with elevations not exceeding 3 m above mean sea level. On the seaward side of the dune base, the beach is narrow, measuring less than 25 m in width from the base of the dune to the high water line. The southern part of the beach is less than 1 m above mean sea level. Moving inland, most of the area does not exceed 4 m above mean sea level.



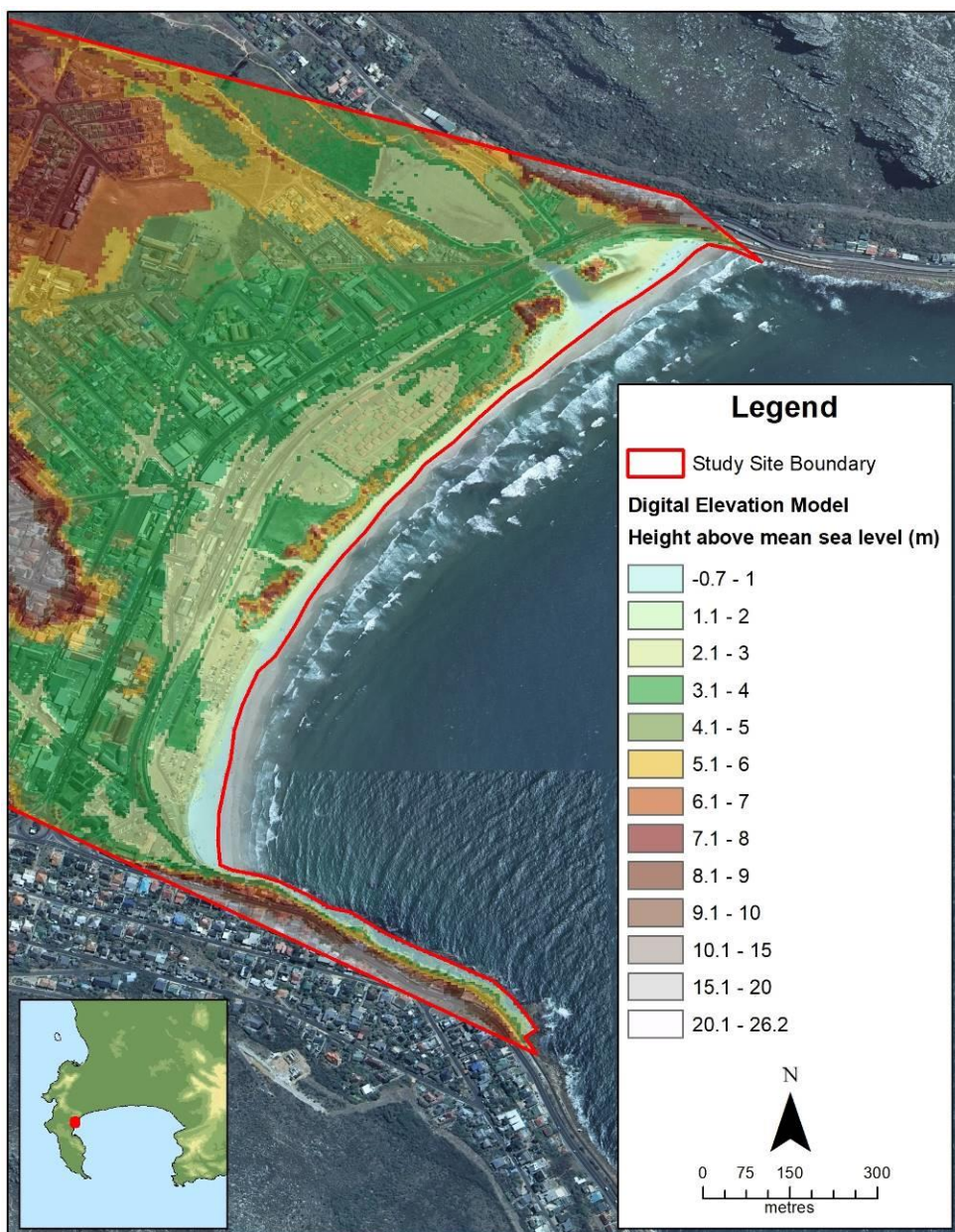


Figure 3.5 LiDAR derived Digital Surface Model (DSM) of the Fish Hoek study site

In terms of previous damages emanating from coastal processes, in 2011 heavy wave action resulted in underscouring of the revetment and erosion of its foundations (Figure 3.6 B, C). A big storm event that occurred on 1 April 2013 resulted in large amounts of kelp being washed up onto the beach (Figure 3.6 D). Later that year (8 September 2013) another storm coupled with a spring tide resulted in the thoroughfare subway being inundated with sea water (Figure 3.6 E). Brundrit (2008) states that previous storms have resulted in disruption of the railway transport system, as well as inundation of Fish Hoek's main road. This is supported by the CCT's GIS based sea level rise assessment (Cartwright, Brundrit & Fairhurst 2008b) and a court case dating back to 1922. The legal application stated that in accordance with a land survey undertaken in 1918, the existing railway line was located below the high water mark and therefore subject to inundation (Fish Hoek Centenary 2018).





Source of A-E: C. Lindeque (various)

Figure 3.6 Damage caused by previous storm events in Fish Hoek

While the area is affected by flooding during spring tides, the primary disruptive coastal hazard is wind-driven sand movement that affects the railway line. It was noticed as early as 1922 that the shoreline had changed specifically due to the attempts to stop sand from encroaching on the railway line and changes in the Silvermine River's water course.



In order to prevent windblown sand from affecting the railway, a palisade of railway sleepers was erected in the late 1920s. By 1970 it was badly degraded due to high tides washing through the rotting wooden sleepers (A). Despite many controversial engagements beginning in 1976, the Fish Hoek Town Council resolved in 1979 that a new seawall amongst other beachfront developments would be constructed. The seawall was completed in 1982 (Figure 3.7 B) and much resembles the seawall existing today Figure 3.8 (Fish Hoek Centenary 2018).

A

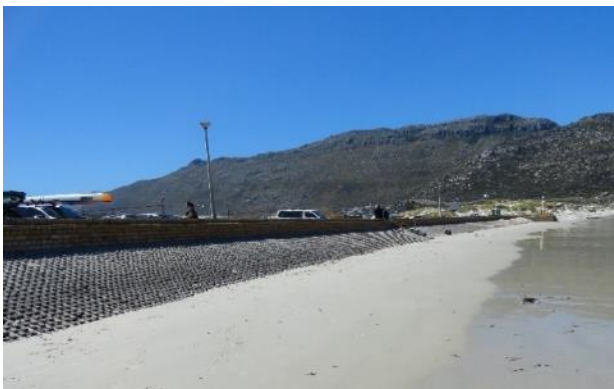


B



Source: Fish Hoek Centenary (2018)

Figure 3.7 Sea walls in Fish Hoek A) Palisade sea wall constructed from wooden railway sleepers, 1980; B) Construction of a new (existing) seawall which was completed in 1982



Source: Author (2017)

Figure 3.8 Existing seawall revetment

Until today, windblown sand remains a problem for the railway line. An article in the local newspaper (The People's Post) from 7 March 2017 states that Fish Hoek beach's sand levels are planned to be lowered in order to reduce the accumulated sand on hard infrastructure (McCain 2017). The consequence of this action would be the movement of the high water mark closer inland towards the infrastructure (Figure 3.9 and Figure 3.10), which would reduce the sand movement by wetting a

larger area of the sandy beach, but in the event of a storm, the infrastructure may experience more energetic wave action.



Source: Author (2017)

Figure 3.9 Water level in relation to the revetment



Source: Author (2017)

Figure 3.10 Kelp washed ashore indicating the high water mark

The railway line separates the beach, recreational space and Seaside Cottages from shops and businesses located in the main road. The distance of the railway line from the high water mark ranges from 20 m at the southern end of the beach, over 150 m in the central beach region to 100 m in the northern area where it crosses the Silvermine River. The main road is set back further from the coast, running almost parallel to the railway line. The distance of the main road from the observed high water mark, taken from the same locations as the railway measurements, is approximately 70 m in the south, 220 m in the central region and 130 m where the road crosses the Silvermine River. The residential area is located directly behind the main road, comprising of medium to high density apartments and single residential properties.

## 3.2 STRAND

The study site in Strand is approximately 2.0 x 1.5 km large (Figure 3.11). The Lourens River estuary, a small dune (Figure 3.11 A) and a recreational park area (Figure 3.11 B) form the northern border of the study site. In this region the beach is wide and sandy (Figure 3.11 C), considering that the photographs were taken approaching low tide. The greenbelt is replaced by a low wall/pavement further south (Figure 3.11 D), which continues towards the location of Figure 3.11 E, beyond which the beach tends to narrow in width. Approaching the location of Figure 3.11 F and G, a sea wall was constructed in 2017 to mitigate the impact of inundation that frequently affected Beach Road, particularly during spring tides and storm events. The sea wall continues southwards up to the Strand Pavilion building which is built on stilts into the water. In this southern part of the study site, the beach is considerably narrower and interspersed with submerged rocky cliffs in the intertidal, forming exposed tidal pools during low tide (Figure 3.11 H).





Source: Author (2018)

Figure 3.11 Locality map of Strand Beach, A: Small foredune towards Beach Road, B: Greenbelt, C: Wide sandy beach, D: Low sea wall and wide sandy beach, E & F: Wide sandy beach, G: Recently constructed sea wall, H: Narrow beach on rocky shallow cliffs

Given the gentle slope of the beach, the intertidal zone is with up to 200m in the northern beach area (Figure 3.12 A) and 40m in the southern beach area (Figure 3.12 B) very wide. The high water mark was observed to partly almost reach coastal infrastructure during high tide on a non-stormy day, particularly in the southern area (Figure 3.12 B).

A



B



Source: Author (2018)

Figure 3.12 Northern beach (A) and southern beach (B) showing the landward extent where the high tide reached on a normal day (yellow arrow)

In the northern part of the study site, the foredune exceeds 10 m in height above mean sea level (brown belt in Figure 3.13). The area behind the foredune is low lying with elevations mostly less than 3 m above mean sea level. Similarly, the built up beach front along the whole study site does not exceed 3 m above mean sea level apart from the small vegetated dunes in the northern area, but these are not built up.



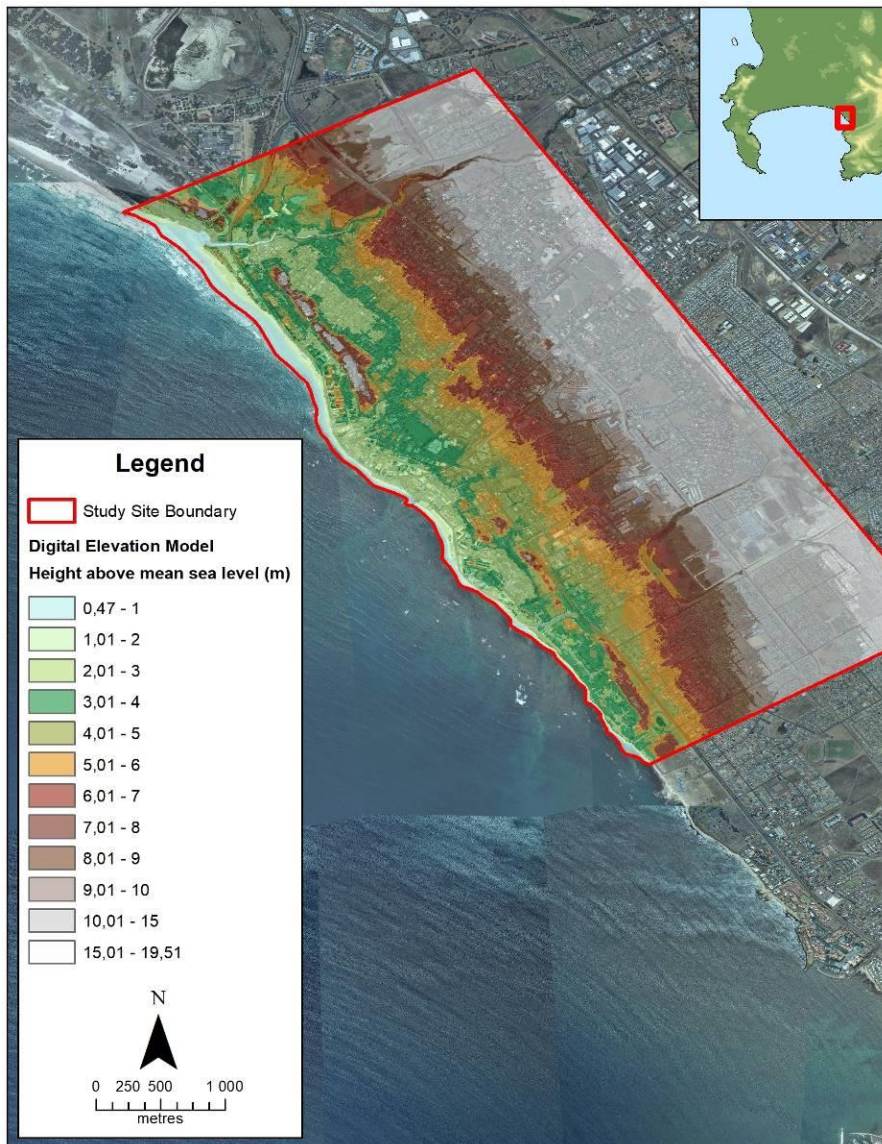
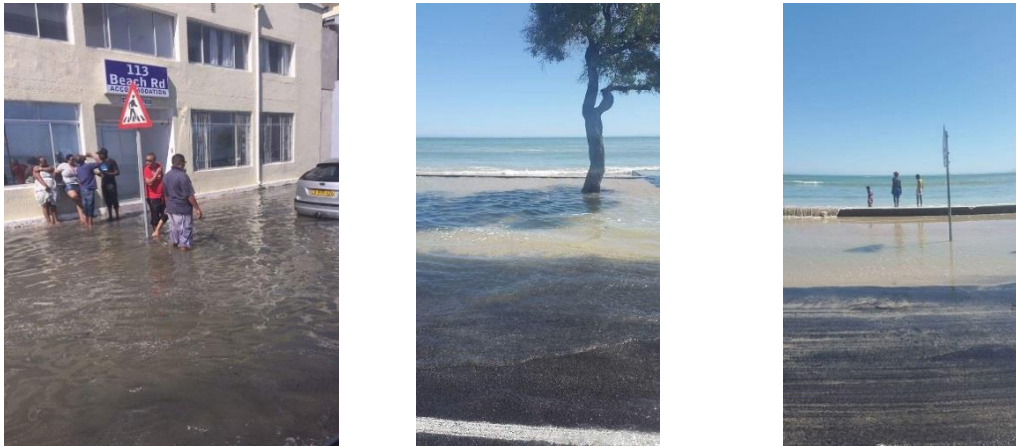


Figure 3.13 LiDAR derived Digital Surface Model of the Strand study site

The Strand area is characterised by residential areas and mixed use developments such as holiday accommodation and businesses located on the beach front. Most of the foredunes have been built over and hardened, resulting in developments extending into the previously active littoral zone. This has subsequently left the developed area vulnerable to flooding and erosion. Developments directly opposite the beach are primarily high rise buildings, frequently without any intentional flood mitigation provisions e.g. the ground floors are not elevated above ground level. The buildings in residential areas are predominantly freestanding single or double storey structures, the majority of which have solid walls which can serve as protection from shallow flooding.

Being generally very low lying, the effects of coastal inundation extend far inland. In addition, many developments are located below river flood lines (Cartwright, Brundrit & Fairhurst 2008b). During

the supermoon experienced in September 2015, Strand was inundated due to the higher than normal sea levels, despite the absence of wave and wind forcing (Figure 3.14) (Bekko 2018, Pers com).



Source: I Bekko (2015)

Figure 3.14 Inundation in Strand caused by the supermoon in September 2015

Contributing to the recurring inundation problem in this area is the condition of the existing subterranean drainage systems. Previous inundation events have resulted in saltwater intrusion and sediment build up in these systems causing damage to drainage infrastructure. In severe storm events coupled with high precipitation, there have been accounts of the drainage systems being saturated and ineffective in removing inundation water (Roux 2018, Pers com).

Prior to the construction of the sea wall in 2015, inundation primarily occurred in the central beach area, particularly near the tidal pool. Greenways Golf Estate also previously experienced inundation near the rock revetment. Since the construction of the new sea wall, which was completed in 2017, inundation caused by wave action has been experienced near the Oceanview apartments, west of the rock revetment due to the deterioration of the old sea wall (Roux 2018, Pers com). Figure 3.15 shows examples of inundation events that occurred in Strand during the last years. The figure shows that flooding affects large stretches of the road and the beach front buildings. The figures also show the derelict condition of the low seawalls, which are in the process of being replaced by a higher, more solid seawall.





Source: A) Cape Town (2013), B-C) Google Search Engine<sup>8</sup>; D) P Roux (2013); E-G) A Theron (2013)

Figure 3.15 Locations of recent storm related inundation events in Strand

<sup>8</sup> The original sources could not be found



## **CHAPTER 4: THE DEVELOPMENT AND VALIDATION OF A COASTAL INUNDATION MODEL AND TOOL**

The development of a coastal inundation model was informed by a written survey and interview processes (Section 4.1). As this process revealed GIS to be the most accessible technology, this component of the study focused on the development of a GIS based eBTM as a baseline for the coastal inundation model. The eBTM outputs were compared to outputs of the traditional sBTM to assess the degree of value addition (Section 4.2). In order to make the model user-friendly and accessible, the model was packaged as a GUI that can be accessed via the ArcGIS ArcToolbox (Section 4.3).

The eBTM was then validated against actual data recorded during a storm event to see how it compares to both observed data and the sBTM (Section 4.4.1). This section also describes tests on the performance of the eBTM using varying input datasets to advise on the most appropriate data to be used (Section 4.4.20). Additional tests include observing the model's response to using elevation data at different resolutions (Section 4.4.3) and different surface roughness values (Section 4.4.4).

### **4.1 GUIDING THE MODEL DEVELOPMENT THROUGH STAKEHOLDER ENGAGEMENTS**

The development of the coastal inundation model was preceded by engagements with coastal practitioners to assess:

- Why South Africa does not have any existing operational ocean models that can be used to inform where coastal inundation may occur?
- What would be the most appropriate technology to develop the coastal inundation model?
- What level of expertise exists within relevant institutions to utilise a model based tool?
- Which datasets are available to assess coastal inundation?

Concurrent to this research, a parallel study had commenced, namely the National Coastal Assessment (NCA) undertaken by the DEA. This presented the opportunity to engage with relevant coastal practitioners and domain experts through the NCA-related stakeholder consultations. Following permission granted by the DEA, two approaches were undertaken, namely:

- A voluntary and anonymous written survey among general coastal management practitioners working in the fields of disaster risk and coastal management<sup>9</sup>; and

---

<sup>9</sup> The tabulated survey results are available in Appendix A2

- Semi-structured interviews with relevant technical experts.

The written survey was primarily self-administered as a hard copy document presented to the participants of the NCA workshops and various other coastal practitioner forums, with permission granted by the respective chairs. In addition, the survey was made available online via Google Forms to respondents. Data collection took place between September and November 2017.

Participants were informed that participation was anonymous and voluntary and that results would be used to inform this research as well as potential future publications. All respondents were either official government employees, academics and/or researchers practising in either coastal management and/or disaster management fields.

The verbal interviews were conducted with identified experts from various institutions. The respondents were directly approached to participate in this study and were selected based on their expertise in coastal management and coastal processes. Each respondent provided their written consent to participate and understood that their participation was voluntary, anonymous, that they would not be remunerated and that they could decline to answer any of the questions. The primary purpose of the interview was to corroborate the information obtained via the written survey and to understand government priorities in terms of coastal management, available resources, technical expertise and challenges in executing their mandates. The interviews were semi-structured and therefore allowed for the respondent to provide detailed responses and the interviewer to ask additional questions for clarity (Greeff 2007).

#### **4.1.1 Survey and Interview Findings**

The written survey yielded 30 responses from a range of professions, which included 16 coastal management practitioners, 3 disaster management officials, 7 specialists<sup>10</sup>, 2 environmental assessment practitioners, 1 compliance monitor and 1 community services practitioner. The interviews were limited to specialists. A summary of the written survey and interview respondent numbers are provided in Table 4.1. While a larger number of responses would have been preferred, it has to be acknowledged that the South African coastal and disaster management community is very small, compared to other countries. The 30 responses constitute a good representation of expertise present in the country.

---

<sup>10</sup> 1 Scientist, 1 Engineer, 5 Geographic Information Systems (GIS) Practitioners

Table 4.1 Summary of survey and interview respondents

Institution	Total written survey respondents	Total interview respondents
National Government	9	1
Provincial Government	7	2
Local Government	4	3
Parastatal	6	2
Private Sector	1	0
Academia	2	2
NGO	1	0
Total	<b>30</b>	<b>10</b>

The interviews were aimed at understanding why South Africa does not have existing operational coastal models, as operational wave and high resolution storm surge models<sup>11</sup> are very useful in forecasting coastal inundation events. International examples show that efforts have been made to develop these operational models, particularly in hurricane<sup>12</sup> and tsunami prone areas.

Experts in operational modelling<sup>13</sup> were consulted to determine why South Africa does not have these systems in place, considering the more frequent and intense storm surges and inundation events being experienced along the coast. The general sentiment was that the lack of operational ocean models in South Africa can be attributed to:

- lack of dedicated funding (investments) and initiatives supporting the development and implementation of an operational model at a required resolution;
- lack of expertise in South Africa in numerical modelling and data assimilation;
- inadequate High Performance Computing being available for development and for operational service delivery;
- numerical modelling developments being typically led by academic institutions with no interest in taking the extra step to become operational<sup>14</sup>;
- a need for high resolution topography data such as LiDAR to be available and acquired on a more regular basis to reflect the current topography.

---

<sup>11</sup> Since November 2017 the South African Weather Services has an operational storm surge model at 4 km resolution which is however too coarse to determine localised coastal inundation events.

<sup>12</sup> Tropical cyclones, monsoons etc.

<sup>13</sup> Listed in Appendix A3

<sup>14</sup> The University of Cape Town is currently the only tertiary institution in South Africa offering ocean modelling as a course, with little focus on operational modelling.

Further, the written survey results clearly showed GIS to be the most accessible technology as it is used by 90% (27) of the respondents. Qualitative techniques such as stakeholder engagements are the second most popularly used technique, with 36.7% (11) respondents indicating that they engage with stakeholders when assessing coastal risk. Only 26.7% (8) of the respondents indicated that numerical modelling (HDm) skills were available within their organisations. Other techniques include site inspections and field measurements, which 23.3% (7) of respondents noted to be undertaken at their organisations. The results are illustrated in Figure 4.1.

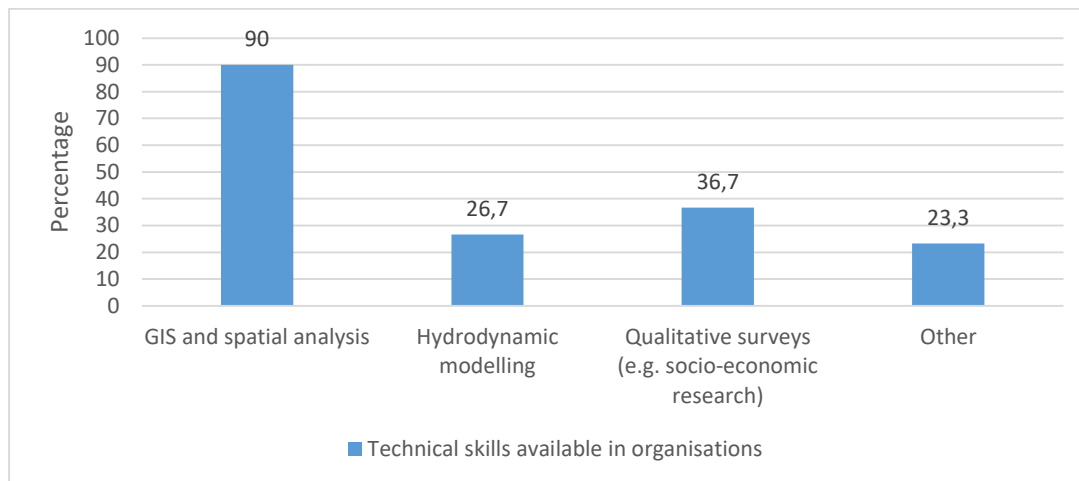


Figure 4.1 Technical skills available in organisations to assess coastal risk

When analysing coastal hazards, GIS data (raster and vector) are the most commonly used datasets (73.3%, 22 nominations), followed by historical climate data (56.7%, 17 nominations), and topographic data, including LiDAR (56.7%, 17 nominations), while oceanographic data are the least used data, utilised by 50% (15) of respondents.

While GIS data are more commonly used, the datasets are static, reflecting conditions at one point in time, and therefore may be outdated if they are not maintained by the relevant custodian. Oceanographic data used as input for HDm are recorded daily and therefore would be more appropriate for reflecting changing conditions over a specified time series.

In agreement with the written survey results, the interviewed technical experts largely confirmed that technical expertise is limited within most government organisations. They revealed that technical analyses are often outsourced, but this presented additional challenges in that the Terms of Reference for the respective tenders are not well articulated and often vaguely formulated because there is insufficient technical knowledge within government to draft adequate technical specifications, potentially leading to compromised results of the analyses.

Broadly, the response to whether the GIS based sBTM was useful in the coastal management context was mixed. sBTM provides the static rise in sea level without atmospheric and oceanographic influence, however, it is valuable in identifying potential areas that could be inundated based on the topography. In the context of HDm, technical experts agree that it is impossible to account for all possible scenarios, taking cognisance of any and every anomaly. Storm surge predictions would require HDm and/or operational models, and the survey results show that there is limited technical capacity in this regard. The verbal interviews further showed that in some cases respondents did not have a clear understanding of the main purposes and applications of GIS bathtub, HDm and operational modelling.

In terms of the types of tools that coastal and disaster management practitioners need, it was clear that while HDm, including tidal and atmospheric forcing, is useful for localised hazard assessments, there is limited expertise to run such models. Practitioners require methods that are technologically accessible and easy to use for non-specialists, such as GIS. Broadly the most useful methods are those that:

- are easily repeatable and structured;
- do not require advanced specialised expertise;
- are implementable over a large area;
- are quickly executable; and
- are able to be undertaken without the need for sophisticated technologies e.g. high-performance computing.

Based on these findings, it was decided that the methodology to be developed for coastal inundation modelling in this thesis needed to be GIS based. The development thereof is described in the following sections.

## 4.2 COASTAL INUNDATION MODEL DEVELOPMENT

This section details the research assumptions (Section 4.2.1) and describes the input data required for eBTM coastal inundation modelling (Section 4.2.2). The sBTM and eBTM workflows are described in Sections 4.2.3 and 4.2.4 respectively, the results of which will be used to determine the improvements that the eBTM offers over the sBTM.

### 4.2.1 Research Assumptions

The inundation model development in this thesis is based on the following assumptions:

- i. The topography remains static for all scenarios as the LiDAR reflects the topography at one point in time (i.e. 2014, as per the acquisition date) as no more recent LiDAR data was available for the study sites at the time this research was undertaken;
- ii. The IPCC AR 5 sea level rise projections are referenced to Land Levelling Datum; and
- iii. Inundation refers to temporary wetting of any surface that is normally dry, as a result of the model output.

### 4.2.2 Input Data

In order to develop the eBTM and the sBTM, a number of input data sets were used. These are described in the following sections.

#### 4.2.2.1 High resolution topography

A key input parameter for the intended sBTM and eBTM flood modelling is high resolution topographic information. Gesch (2009) states that the confidence in flood modelling results is improved through the use of higher resolution DEMs. Therefore, LiDAR data were used in this study, provided by the CCT in LASer (LAS) point file format for both the bare earth as well as other surfaces (including vegetation and man-made objects), with a density of 2–3 points per square meter. From these data, a DTM was produced from the bare earth LAS points and a DSM was produced using all first return points, with a 1 x 1m horizontal and 0.01 m vertical resolution.

For test three (Section 4.4.3), 5 m and 10 m resolution DSMs were created by degrading the 1 m resolution LiDAR derived DSM. For both cases the resampling technique was set to ‘majority’ i.e. the new cell assumes the most popular value in the filter window (ESRI 2016).

The projection used for both the DTM and DSM was Universal Transverse Mercator Lo19. The vertical datum used was Land Levelling Datum (LLD), which is South Africa's official vertical datum based on mean sea level, determined from tidal observations in Cape Town and verified by the mean sea level determinations from tidal observations in Durban, Port Elizabeth and East London over varying time periods (CD:NGI 2013).

Fish Hoek was covered by LiDAR tile W057D and Strand was covered by tiles W17A, W17C and W17D. The LiDAR acquisition period for both study sites was December 2013 – January 2014 as more recent LiDAR was not yet available. It should particularly be noted for Strand that the LiDAR was acquired prior to the construction of the sea wall which commenced in June 2015 and concluded in 2017. Therefore, the results achieved here do not reflect the current situation on the ground.

#### 4.2.2.2 Coastline

The development of the eBTM requires the definition of the coastline. The coastline in this context is a line drawn along the coast which tells the model where the water is originating from, i.e. the water source. Essentially this is where the model begins to run and propagates the inundation water inland. For this study, the coastline was created using the LiDAR derived DTM by means of connecting the centroids of the DTM raster cells where the cell value, i.e. the elevation above mean sea level was 0. This created a zero meter (0 m) contour along the coasts of each study site which was extracted as a line shapefile (.shp).

#### 4.2.2.3 Inundation water levels

Sea state observations i.e. long term water level recording are primarily undertaken by the South African Navy Hydrographic Office (SANHO), the CSIR for the National Ports Authority, and the Marine Office of the South African Weather Service. This thesis combined the average rise in water levels during (1) a storm surge event for different return periods (Rossouw et al. 2012) and (2) a high water spring tide of 0.95 m (South Africa 2009) to derive the combined water level baselines. All water levels were relative to LLD (Table 4.2).

Table 4.2 Combined water levels derived for False Bay relative to LLD under current sea level conditions

Return period	Storm surge (m) as per Rossouw et al. (2012)	Mean High Water Spring tide (m above LLD) as per SANHO (2009)	Derived combined water level (m)
Once per 100 years	0.84	0.95	1.79

Currently in South Africa, localised sea level rise projections and/or estimates are currently not undertaken, with the most recent study being published in 2009 (Mather, Garland & Stretch 2009). Mather (2007) has previously stated that South Africa's local rate of sea level rise is within the range



of global trends and it is undisputed that the sea levels are indeed rising (Cartwright 2011; Kretzmann 2019). Hence, due to the lack of local data, the IPCC (2014) global sea level rise estimates were used for this purpose.

For the purpose of this thesis, three scenarios were developed, namely:

- scenario one uses the baseline water level i.e. 1.79 m;
- scenario two uses the baseline and adds the IPCC (2014) likely medium term sea level rise scenario of 0.38 m; and
- scenario three uses the baseline and adds the IPCC (2014) likely long term sea level rise scenario of 0.82 m.

The water levels are summarised in Table 4.3.

Table 4.3 Water levels for inundation hazard scenarios

Scenario number	Return period	Derived combined water level (m)	IPCC AR5 sea level rise projection (m) <sup>15</sup>	Resulting hazard scenario water levels (m)
1	Once per 100 years	1.79	None	1.79
2	Once per 100 years	1.79	0.38	2.17
3	Once per 100 years	1.79	0.82	2.61

#### 4.2.2.4 Roughness Coefficient (RC)

The eBTM required information on the dry coast roughness as input. The roughness or smoothness of the receiving environment plays a critical role in influencing water movement. FEMA (2007) provides generic surface roughness ratings between 0 – 1 that can be used as a roughness coefficient (RC) in the eBTM to accommodate for different receiving environments. In this rating a value of 0 indicates a very rough surface and 1 is a hydraulically smooth surface. As both study sites used in this research are sandy, a RC value of 1 was assumed<sup>16</sup>.

#### 4.2.2.5 Historical Inundation Event and Extent data

As mentioned within the literature chapter, despite its known weaknesses, the sBTM is used widely to assess both sea level rise (permanent change of the coastline) and coastal inundation

---

<sup>15</sup> Due to its global reporting structure, the IPCC projections are not referenced to a specific datum. The assumption used in this analysis is that it is referenced to LLD (Mather 2017, Pers com). The values reflected are for the upper likely values presented in IPCC (2014).

<sup>16</sup> See Appendix A4 for details on the FEMA roughness index.

(temporary/episodic event). In order to assess the model results produced by the sBTM and eBTM, coastal inundation extent data from a storm event that occurred in Cape Town on 30 August 2008 were used as reference. This was the most intense storm to impact the region since 2001 (RADAR 2010). The event included high rainfall and wind speeds between 35 – 82 km/h recorded on both the False Bay and Atlantic coastlines. Rossouw et al. (2012) state that during this storm the significant wave height exceeded 9 m, which was compounded by the coinciding spring high tide. The largest individual wave measured during this storm had a height of 17.8 m (Rossouw et al. 2012). The maximum tide water level (still water level i.e. without waves) recorded during the event was 2.3 m, excluding the effects of wind and waves (South Africa 2008).

During the storm, the CCT recorded the inland inundation extent using a GPS. The data thus reflect the height above mean sea level that the maximum inland inundation extent reached. For Fish Hoek, one data point was captured. In Strand, 3 data points for the edge of the maximum inland inundation extent were recorded during the event. These four data points were available for this thesis as point shapefiles.

#### **4.2.3 Simple BTM (sBTM) modelling**

The sBTM model was produced using a 1 m resolution LiDAR derived DTM as described in Section 4.2.2.1.

Inundation levels for 3 independent inundation scenarios were calculated in ESRI ArcGIS version 10.3 using the Raster Calculator Tool in the Spatial Analyst Extension Toolbox, based on the 3 extreme sea level scenarios, as per Table 4.3. The extreme sea levels i.e. 1.79 m, 2.17 m and 2.61 m respectively, were subtracted from the DTM so that all areas below the extreme sea level thresholds were considered to be inundated. The so derived flood masks were compared to the corresponding eBTM outputs.

#### **4.2.4 Enhanced Bathtub Model (eBTM) modelling**

The novel approach developed in this thesis for coastal inundation mapping was the eBTM in order to overcome the sBTM shortcomings. The eBTM process improves on the work conducted by both Li, Grady & Peterson (2014) and Perini et al. (2016), taking cognisance of the work conducted by Hejazi, Ghavami & Aslani (2017), who proved that both roughness and beach slope influence wave runup and subsequently inundation. The approach used in this thesis amalgamates the previous works conducted and hence required the following input datasets:

- high resolution topography;

- coastline (water source);
- inundation water level; and
- roughness coefficient.

The model was developed in ArcGIS 10.3 and requires the Spatial Analyst extension. All ArcGIS models need to be stored in an ArcGIS Toolbox environment and hence a new toolbox was created called 'ArcCoastTools' (Williams 2019a). The modelling steps, which are also depicted in Figure 4.2, are as follows:

1. The input surface and user specified inundation water level were added to the Raster Calculator tool to identify areas lower than the specified inundation water level. For this study a DSM was used. The output layer was a binary layer 'grid1', where a value of 0 was assigned to areas higher than the pre-set inundation water level and a value of 1 to areas lower than the pre-set inundation water level;
2. Grid1 was reclassified into 2 classes where zero values were recoded to 'NoData'. This step eliminated areas higher than the input inundation water level, which are now acting as barriers, forcing inundation to go around them when using the Cost Distance tool (in step 5). Therefore this step also converted buildings and other objects into barriers. The output is 'grid2';
3. Grid2 was then converted into a polygon .shp mask. The output is 'Shp1';
4. Shp1 was used to extract the DSM of the area to be inundated, excluding buildings. The output is 'grid3'
5. Grid3 was used as the input elevation model for the slope tool which calculates the steepness of each cell across the study site. The output comprises of the slope angles. The output is 'grid4'. According to Perini et al. (2016), the slope influences inundation water distribution;
6. Grid 4 was divided by the RC (based on Sekovski et al. 2015), using the raster calculator, which in this case was 1. While for a homogenous RC of 1 for the whole area, this step technically could be omitted, it was kept in the model to allow for easier ingestions of (variable) RC data in the future. The output is 'grid5';
7. The Cost Distance tool used grid5 and the coastline (.shp line) to calculate the inundation progress from the coastline and pathways which favoured water movement (Perini et al. 2016; Sekovski et al. 2015), based on the least cumulative cost route per cell. The output is 'grid6' (the cost raster) where the value of each cell represents the least horizontal cost distance from

the coastline<sup>17</sup> (Perini et al. 2016). In the preceding steps, both the vertical elevation of the DEM and slope angle contributed to the ‘cost value of the cell’ i.e. higher and steeper cells were assigned higher cost values, which also increased based on the horizontal distance between the cell and the coastline. This step included an optional output, the Backlink Raster, that can be used to show directional pathways;

8. The following steps require the input data to be in integer format, however, grid 6 is in floating point format. In order to preserve grid 6’s decimal values, the raster calculator was used to multiply grid 6 by 1000 (producing grid 7);
9. Grid 7 was converted into an integer raster, using the Integer tool (grid 8);
10. The Raster to Polygon tool is used to create an inundation mask ‘shp2’ in shapefile format;
11. Shp2 was used as a mask to extract the inundated area from the input DSM. The output is grid 9 which contains the original elevation values of the DSM;
12. The raster calculator is then used to subtract grid9 from the user defined initial inundation water level. The output is ‘grid10’ which gives the actual inundation depth;
13. The raster calculator is used to eliminate cells where the inundation water level is calculated to be negative i.e. below the DTM, so only water levels occurring on the ‘surface’ are reflected. The final output is the Inundation Depth Raster.

All intermediate grid and shape outputs are stored in a temporary file geodatabase and can be retrieved by the user. Only the final inundation raster and the optional backlink raster layer are displayed by default.

---

<sup>17</sup> The output raster no longer reflects elevation but the product of the cell size and the cost value e.g. if the cost raster cell size = 30, and particular cell’s cost value = 10, the final cost of that cell is 300 units (ESRI 2016).

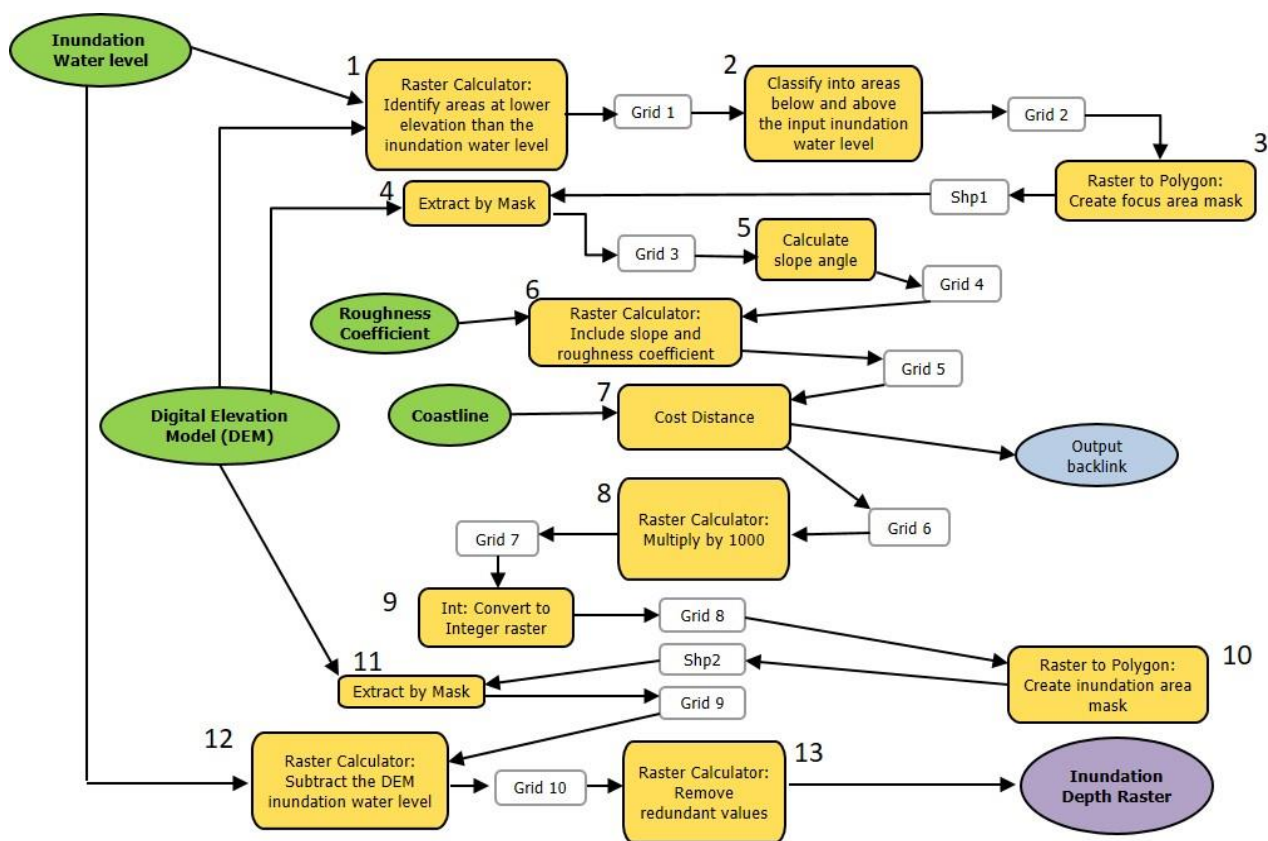


Figure 4.2 Enhanced Bathtub Model (eBTM) developed for this study. Large numbers correspond to the processing steps described in the text

### 4.3 eBTM TOOL DEVELOPMENT

On completing the development of the model (Figure 4.2), a GUI was created so that the model is now presented as a tool. The packaging of the model into a geospatial tool was undertaken because:

- the GUI provides a simple user interface where the user is prompted to provide the input datasets and formats. It is therefore more user friendly than a model, particularly to those with limited GIS skills as it merely has to be added to ArcGIS as an additional toolbox;
- the GUI can be used without understanding the complexities of the model itself; and
- the model itself is embedded within the tool and therefore ‘protected’ from erroneous manipulation.

However, the GUI also allows access to the model for more experienced users to customise as needed.

The tool development required two essential steps. First, all input parameters required for the model to run needed to be specified in the ArcGIS Toolbox environment. This provides a basic GUI interface with the predetermined fields for the input data, required by the embedded model specifications. These parameters were customised via the ‘properties’ menu, to specify datasets that are optional or

mandatory, format requirements (e.g. vector or raster datasets) and any additional data parameters. The model parameters which are enforced by the GUI are shown in Figure 4.3.

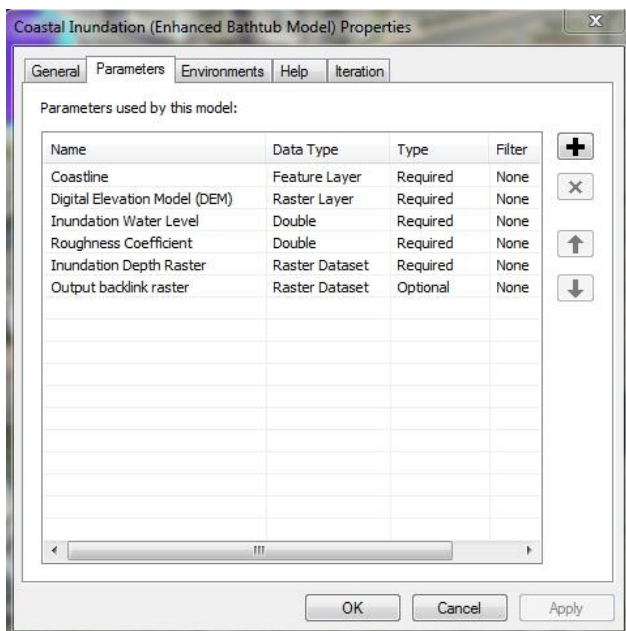
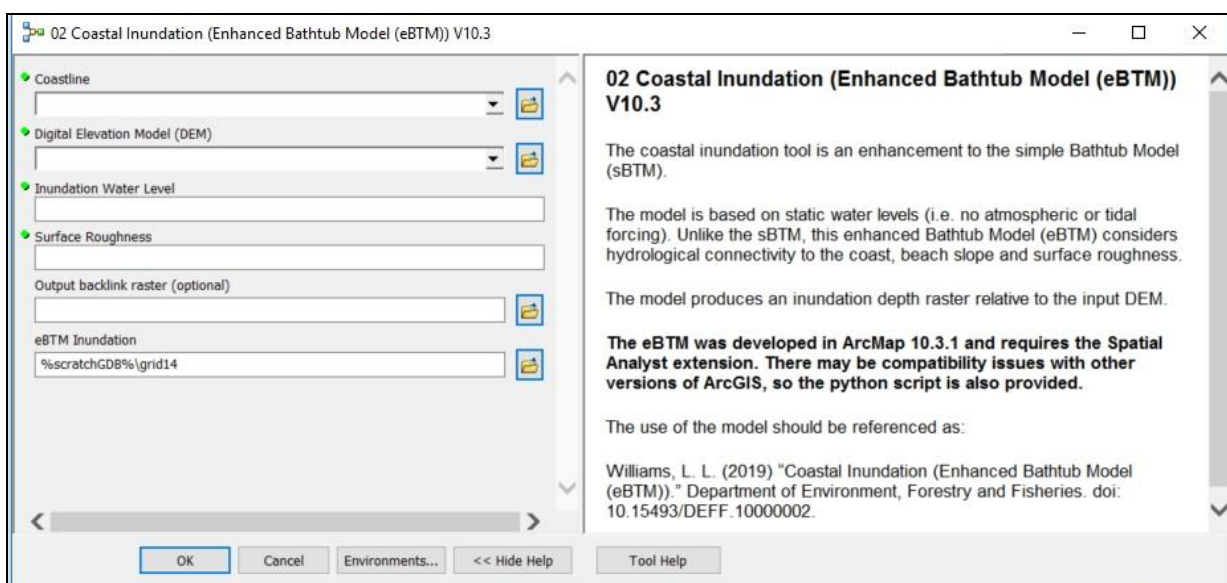


Figure 4.3 Model parameters enforced by the GUI

Once the model parameters were defined, ArcCatalog was used to add descriptive text to the GUI. The text was customised so that upon clicking on an input dataset a description of the requirements, including the relevant parameters are displayed. An example of the GUI and descriptive information is shown in Figure 4.4.



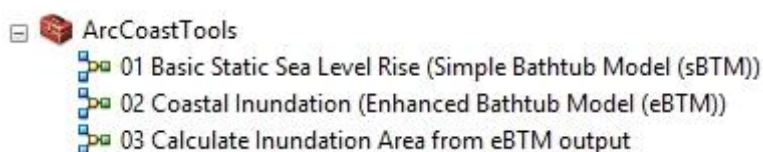
Source: Williams (2019b)

Figure 4.4 The eBTM GUI tool

In developing the toolbox, which was named ‘ArcCoastTools’(Figure 4.5), additional analysis tools were included to further support GIS based coastal analyses. The tools are:

- Basic static sea level rise (Bathtub Model): The sBTM model (section 4.2.3) was packaged into a tool to provide users with a GUI interface to undertake simple bathtub based assessments which is more applicable to long term sea level rise;
- Coastal Inundation (Enhanced Bathtub Model): To run the eBTM described in Section 4.2.4.
- Calculate inundation area: Once users have run the eBTM, this tool allows to calculate the surface area determined to be inundated; and

The ArcCoastTools toolbox is presented in Figure 4.5 below:



Source: Williams (2019a)

Figure 4.5 The ‘ArcCoastTools’ toolbox developed

The python script for the eBTM (described in Section 4.2.4) is included in this thesis as a digital appendix (Appendix A5). The latest version of the toolbox can be downloaded from this link: <https://doi.org/10.15493/deff.10000001>. After downloading and extracting it in a user-defined location, it can be loaded directly into ArcGIS by selecting to “add toolbox” in the toolbox menu.

#### 4.4 MODEL TESTING AND VALIDATION

In order to determine:

- the performance of the eBTM in comparison to the sBTM,
- the response of the eBTM to the use of a DTM instead of a DSM,
- the performance of the eBTM using different resolution DSMs, and
- the impact of the use of different roughness coefficients

four tests were devised by using the sBTM and eBTM models as implemented in the developed toolbox. For all tests, excluding test one, the input coastal inundation water height was 2.61 m, equivalent to scenario three of the primary analysis. All four tests are described in detail in the following sections.



#### **4.4.1 Test One: Comparing EBTM and SBTM outputs to observed data**

In order to assess the differences in the sBTM and eBTM, both models were run for Strand and Fish Hoek with an input water level of 2.3 m above LLD. This water level was recorded during the big storm event that occurred in August 2008. For both the sBTM and eBTM analyses, a DSM was used as the elevation model. The coastal inundation extent data recorded in 2008 by the CCT were used to assess the quality of the respective model results.

#### **4.4.2 Test Two: The model's response to a DTM vs. a DSM**

Strand was used for running the eBTM model using a 1 m resolution DSM vs. a 1 m resolution DTM, in order to determine the respective response of the model and to identify the limitations associated with the use of either of the elevation models. This test was undertaken as literature often makes reference to the use of a DTM for sBTM inundation analyses, possibly due to DTMs being more easily available. However, the use of a DTM prevents the modelling of the impact of surface structures acting as hydrodynamic barriers. The difference between the outputs using a DSM vs. DTM in the context of eBTM thus needed to be tested. For this test, the input coastal inundation water height was 2.61 m, equivalent to scenario three of the primary analysis. All other input parameters were kept the same (e.g. roughness coefficient).

#### **4.4.3 Test Three: The model's response to different DSM resolutions**

In this test the eBTM's performance to 1 m, 5 m and 10 m resolution DSMs was assessed with otherwise identical input parameters to determine the most appropriate resolution to use when assessing coastal inundation at a local level.

This test was only run on the Strand study site as it has a highly developed beachfront, using 2.61 m water levels as per scenario three. The presence of buildings and surface structures of varying height and width creates more complexity for the model, which is ideal as the model is intended to determine water movement by navigating through these structures. The model was not constricted by time and/or iteration parameters. Each of the eBTMs were run once until completion.

#### **4.4.4 Test Four: Varying the Roughness Coefficient**

In order to test how the Roughness Coefficient (RC) influences the inland extent of inundation, the 1 m DSM for Strand was used as the input surface model and the RC was set to both the original value of 1 and to 0.5, indicating higher roughness, as to be found e.g. for cast-concrete armour units (FEMA

2007). The rationale for this test is the hypothesis that smooth surfaces offer less resistance and should allow water to travel further inland.

## 4.5 RESULTS AND DISCUSSION

An enhanced GIS based BTM (the eBTM) was developed, which used a high resolution DEM, slope (generated by the model), user defined water level and a roughness coefficient to model storm surge related coastal inundation limits in Fish Hoek and Strand in False Bay, Cape Town. In order to assess the eBTM's performance, four tests were conducted with varying input parameters. The results of these tests are presented and discussed in the following sections.

### 4.5.1 Test One: Comparing eBTM and sBTM outputs to observed data

The first test simulated the storm surge height of 2.3 m of a 2008 storm event and compared the respective eBTM and sBTM generated flood extents to historically observed inundation limits (Figure 4.6).

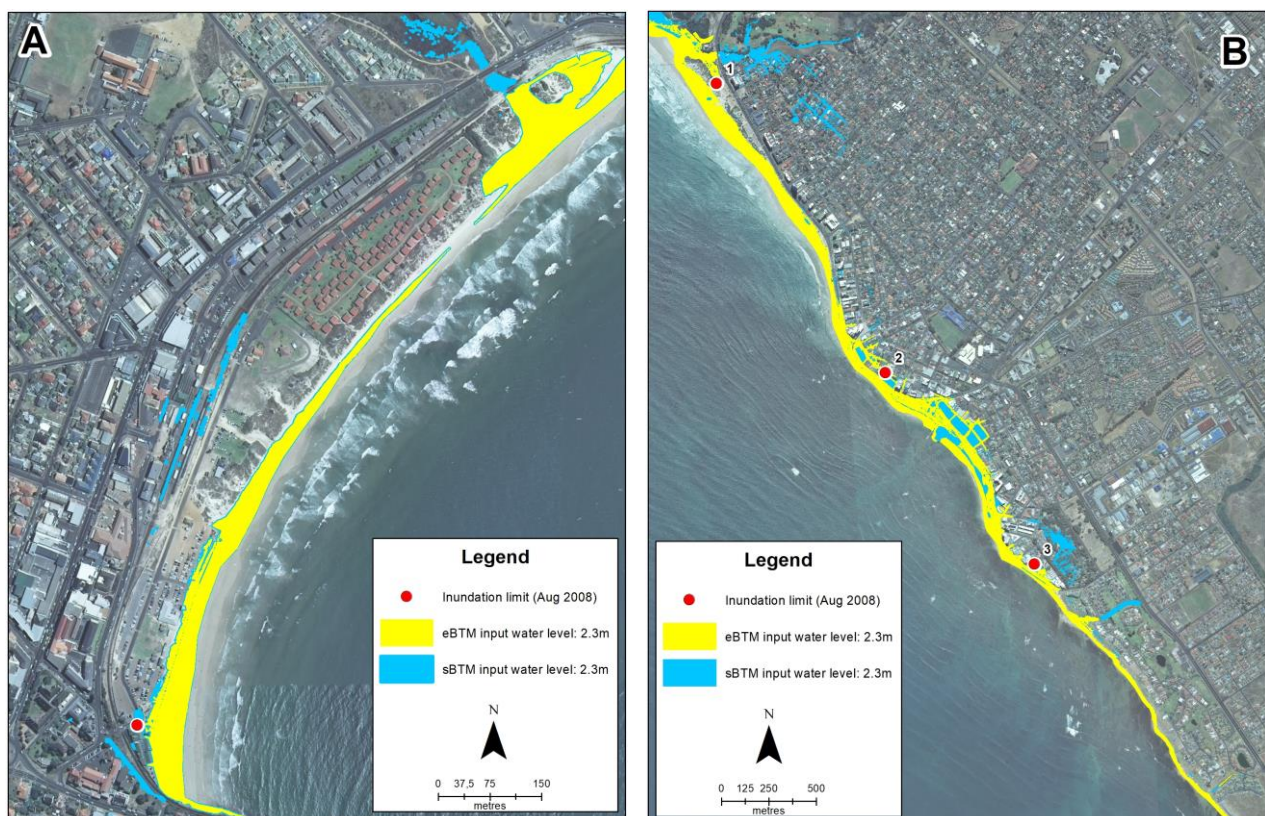


Figure 4.6 Locations of field recordings of the 2008 flood extent (red dots) overlaid with sBTM (blue) and eBTM (yellow) results for (A) Fish Hoek and (B) Strand

Figure 4.7 zooms into the areas where reference points were taken during the storm event. In Strand (Figure 4.7 A) both the eBTM and sBTM show that inundation occurred in the recreation area behind the dune, in agreement with the recorded GPS point. Here the 2008 recorded inundation level was 3.35 m above mean sea level. Both the eBTM and sBTM suggest that inundation water may have emanated from the Lourens River. However, on closer investigation (Figure 4.8) it is evident that there is a pedestrian thoroughfare through the dune at that point, it is therefore also plausible that the coastal inundation water entered the recreational area via the thoroughfare. The driving factors may be attributed to the wave energy driving the wave runup, coupled with onshore wind push and further facilitated by the gentle beach slope and sandy beach (and therefore reduced friction).

Point two in Strand (Figure 4.7 B) was captured in De Beers Road, running parallel to Beach Road on the landward side. The inland inundation limit recorded was 2.32 m above mean sea level. The GPS point corresponds well to the eBTM result, while the sBTM shows buildings being submerged and water penetrating further inland. In Figure 4.7 C, point three in Strand shows close correspondence of both the eBTM and sBTM with the historical GPS point, however the sBTM shows overestimation in surrounding areas.



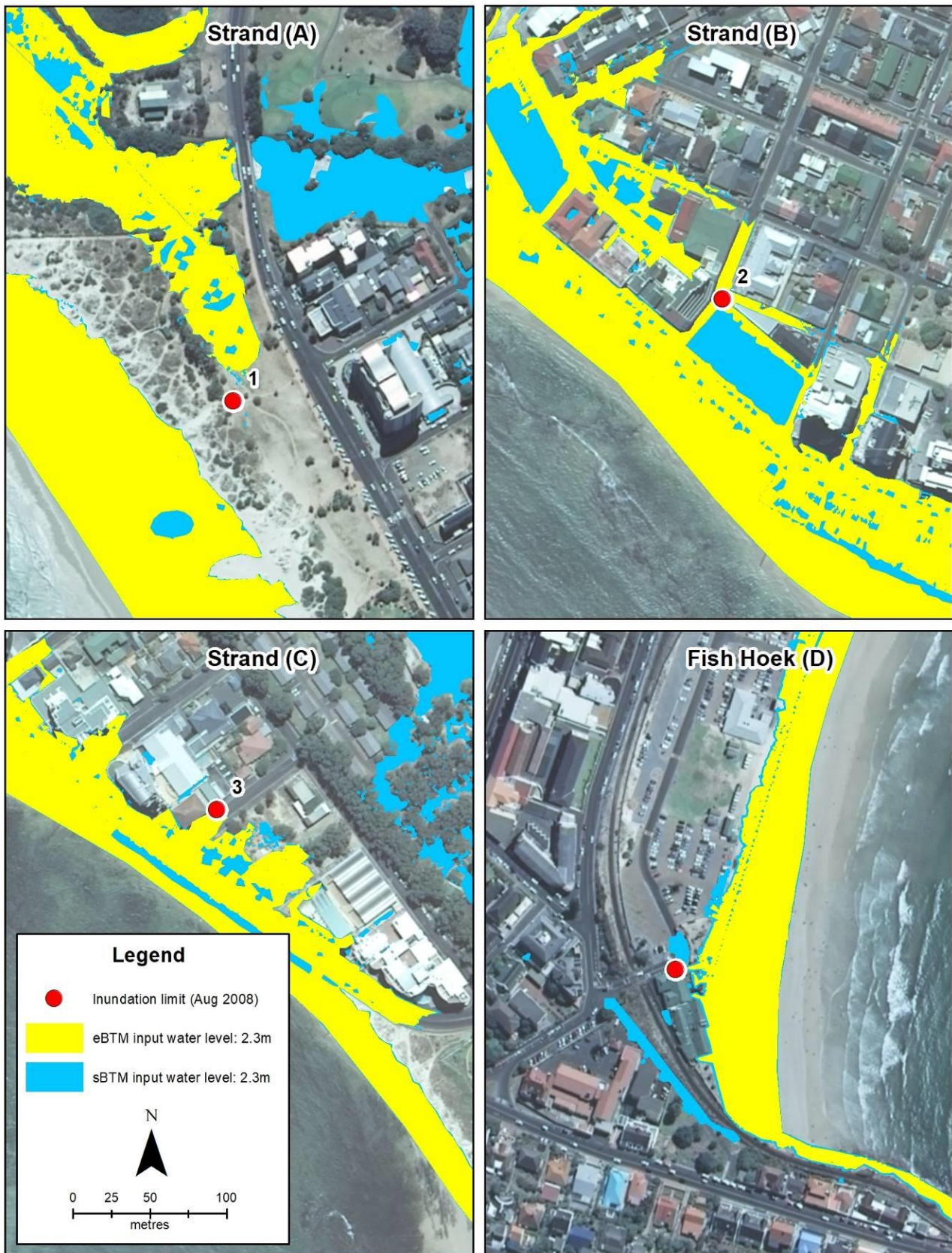


Figure 4.7 Recorded 2008 flood line (red points) compared to the eBTM (yellow) and sBTM (blue) outputs for Strand (A – C) and Fish Hoek (D)

The recorded point in the southern region of Strand is also landward of Beach Road, with inundation reaching 2.32 m above mean sea level. In both Figure 4.7 A and C, the overestimation of the sBTM can be attributed to the lack of hydrological connectivity to the coast, which is more relevant for Figure 4.7 C as Figure 4.7 A demonstrates the eBTM limitation as explained previously.

In Fish Hoek (Figure 4.7 D) the results were similar to that of Strand point 3. While there was alignment between the sBTM and eBTM at the GPS point location, in the point vicinity the sBTM produced inundation occurring further inland.

Overall, there is better alignment between the eBTM results and the actual inundation limit points recorded during the storm inundation event than for the sBTM which overestimates the flood extent. The eBTM in some cases slightly under and over estimates the ground-truthed flood extent, however the variation is minimal. It is important here to note that the eBTM output does not include inundation as a result of wind push by surface winds or wave action. Inclusion of these additional parameters may likely result in the inundation extending further inland.

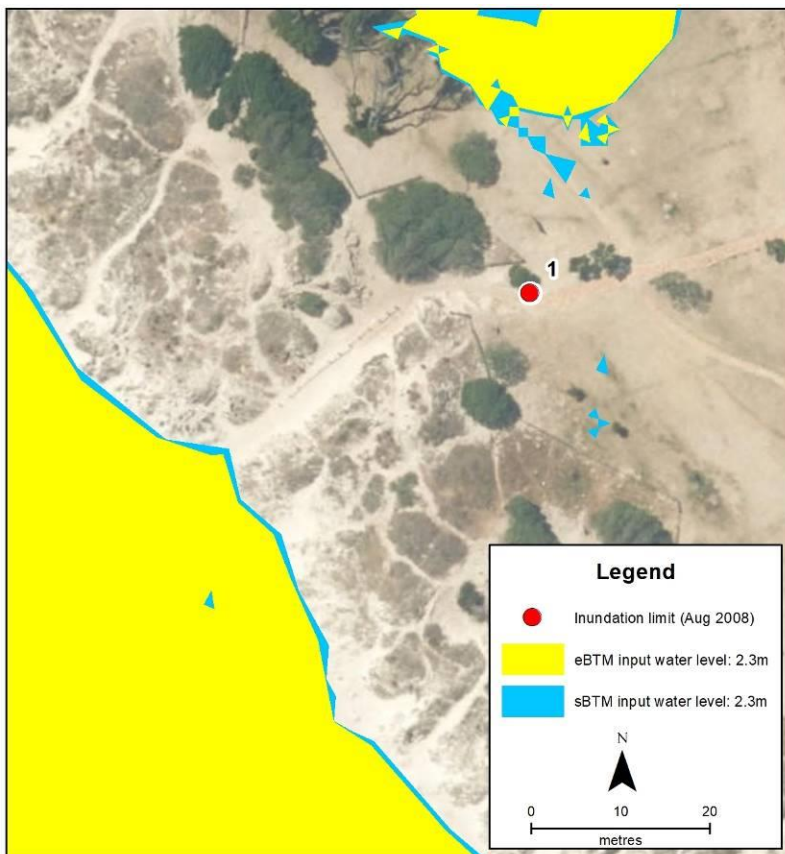


Figure 4.8 Thoroughfare through the dune in Strand (as per Figure 4.7 A)

However, on closer inspection the sBTM also reveals a weakness in the eBTM. The first return LiDAR points were used, which shows bridges and overhead structures as solid structures that do not allow passage underneath. This is an inherent problem with DEMs, but in this instance the sBTM



better describes the inundation on landward side of the bridge, while the eBTM output abruptly stops where the road bridges cross the respective rivers (Figure 4.9). The eBTM weakness can be attributed the cost-distance tool instilling hydrological connectivity to the coast.

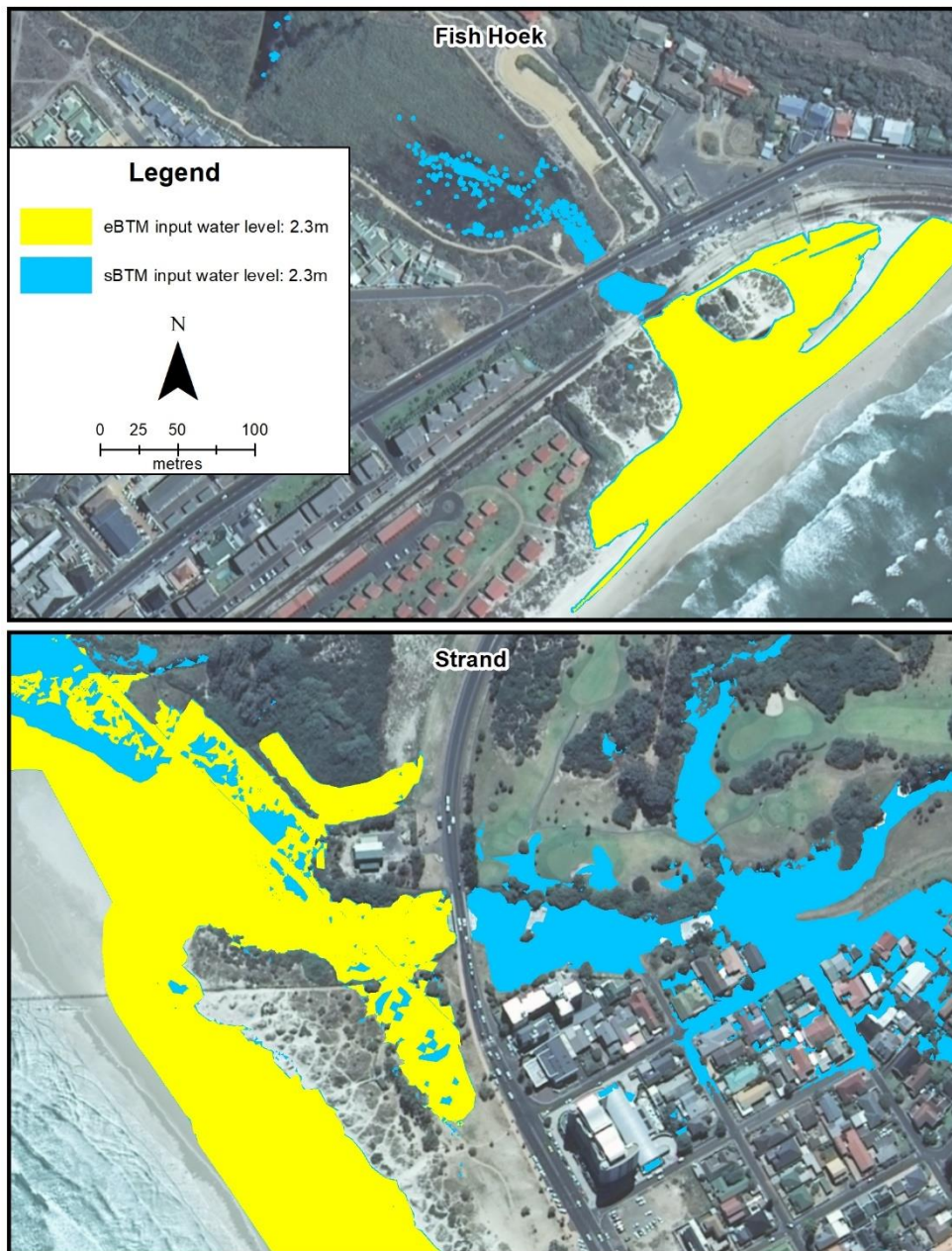


Figure 4.9 eBTM (yellow) and sBTM (blue) results for bridges over rivers in Fish Hoek (top) and Strand (bottom).

Overall, the sBTM predominantly produces overestimations of coastal inundation which is largely attributed the hydrologically disconnected outputs. As the water levels are increased, the degree of overestimation will therefore also increase. The sBTM should thus be used with a degree of caution, specifically in the many online sea level rise applications (see examples in Table 2.4) used to inform development planning. The use of the sBTM to produce these ‘drown your town scenarios’ will require data to be cleaned (e.g. removing isolated inundated areas) prior to use, whereas the eBTM

provides the advantage of excluding these areas based on hydrological connectivity. Therefore the eBTM may prove to be a useful contribution to these dynamic applications, and the following tests were therefore conducted with the eBTM alone.

#### **4.5.2 Test Two: The model's response to a DTM vs. a DSM**

The second test (Section 4.4.2) compared the use of a DSM vs. DTM in the eBTM. The results show that the flood mask generated using the 1 m resolution DSM as input excludes surface features such as buildings (Figure 4.10). In contrast, the flood mask generated by the 1 m resolution DTM appears more solid (Figure 4.10), as the DTM represents the bare surface, thereby excluding buildings and other structures.

This virtual reduction of obstructions introduced an overestimation of the total inundation area across the study site (Figure 4.10).

It appears that the 1 m resolution DSM produced the more accurate results in terms of reduced generalisation and maintaining hydrological connectivity to the coast. The improved accuracy however is at the expense of dramatic increase in processing runtime.



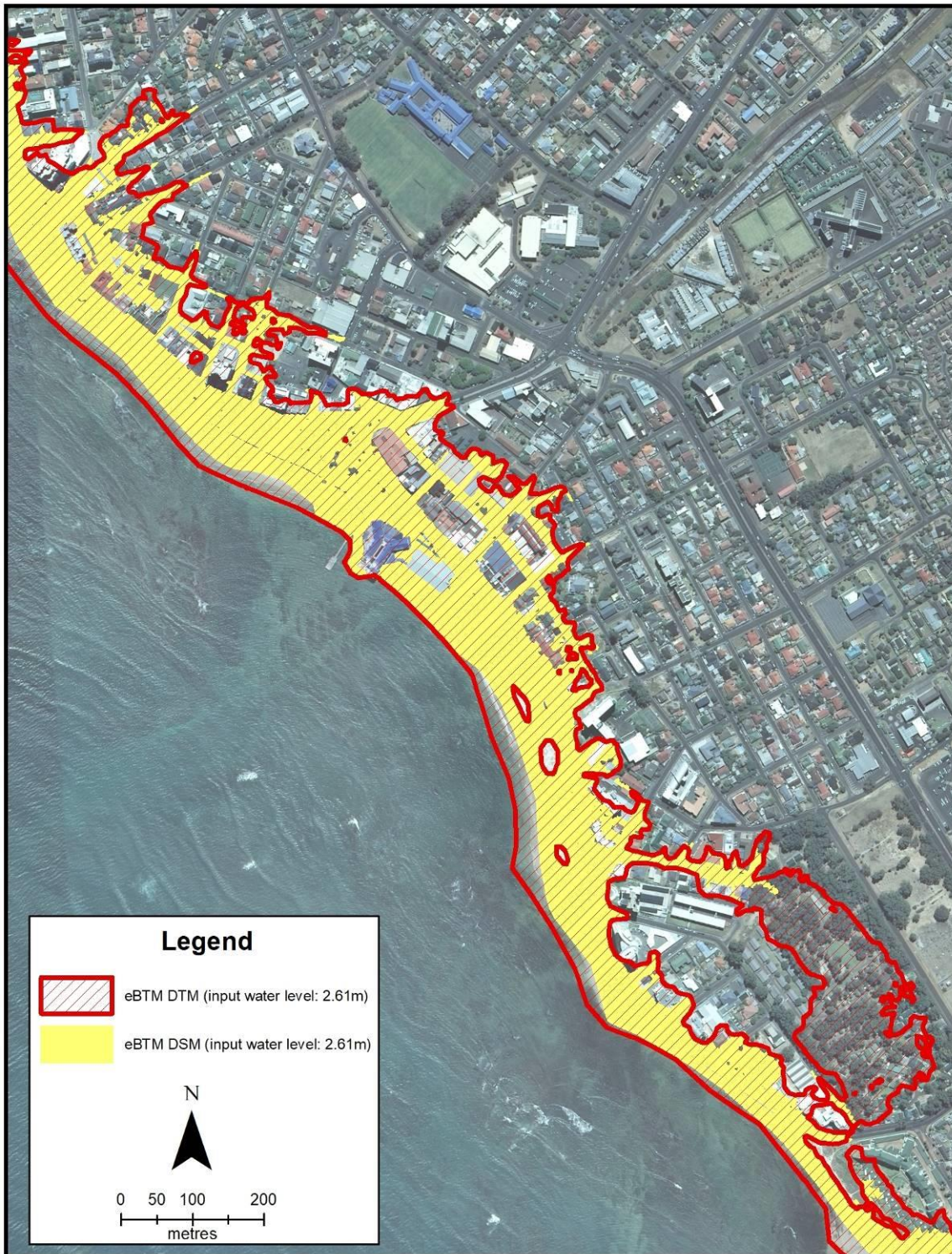


Figure 4.10 Comparison between the modelled flood area outputs using a DSM (yellow) and DTM (red)

### 4.5.3 Test Three: The model's response to different DSM resolutions

The third test considered the use of DSMs with varying resolutions, namely 1 m, 5 m and 10 m in the eBTM model for the 2.61 m water level scenario (Section 4.4.3). The DSM resolutions were shown to influence the total model run time. The model runtime and resulting inundated areas are summarised in Table 4.4 below.

Table 4.4 Summary of the model test 3 results

DSM resolution	Model Runtime	Inundation Area (km <sup>2</sup> )
1 m resolution DSM	50 min, 4 s	0.526 km <sup>2</sup>
5 m resolution DSM	1 min, 37 s	0.508 km <sup>2</sup>
10 m resolution DSM	0 min, 38 s	0.520 km <sup>2</sup>

The runtime using the 1 m resolution DSM far exceeded the runtime taken for lower resolution DSMs. The difference in the total inundated area was negligible for all the DSMs. Upon visual inspection of the results, the 1 m resolution DSM (Figure 4.11 A) tended to preserve solid structures such as buildings quite well. The inundation tends to follow the road network as it penetrates inland, notably maintaining hydrological connectivity to the coast throughout the study site. Overall, the 1 m resolution DSM provided a visually realistic output.

The 5 m resolution DSM also represented the roads as conduits facilitating the movement of the inundation inland (Figure 4.11 B). The obstructing effect of the buildings was also well represented. Visually, the output appeared more pixelated than the 1 m resolution DSM output.

The 10 m resolution DSM tended to underrepresent the inundation extent (Figure 4.11 C). The reason for this difference is that the 10 m resolution DSM contains more mixed pixels including road and building elevations than the 1 m and 5 m DSMs. As the building rooftops cover larger surface areas than the roads, the cell values would therefore assume the height values close to the building heights. When running the eBTM model, the model therefore assumes that the mixed pixel cells form a barrier that restricts the coastal inundation from penetrating inland. Subsequently, the total inundation area for the 10 m DSM model run is the smallest.





Figure 4.11 Results of the eBTM resolution test with (A) 1 m, (B) 5 m and (C) 10 m resolution DSM

This test thus revealed that the high resolution 1 m DSM provided the most detailed output in that hydrological connectivity is clearly maintained and inundation penetrated further inland through relatively narrow thoroughfares. These results are in line with Gesch (2009). The processing time however, was considerably longer than for models run with the coarser resolution DSMs, running for almost an hour for the Strand study site.

As Neumann & Ahrendt (2013) stated, the DEM is the model's playground and interpolations may introduce topographic uncertainties. Marks & Bates (2000) further elaborate that the difference in the DEM resolution and model output may result in further inaccuracies, which was confirmed in test 3 (Section 4.4.3).

The eBTM model relies on high resolution topographic data (Section 4.2.2.1 and 4.4.3). The preference for high resolution DEMs for coastal application is echoed by many authors (e.g. Brock & Purkis 2009; Gesch 2009; Lück-Vogel, Macon & Williams 2018; Marks & Bates 2000; Neumann & Ahrendt 2013; Slatton et al. 2007; Xharde, Long & Forbes 2006; amongst others). This in itself may be a limitation as access to such data, particularly in South Africa, is a challenge, primarily due to the high costs associated with acquiring such data (Lück-Vogel, Macon & Williams 2018).

#### 4.5.4 Test Four: Varying the roughness coefficient

The results of the final test (Section 4.4.4) showed the impact that surface roughness has on inundation propagation (Figure 4.12). The use of a high RC, implicating a smooth surface, produced an inundation extending further inland than the use of a lower RC of 0.5, indicating a rougher surface.



The inclusion of a RC therefore allows the model to be applicable in more scenarios e.g. where coastal defences such as sloping revetments and vegetation are in place, however it would not eliminate the need for further testing and considerations.

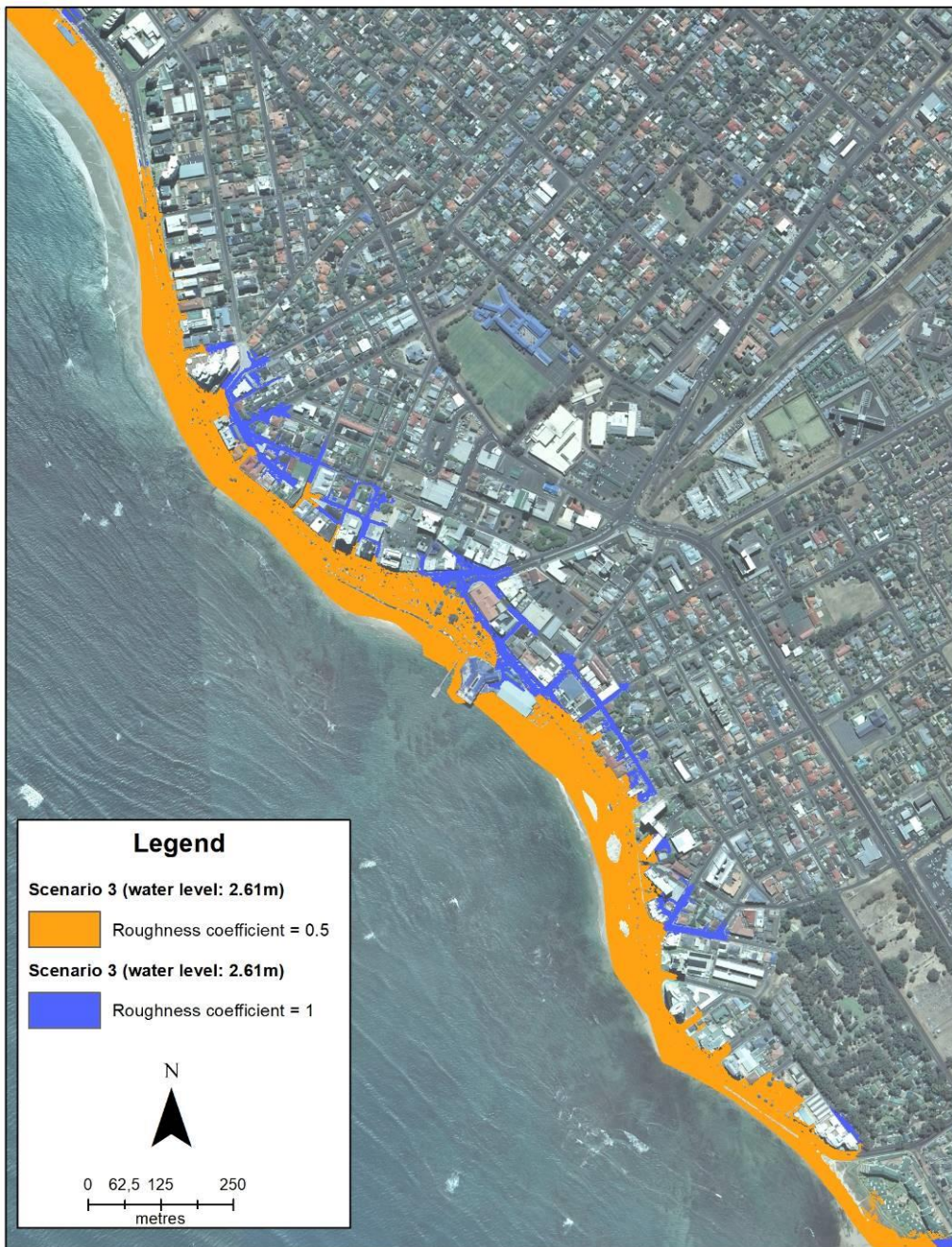


Figure 4.12 eBTM outputs for runs with a RC of 0.5 (orange) and 1 (blue)

Hejazi, Ghavami & Aslani (2017) state that the effect of roughness is dependent on both the surface roughness and beach slope that the inundation water is traversing. This result is in line with Hejazi, Ghavami & Aslani (2017) who observed that wave runup over a smooth slope achieved a higher runup height than the wave runup over a rough slope at the same angle of inclination.

## 4.6 SUB-CONCLUSION

As only few ground truth points for historical flood extents are available, it is impossible to validate the outputs of the eBTM model in a statistically robust manner. The visual interpretation of the results, together with the comparison of the 2008 flood line reference data and discussion of the results with domain experts imply however that the eBTM produces more realistic inundation extent results than the sBTM. The eBTM can thus be used for rapid coastal (temporary) inundation assessments, undertaken on existing (low-spec) computing infrastructure and without the need for specialist inputs. The eBTM results can therefore add value for the purpose of disaster management, coastal management, spatial development etc. particularly in the risk assessment context to improve on existing coastal development planning processes.

However, the GIS based models use static input data and produce a static output, unlike HDm models which enforce the laws of physics (Woodruff, Vitro & BenDor 2018). Therefore, the inundation produced by the eBTM may underrepresent coastal inundation resulting from wind driven storms (Wong et al. 2014). Nock (2014) states that all coastal inundation assessment approaches invariably rely on modelling techniques and that it is important to understand the purpose of the model and what the model aims to achieve.

It is therefore important to reemphasise that the purpose of the eBTM is to achieve the most accurate ‘average’ result. It ‘sacrifices’ theoretical accuracy i.e. atmospheric and tidal forces such as wind and surface waves, but improves on the empirical accuracy i.e. including slope, surface roughness and hydrological connectivity (Shmueli 2010). Provided that the purpose and limitations of the eBTM are clearly stated, the model is nevertheless useful as a static method for communicating coastal risk and raising awareness (Gallien, Sanders & Flick 2014). **It is not intended to be used as a predictive tool** as it excludes components such as atmospheric and tidal forcing, which vary with each storm event.

When comparing the DTM-DSM outputs (Section 4.5.2), the high (1 m) resolution of the raster data influenced the inundation extent such that the overestimation of the DTM is largely due to less obstructed horizontal movement rather than penetrating further inland. However there are exceptions where inundation using the DTM does penetrate further inland (Figure 4.10). The use of the DTM is therefore less realistic for short term inundation scenarios as it provides an unobstructed environment over which the inundation can move. However, it may be useful for determining shorelines in the light of longer term sea level rise and in storm related inundation scenarios where the presence of surface structures may not play a role e.g. in undeveloped areas. The inundation mask produced using the DSM shows clearly defined water pathways based on the inclusion of buildings and slope of the

land. This is useful in planning for short term events where evacuation routes can be determined. Storm surge data are important to inform coastal planning interventions such as managed retreat as well.

Test three (section 4.5.3) showed the implications of using different DSM resolutions and confirmed that high resolution (1 m) is preferred. In the context of the study site, many roads and thoroughfares were less than 5 m wide and therefore using a DSM resolution  $\geq 5$  m as the downscaling of the original 1 m resolution DSM led to the creation of mixed pixels in these “street canyons” with artificially higher elevations. These areas worked as barriers in the eBTM process and wrongly constrained the propagation of inundation. A recommendation in this regard would thus be that in the absence of a high resolution DSM ( $< 5$  m) to rather make use of a coarser resolution DTM ( $\geq 5$  m) to avoid creating artificial barriers.

Both the surface roughness and beach slope were incorporated into the development of the eBTM. The eBTM includes beach slope discretely i.e. it is derived from the input DEM without any user intervention (step 6 of Figure 4.2). The user is however required to specify a surface roughness coefficient that is representative primarily of the beach, but ultimately the rest of the study site. Test four showed that the impact of the roughness on the flood extent is significant. However, the static and uniform roughness coefficient that is currently used as input in the eBTM, is a known limitation of the model as in reality, inundation water would traverse over different surfaces like beach sand, tarred roads and vegetation, which have different roughness coefficients. A desirable improvement for the eBTM would therefore be the use of a continuous ‘roughness raster surface’ for the respective study site, ideally at the same spatial resolution as the input DSM, rather than a single roughness coefficient. A land cover map could serve as the baseline for such a continuous roughness layer. However, in South Africa, existing land cover data such as the National Land Use/Land Cover dataset are available at 30 m resolution which might be too coarse for use in this context. It is however possible to produce different versions of the eBTM model and tool which would provide the choice of using either a single RC value for novice users or a spatially continuous RC raster layer for more experienced GIS practitioners.

One of the eBTM’s primary benefits in its current version is that it is not ‘data hungry’ and effectively only requires a DEM as tangible input layer to define the topography and slope of the study site and derive a coastline (in the absence of an existing one). A limitation is however that the use of the eBTM requires an ArcGIS Spatial Analyst extension in addition to the ArcGIS desktop software.

Coastal practitioners making use of the eBTM (or other coastal inundation models) should be aware that mismatching vertical datums have the potential to influence the accuracy of the model i.e. bathymetry is referenced to chart datum while terrestrial elevation models are referenced to LLD. These usually have a vertical offset of several decimetres (in Cape Town the offset of chart datum to LLD is approximately -0.8 m). This offset differs between areas. Therefore, when undertaking inundation modelling, all data must be corrected to the same vertical datum. In terms of utilising the eBTM, the model produces water levels relative to the vertical datum of the DSM, which in this case is LLD.

In order to make the eBTM accessible to practitioners it was packaged as an ArcGIS Toolbox with GUI interface. The GUI tool therefore responds to the need voiced by the practitioners for an approach that is:

- easily repeatable and structured;
- does not require advanced specialised expertise;
- implementable over a large area;
- quickly executable; and
- able to be undertaken without the need for sophisticated technologies e.g. high-performance computing.



## CHAPTER 5: DETERMINING THE INUNDATION HAZARD AND BUILDING HAZARD EXPOSURE PER SCENARIO AND HAZARD PROBABILITY

### 5.1 DETERMINING THE INUNDATION HAZARD PER SCENARIO AND HAZARD PROBABILITY

Chapter 4 aimed at developing the eBTM and to assess its performance through testing against ground-truthed historical inundation data, the sBTM and by varying some of the input parameters. Having its validity established, in this chapter, inundation extent maps for a statistical 1-in-100 years storm surge event and two predicted sea level rise scenarios will be produced (section 5.1.1), based on which coastal inundation hazard probability scores for buildings in the coastal zone will be established (Section 5.1.2). The purpose of this approach is to provide quantifiable information for long term spatial planning and adaptation in the coastal zone.

#### 5.1.1 Producing coastal inundation extent maps

##### 5.1.1.1 eBTM setup for hazard map development

Hazard maps are intended to spatially depict the areas that may be affected by a defined hazard (Nandi et al. 2016). For the development of inundation hazard maps relating to a statistical 1-in-100 years storm surge scenario and considering two different sea level rise scenarios as established in Table 4.3, the eBTM was used. The datasets used in this analysis are summarised in Table 5.1. The technical details on how these datasets were derived were presented in section 4.2.2.

Table 5.1 Datasets used for coastal inundation hazard modelling using the eBTM

Dataset requirement	Input data
Digital elevation model	1 m resolution digital surface model (DSM)
Slope	Derived automatically from the 'grid 3' LiDAR DSM derivative (section 4.2.4)
Coastline	Shapefile line derived from the DSM
Sea levels	As per Table 4.3: scenario one = 1.79 m, scenario two = 2.17 m and scenario three = 2.61 m
Roughness coefficient	A uniformly assumed value of 1

The eBTM was run in ArcGIS 10 and required the Spatial Analyst extension. The computer used for the processing had an i7 CPU with 8GB RAM.



### 5.1.1.2 Results and discussion

For each study site and scenario, binary maps were produced illustrating where coastal inundation is likely to occur in the absence of external atmospheric and oceanographic forcing factors. These maps are displayed in Figure 5.2 for Fish Hoek and in Figure 5.3 for Strand. The total surface area that would be inundated under such conditions on both sites is shown in Figure 5.1.

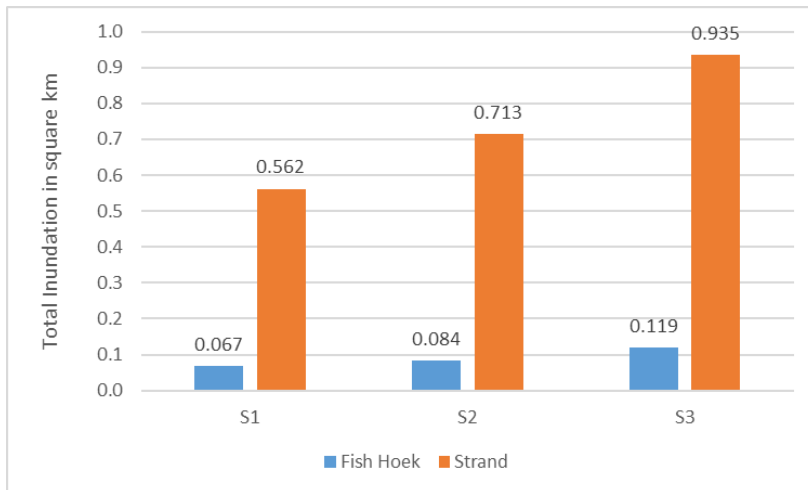


Figure 5.1 Comparison of total inundated area the 3 sea level scenarios for Fish Hoek and Strand

As expected, for both sites the total inundation area increases with increasing input inundation water level. Give the smaller extent of the Fish Hoek study area, the total inundation area is smaller than for Strand.

Figure 5.2 shows the inundation extent for the three scenarios in Fish Hoek. This figure shows that the residential and/or holiday accommodation in the Seaside Cottages development, despite its proximity to the beach are unaffected by all three the coastal inundation scenarios. The buildings are located behind a large dune which, according to the model outputs, provides protection against high water levels.

If inundation were to be experienced in that area, it would likely be caused by either the Silvermine River bursting its banks or due to saturation of the water table which is not featured in the eBTM. Since the area is relatively low-lying, the dune may contribute to the pooling effect if water is trapped behind it and there are no subterranean drainage systems present to channel water away. The cottages directly behind the dune however may be slightly less affected as they tend to be higher lying than those located in the more central area of the development.

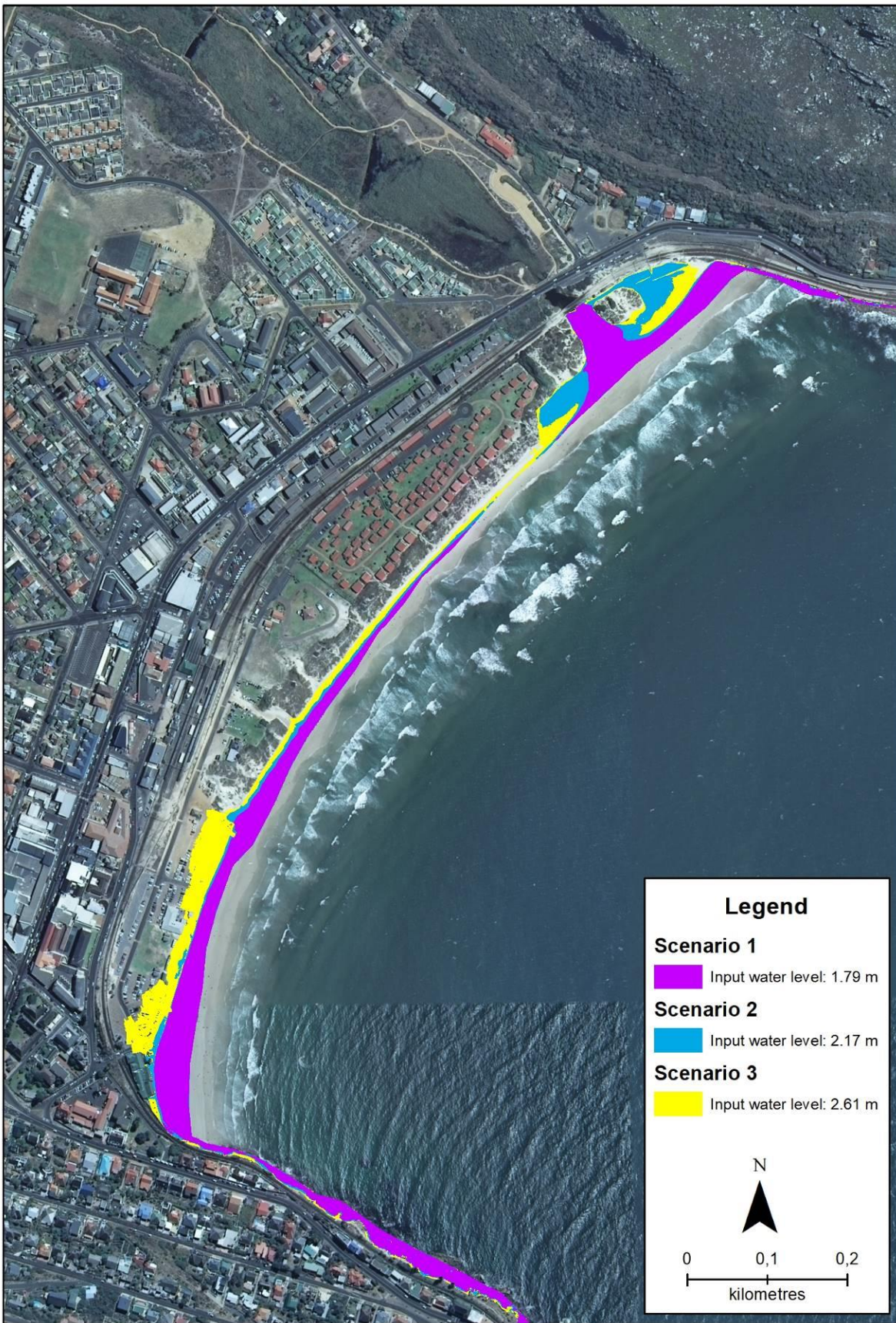


Figure 5.2 eBTM results for Fish Hoek for all three inundation scenarios

Scenario two and three in Figure 5.2 show that if coastal waters are pushed into Silvermine River mouth, there is the potential for inundation of the banks near the river mouth, however there are no buildings or structures present in that area. While protected from direct coastal inundation, it is unclear if these developments would be affected by flooding originating from the river catchment e.g. after heavy rainfalls or in a compound event of a combined coastal surge and river flood. In the absence of a protective dune, the parking area and restaurant in the southern area part of the study site will likely be affected by coastal inundation, which is most prominently demonstrated in scenario three (Figure 5.2).

The developed areas in the study area in Strand are more affected by flooding than in Fish Hoek, given the generally low elevation of that area with less than 4 m above mean sea level. Unlike Fish Hoek, dense development occurs directly opposite the beach. Consequently, all the scenarios presented in this study result in inundation occurring that affects buildings (Figure 5.3).

The northern Lourens River bank in the north of the Strand area shows inundation for all scenarios, increasing in severity as the input inundation water levels increase. South of the Lourens River, the wider beach as well as a dune belt protect the buildings from inundation, unlike the remainder of the study site. Scenario one (Figure 5.3) produced some inundation in the more southern area of the study site, while buildings in the rest of the study site remain unaffected. Scenarios two and three however show widespread inundation in the central and southern areas.

Through scenarios two and three, water pathways can be determined as the high resolution DSM demonstrates where inundation water may enter the developed area and move relatively unobstructed. These pathways may allow water to travel further inland, guided primarily by topography and surface structures as wave and wind energy may dissipate the further water moves inland. This is particularly evident in scenario three (Figure 5.3) where many roads are serving as conduits for water passage.

Considering the ability of the eBTM tool to produce scenario based inundation outputs, the model runtime for each scenario was recorded. For all six model runs (three for Fish Hoek and three for Strand) the runtime ranged between 2 min 13 s to 2 min 39 s and 6 min 27 s to 7 min 41 s and respectively. These figures demonstrate that the eBTM tool can be executed without requiring high power computing infrastructure or specialist knowledge. This is important as meaningful results can be provided to relevant decision makers for improved coastal development planning without high spec computers being required.



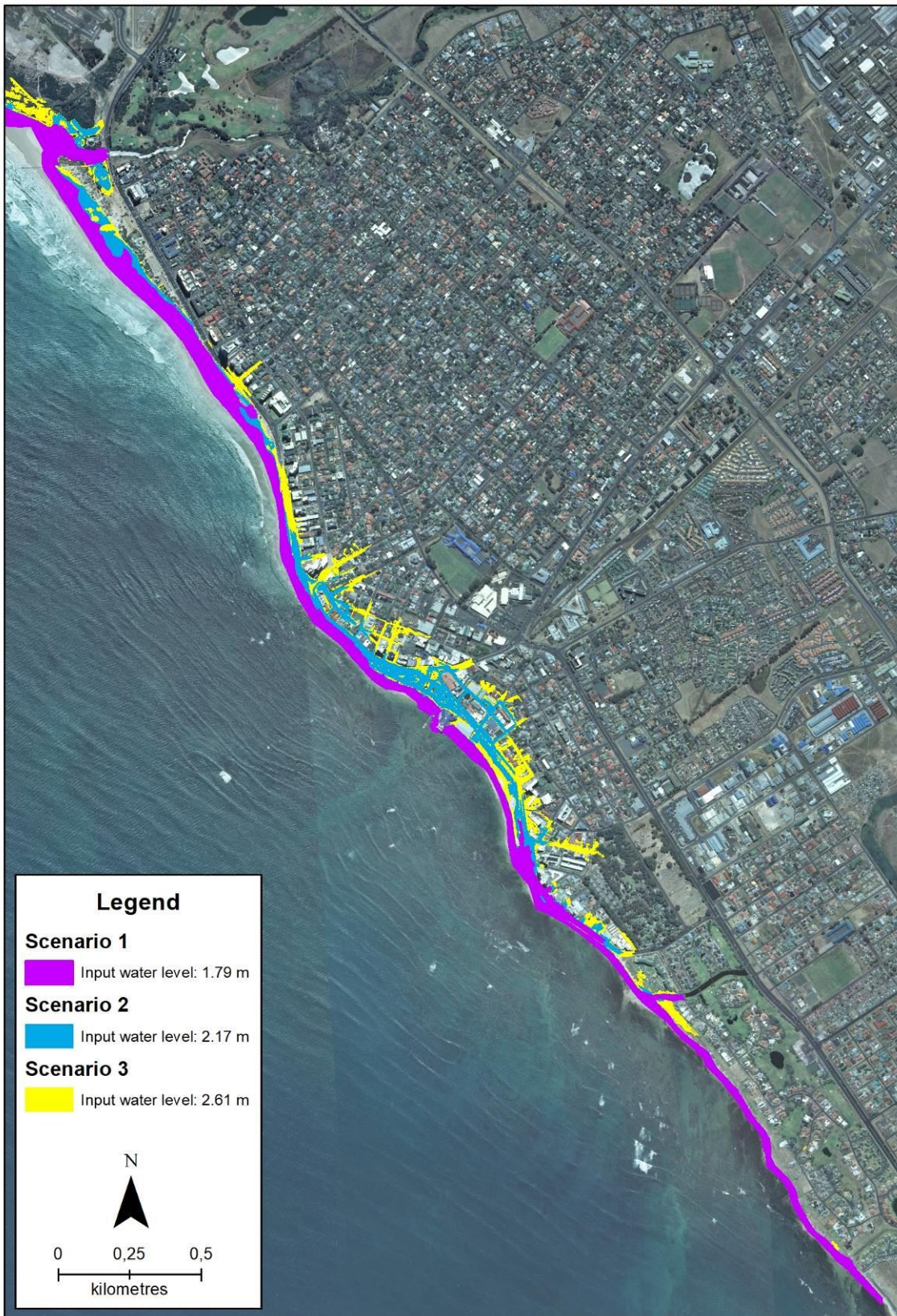


Figure 5.3 eBTM results for Strand for all three inundation scenarios

Based on historical inundation observations in Strand, the eBTM scenarios show good correlation with observed results in terms of general location of previously occurred inundation i.e. the central region of the study site (Bekko 2018, Pers com). Buildings in this area were regularly affected by inundation hazard (Roux 2018, Pers com).

The use of the DSM as input data to the eBTM was beneficial as the outputs present inundation pathways and also the potential inland inundation extent. The inundation pathways are useful for disaster management officials as they provide insight as to which roads would potentially be unsafe to travel on during a storm event as it is likely to be subject to inundation. Similarly, 'safe roads' are therefore also identifiable through the use of the eBTM. This is particularly evident in Strand (Figure 5.3), with many roadways acting as water conduits. Conversely, in Fish Hoek (Figure 5.2), there is limited coastal development and the southern part of the study site allows inundation to travel without many obstructions. The eBTM derived inundation limits are useful even with tidal and atmospheric forcing excluded, as it shows the areas that are likely to be affected by inundation and allows decision makers to focus on these hotspots.

One challenge with the derived results is to validate their accuracy. The work presented in Chapter 4 used some few historical inundation extent data to estimate the eBTM's performance. However, the inundation maps developed and presented in Section 5.1 are based on forward looking, predicted storm and sea level rise scenarios. It is therefore inherently difficult to assess their validity with currently available data. In addition, It is important to note that the results achieved here in terms of the eBTM differs from other initiatives such as the development of coastal management lines (in terms of the Integrated Coastal Management Act) where risk lines, comprised of multiple hazards, have been determined for different time horizons and at coarser resolutions i.e. >100 m, predominantly using HDm. The eBTM produces high resolution (1 m) inundation masks in a GIS environment.



## 5.1.2 Determining the building hazard probability

Following the production of the coastal inundation hazard maps (Section 5.1.1), this section describes the hazard scoring framework against which the buildings were assessed.

### 5.1.2.1 Hazard probability scoring

From the coastal inundation hazard results (section 5.1.1), the hazard probability scoring for each building in the coastal zone was derived. The second input data for this component were building roofprints that were manually digitised into .shp polygons (buildings.shp) from 2014 aerial imagery available from the City of Cape Town for each study site. The hazard score indicated how many of the three scenarios would affect a building. The hazard probability scoring framework is presented in Table 5.2:

Table 5.2 Hazard probability scoring framework

Total number of scenarios affecting buildings	Hazard Score
Affected by at all three scenarios	4 (high)
Affected by two scenarios	3 (medium)
Affected by one scenario	2 (low)
Not affected by any of the presented scenarios	1 (very low)

### 5.1.2.2 Hazard probability mapping

As each building is only scored in accordance with Table 5.2, the maximum achievable score is four and the minimum is one. The hazard probability scores were added to the building.shp file in a new attribute column in ArcGIS software.

In Fish Hoek, all buildings below Main Road were assessed. In Strand all buildings along Beach Road and seaward of De Beers road were assessed, in addition to the buildings identified as being affected by the scenarios. Where buildings further inland were found to be affected, the surrounding buildings were also assessed. Buildings that were excluded were those where the author did not have access to the premises or the building was not visible e.g. in gated community surrounded by solid walls. However, it must be noted that these buildings are likely to be unaffected due to the solid walls serving as protection for those buildings.

### 5.1.3 Results and discussion

The spatial statistics for the scores are shown in Table 5.3. There are large numbers of unaffected buildings as the mapped buildings extend far beyond the inundation risk zones for all three scenarios. For both Fish Hoek and Strand, there are very few buildings that would be affected by all three scenarios (1 and 6 buildings respectively). Scenario 3 (score = 1) represents the worst case for this study and therefore buildings only affected by this scenario are considered to be in relatively safer locations than buildings affected by scenario 1 and scenario 2. Most affected buildings occur in Strand. The total number of buildings affected in both sites for the three scenarios is given in Table 5.3 and the maps indicating locations of the buildings and hazard scores in Figure 5.4 and Figure 5.5.

Table 5.3 Number of buildings per study site affected by the coastal inundation hazard scenarios

Study site	Total buildings assessed	Not affected (hazard score = 0)	Affected by scenario 3 (hazard score = 1)	Affected by scenario 2 & 3 (hazard score = 2)	Affected by scenario 1, 2 & 3 (hazard score = 3)
Fish Hoek	206	202	3	0	1
Strand	716	524	114	72	6

In Fish Hoek, 202 out of the total 206 digitised buildings are unaffected (indicated in blue in Figure 5.4) with only four being affected. Three buildings are indicated to be affected by scenario three and the one building to be affected by all scenarios (green and red in Figure 5.4 respectively). These affected buildings are located in the southern area of the study site and relatively close to the beach with little or no protection that could serve as a defence against incoming inundation water.

The revetment and low sea wall in the southern area serve as protection for the buildings located directly behind it for scenarios one and two. On close inspection of these eBTM outputs in Figure 5.2, it is clearly observable that scenarios one and two abruptly stop at the top of the revetment where the sea wall occurs. In some areas scenario two does present some inundation landward of the sea wall, but still does not affect the buildings. However, scenario three breaches the sea wall resulting in the buildings behind it being affected (Figure 5.4). Unlike the buildings that benefit from the protection of the revetment and sea wall, the restaurant is affected by all three scenarios.



Figure 5.4 Building hazard score map of Fish Hoek (numbers in brackets give the total number of buildings per class)

In the northern area the dune seemingly serves as good physical protection for the Seaside Cottages development, provided it remains stable. However it is already observed to be subject to erosion (author's observation in Dec. 2017, Figure 3.6). In this context, the current activities described by the CCT of sand being actively removed from the beach in order for the high water mark to move further inland for the purpose avoiding wind-blown sand is of concern, as this may result in more energetic wave action affecting the dune during storm events, thereby further encouraging erosion.

In Strand (Figure 5.5), six buildings are exposed to all three scenarios (red), 72 buildings are exposed to scenarios two and three (yellow) and 114 buildings are affected only by scenario one (green). In total, 524 buildings are unaffected by the scenarios.



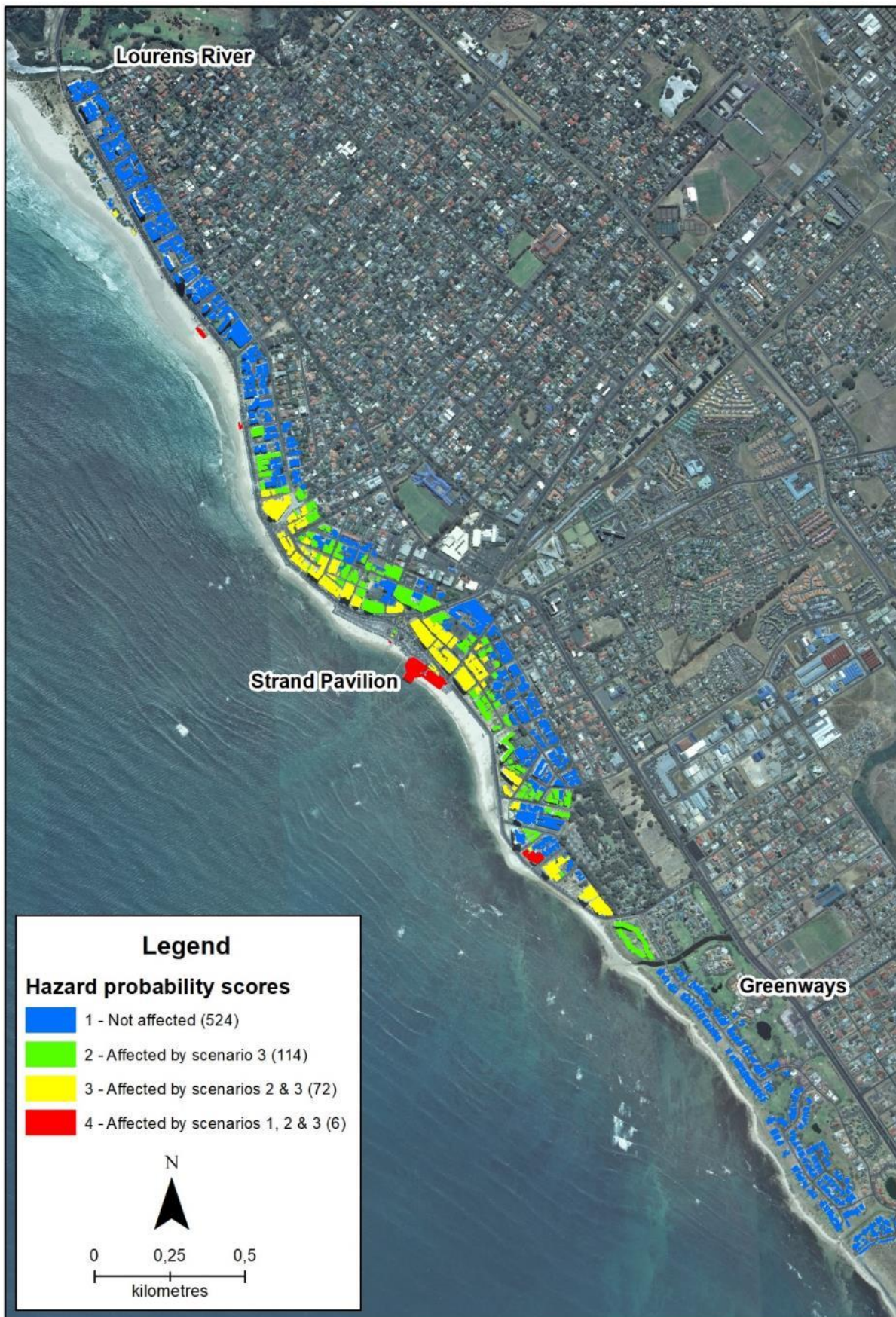


Figure 5.5 Building hazard score map of Strand (numbers in brackets give the total number of buildings per class)



The northern area of this site is dominated by buildings that are unaffected by any of the inundation scenarios. This is likely due to the wide beach, protective dunes and recreational area that separates the buildings from the sea. Notably, the affected buildings are predominantly located in the central region of the study site and further southwards where the beach is narrow and the dunes and recreation area are discontinued. At the Greenways Estate in the south of the study site, the buildings are also unaffected despite the beach being very narrow. This is due to the area being elevated relative to the beach level and due to the construction of a rock revetment to prevent erosion. However, following the construction of the revetment, it has been observed that wave energy is now being deflected northwards i.e. towards the central and southern region of the study site (Bekko 2018, Pers com). The energy contribution is most notable during storm events (Figure 3.15).

## **5.2 ASSESSING BUILDING HAZARD EXPOSURE**

Hazard exposure manifests as the interaction between the hazard and the receiving environment and provides an indication of what is at risk (or negatively affected) when a hazard takes place (Dilley et al. 2005; Hahn, Villagrán de León & Hidajat 2003; van Westen 2013). While in section 5 the probability for buildings to be exposed to coastal inundation was assessed, this section will assess how severely the respectively buildings will be affected in terms of inundation depth. The methods and the results will be presented for both study sites.

### **5.2.1 Building hazard exposure assessment**

Input data for this assessment are the building.shp file created in section 5.1.2.1 and the inundation maps for the third inundation scenario produced in section 5.1.1, assuming this scenario to be the worst likely. The way the eBTM is set up, the inundation depth per pixel is written out in the attribute table of the respective inundation maps, as described in section 4.2.4 (Figure 4.2, steps 12 and 13). These inundation depths however exclude wind-driven surface waves, whose influence might cause the actual inundation depth to be higher.

The continuous inundation depth values were then re-classified into “severity” classes. Generally, as to the author’s knowledge, no data exist that explicitly define and quantify flood (or inundation) water levels and/or flow rates that would potentially pose a threat to human life and/or disruption to activity.

For the purpose of this study, the indicators, scoring and weightings were developed in consultation with the Western Cape Government Disaster Management Centre (WCDMC) in October 2016 as the existing hazard scoring criteria suggested by the National Disaster Management Centre (South Africa 2016) were deemed to be too broad. The criteria proposed by the NDMC for the respective categories

(i.e. probability, frequency, predictability and magnitude) were not well defined and relied primarily on qualitative assessment e.g. “low” to “medium” magnitude. Qualitative responses are generally based on individual perception rather than factual or quantitative measurements. Consequently FEMA (2013) was used as a “more quantitative” reference which defines “shallow flooding” as water levels not exceeding 3 feet (approximately 0.9 m). This approach was agreed on in consultation with disaster management officials as well as local and international experts in risk assessment processes.

For better discrimination, the experienced inundation depths with a range between 0.0 m and 0.61 m were subdivided into 0.3 m intervals (i.e. ~1 foot) for shallow flooding<sup>18</sup>, following FEMA (2013) as per Table 5.4.

Table 5.4 Building hazard exposure scoring categories

Inundation depth	Hazard exposure score
0 m	0 (not exposed)
0.1 m to 0.3 m	1 (low)
0.31 m to 0.6 m	2 (moderate)
> 0.61 m	3 (high)

Based on the scoring (Table 5.4), the minimum and maximum scores that can be achieved in terms of the building hazard exposure are:

- Minimum hazard exposure score value = 0
- Maximum hazard exposure score value = 3

The use of the DSM to produce eBTM inundation masks means that buildings were excluded and thereby produced ‘holes’ in the inundation mask. The maximum inundation depths were therefore attached to each building using the ‘select by location’ tool in ArcGIS and applying a search radius to each building e.g. search for the inundation mask(s) located within 2 m of the building. The buildings were then scored according to Table 5.4. Where buildings were located across class boundaries, the individual building was assigned the maximum inundation depth value, and scored accordingly.

---

<sup>18</sup> Shallow flooding is defined as flood waters not exceeding 3ft (i.e. ~ 0.9 m) (FEMA, 20013)

## 5.2.2 Results and discussion

Those 202 buildings in Fish Hoek and 524 in Strand that were unaffected by any inundation scenario (Section 5.1.3) were assigned a hazard exposure score of 0 (not exposed). In Fish Hoek, three buildings experienced water depths of 0.3 m or less, while one building experienced water depths of 0.31 m to 0.6 m. No buildings experienced water depths exceeding 0.61 m. The hazard exposure score map for Fish Hoek is reflected in Figure 5.6.

In Strand, of the affected 192 buildings, 96 buildings experienced inundation water depth of 0.3 m or less (low exposure), 59 buildings experienced water depths between 0.31 to 0.6 m (moderate exposure) and 37 buildings are experience water levels greater than 0.61 m (high exposure) (Figure 5.7). Notably most buildings classified as having high exposure experience maximum water levels in the range of 0.62 m to 0.65 m and are located on the landward side of Beach Road, with the exception of the Strand Pavilion building which experiences water a maximum water level of 2.2 m.

Figure 5.7 shows that the buildings in the northern region of Strand are unaffected by all scenarios (blue). The northern area includes a small dune, green belt and has a wide gently sloping beach. Buildings with low (green), moderate (yellow) and high (red) hazard exposure scores are observed in the central region of the study site, extending southwards. This area has a much narrower beach than the northern area. Notably in the central area affected buildings occur further inland, indicative for the very low surface elevation in this area. Observing southwards, only buildings occurring directly along the beach have either moderate or high scores. Few buildings scoring low (green), indicating <0.3 m inundation depth, are observed further inland. In the Greenways Golf Estate, south of the canal, all buildings have low hazard exposure scores which can be attributed to the rock revetment which was constructed to protect properties.



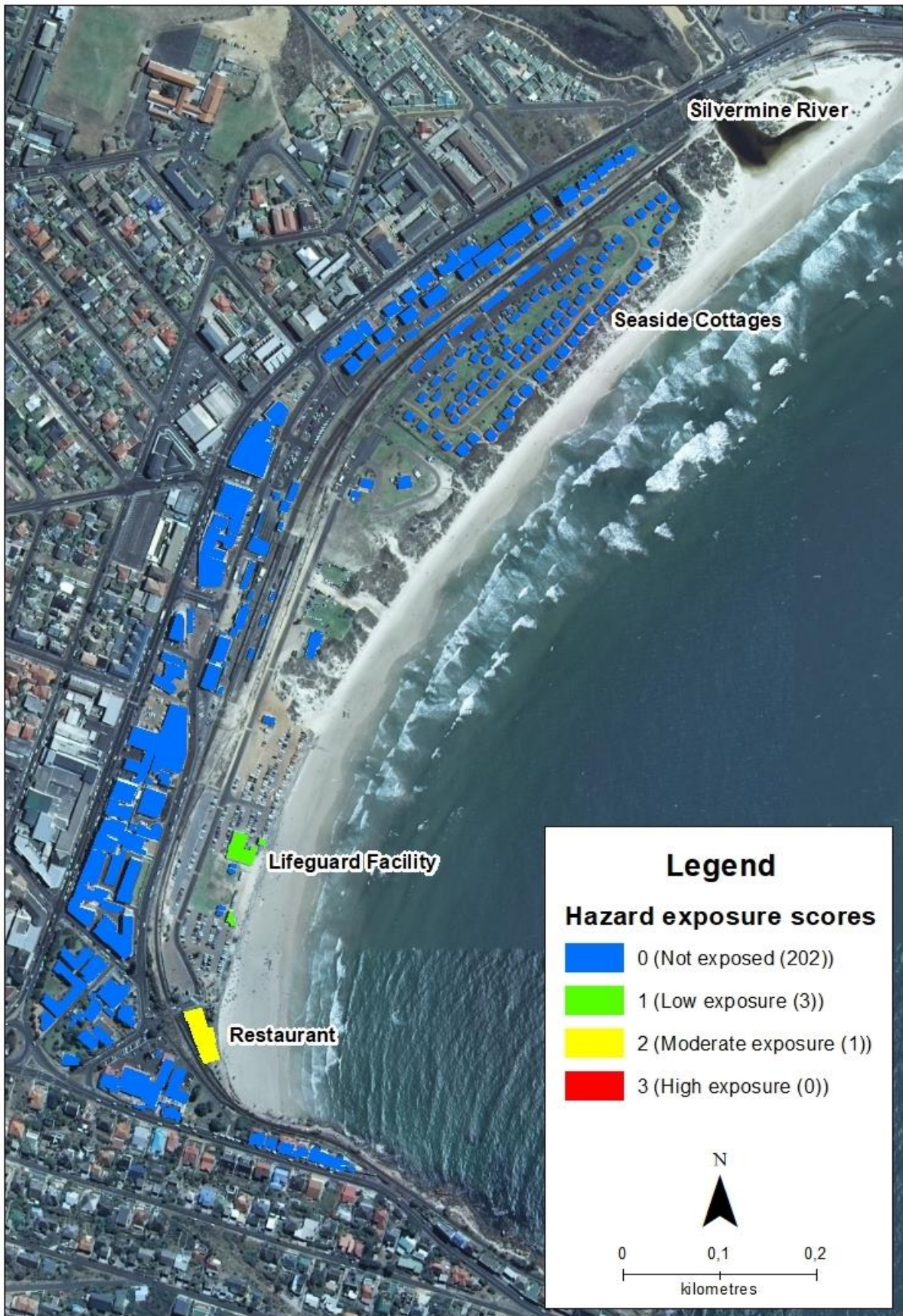


Figure 5.6 Hazard exposure score for buildings in Fish Hoek



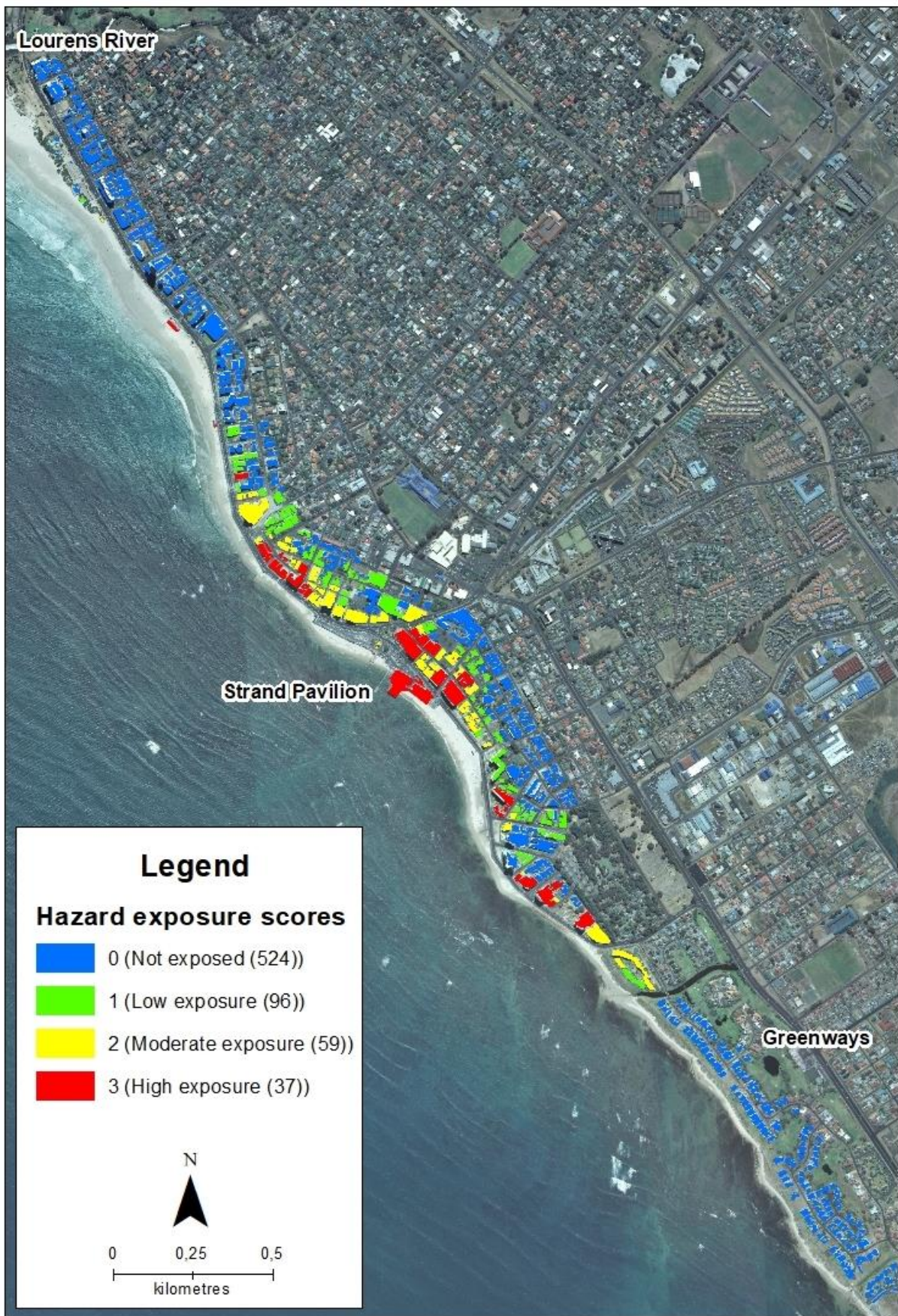


Figure 5.7 Hazard exposure score for buildings in Strand



### 5.2.3 Sub-conclusion

Section 5.1, together with Chapter 4 concludes the response to the first research question i.e. *How can a GIS based coastal inundation model be developed that is more accurate than the existing simple Bathtub Model (sBTM), but simpler and quicker to apply than Hydrodynamic Modelling?*

Based on the eBTM derived inundation extent, it was determined where inundation will occur (Section 5.1.1) and the probability of the buildings being impacted by the inundation hazard (Section 5.1.2). Altogether the results show fewer buildings being affected by coastal inundation than initially anticipated, particularly considering that many buildings are located close to the shore in both study sites.

The hazard probability scoring framework presented here was based on the three pre-defined hazard scenarios. However, it can easily be customised to other user defined scenarios. The hazard score maps presented (Figure 5.4 and Figure 5.5) can be used to effectively identify and communicate buildings that are likely to experience coastal inundation hazard. In the broader context of this study the results satisfy the hazard part of the risk equation i.e.

$$\text{Risk} = \text{Hazard} * \text{Hazard Exposure} * \text{Vulnerability}$$

Equation 5.1 Risk equation used in this study

Papathoma-Köhle et al. (2017) stated that the limitation of assessments using vulnerability indicators was that they primarily considered building characteristics and not the intensity of the hazard process. This study addressed that gap by assessing hazard exposure independently (following Dilley et al. 2005; Hahn, Villagrán de León & Hidajat 2003; van Westen & Greiving 2017). The hazard exposure maps (Figure 5.6 and Figure 5.7) presented in Section 5.2.2 inform the user of the potential maximum water depth that can be experienced relative to the DSM and the inundation water height.

Having these hazard exposure maps for coastal inundation has multiple benefits. They can inform mitigation planning and responses as it was demonstrated that not all buildings may be exposed to coastal inundation hazard events though they may be located in close proximity to the coast. Secondly, these maps provide an exposure footprint of the receiving environment for coastal inundation hazard. Bigger inundation hazard events are likely to result in bigger exposure footprints and therefore having these data available can assist in improved planning for extreme inundation events. Lastly, maps reflecting hazard exposure at the local level can be used to inform communities of how they could be affected during an inundation hazard event and therefore allow individual property owners to take decisions on how they could protect their assets (Hahn, Villagrán de León & Hidajat 2003).

Section 5.2 responds to the exposure classification component of the second research question i.e. *How can buildings be categorised according to their exposure and vulnerability to coastal inundation hazard?*

## **CHAPTER 6: ASSESSING BUILDING VULNERABILITY**

As presented in Chapter 2 (Table 2.1), there are many different approaches to calculating risk. Often hazard exposure (as per Section 5.2.1) is included as a component of vulnerability, however for the purpose of this study it was intentionally evaluated independently, following Dilley et al. (2005), Hahn, Villagrán de León & Hidajat (2003) and van Westen & Greiving 2017.

One of the reasons for this separation is that, as mentioned in Chapter 2, buildings are currently not assessed in terms of their vulnerability in South Africa, nor are there relevant buildings codes (standards) to encourage the construction of hazard resilient buildings.

Other vulnerability assessments undertaken in South Africa (and elsewhere) frequently lack focus and need to more specifically address questions such as “Vulnerability of what? To what?”. This component of the research therefore aimed to develop a framework to serve as a baseline for assessing buildings in terms of their vulnerability to coastal inundation and to potentially guide and inform future standards. The process of the development and the results for the two study sites are presented in the following sections.

### **6.1 BUILDING VULNERABILITY ASSESSMENT**

#### **6.1.1 Framework development**

Assessing vulnerability depends on reliable information, including population distribution and descriptive data, exposure of assets, location of buildings and building types as well as the function and purpose of critical infrastructure (Strunz et al. 2011). While vulnerability itself is an evolving concept, there is growing consensus that it needs to capture direct physical impacts as well as the fragility of populations (Birkmann et al. 2006; Polsky et al. 2007; Cutter, et al. 2009; Cho and Chang 2017, amongst others). This led the study to incorporate the occupancy of buildings as a measure of residents’ exposure to inundation, which potentially creates vulnerable situations for people (Wisner et al. 2003).

In order to develop a building vulnerability framework which covers all relevant aspects, it was developed through close interaction with domain experts in order to acquire relevant expert opinion from people familiar with the area and localised hazards, specifically through:

- a workshop with Disaster Management practitioners employed by the Western Cape Government (WCG) on 18 October 2016; and

- personal communication with Dr Juan Carlos Villagrán de León, the Head of the United Nations Platform for Space-based Information for Disaster Management and Emergency Response (UN-SPIDER) on 10 May 2018.

Through these interactions, additional follow up with experts and a review of the literature, a series of indicators relating to four risk categories was determined to assess factors contributing to the vulnerability of the building and its occupants. These are summarised in Figure 6.1 below.

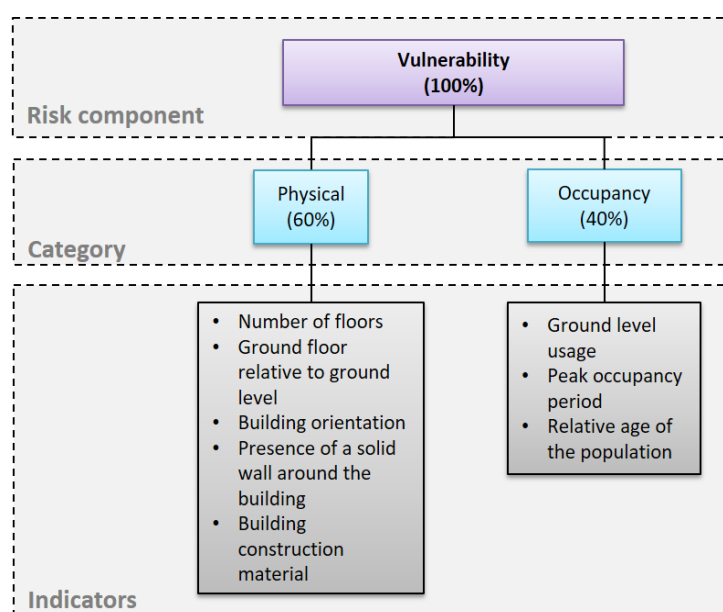


Figure 6.1 Summary of categories, indicators and weightings for assessing building vulnerability

The figure above also shows that the four categories were assigned different weightings (percentages in brackets). These weightings were established through the abovementioned stakeholder interaction. There was general agreement with the WCDMC's practitioners that the physical component should have the most weight (60%). In addition, the physical component also had the most vulnerability indicators against which the individual buildings were evaluated. The occupancy weighting carries the remaining weight (40%) as the physical buildings support various activities and/or functions e.g. residential, restaurants, shops, schools etc. The activities occurring within buildings also provide an indication of the exposed population, e.g. a primary school will have predominantly large numbers of young children, compared to the number of adults, and would thus have a higher vulnerability relative to other occupancy groups.

The vulnerability scoring was designed so that higher vulnerability will get a higher score. The indicators and their respective rationale are presented in Table 6.1 below:



Table 6.1 Building vulnerability categories, indicators and scoring

Grouping	Category	Indicators	Score	Rationale
Physical (60%)	Number of floors (P1)	1	3	The more floors a building has the more scope there is for people to evacuate to higher levels away from the inundation hazard. If a building only has one floor, the primary living space will be affected.
		2	2	
		3 or more	1	
	Height of the ground floor relative to ground level (P2)	Above ground	1	Elevated buildings or buildings with their ground floor higher than ground level will be less prone to inundation and the effects of pooling
		Ground level	2	
		Below ground level	3	
	Building orientation (P3)	Directly facing the coast	3	Buildings facing away from the coast are considered less vulnerable as they have less points of water entry e.g. doors, windows directly facing the incoming inundation hazard
		Orientated away from the coast	1	
	Is the building surrounded by a solid wall? (P4)	Yes	1	A solid wall may act as a barrier by dissipating the energy.
		No	3	
What type of material is the building constructed from? <sup>19</sup> (P5)	Reinforced concrete	1	The construction material used for buildings is directly related to the buildings vulnerability and how it responds to inundation water e.g. buildings constructed from natural materials will be more vulnerable to inundation and soaking than a building constructed from concrete. In this case buildings with similar robustness are grouped based on descriptions available in literature.	
	Masonry or framework <sup>20</sup>	2		
	Prefabricated or baked/natural materials	3		
Occupancy (40%)	Ground level usage (O1)	Medium - High density use	3	The people utilizing the building may be exposed to varying degrees of vulnerability depending on the number of people present. Evacuation may also be hampered in more populated places. The density is defined as follows: Medium - High density use e.g. restaurant, shopping complexes, public transport, indoor markets Low density use e.g. private offices, reception, residential Very low density use e.g. parking, storage
		Low density use	2	
		Very low density	1	
	Peak occupancy period (O2)	Day	1	The time of day that a building is occupied at peak capacity can influence their state of vulnerability. Evacuation is easier during the day than at night.
		Night	3	
	Relative average age of the population occupying the building (O3)	Young children (<10yrs)	3	The average age of people occupying a building can influence the state of vulnerability. Children and elderly citizens are considered to be more vulnerable population groups. Their level of mobility and ability to evacuate to a place of safety contributes to their vulnerability. The building type e.g. school, hospital played a role in guiding the assessment.
		Mixed ages (residential)	1	
		Elderly (>65yrs)	3	

The indicators within each category were developed based on the premise that they would be made available as baseline information to serve in other localised assessments, and that the indicators were transferable to other areas rather than being location specific. They can also be expanded through the introduction of additional indicators, reweighted according to the study objectives and/or customised to be more location specific. In addition, the indicators used were carefully selected and designed

<sup>19</sup> Schwarz and Maiwald, 2008

<sup>20</sup> Reinforced concrete frames with masonry infills (Grünthal, 1998)

such that the vulnerability score of the building will only change if the building is structurally/physically altered and/or the use of the building changes.

The physical, environmental and technological indicators can be assessed through visual inspection or using available data including desktop tools such as Google Maps Streetview, GIS and on site building assessments. The use of these tools and technologies also allows the assessment of buildings for which no local data are available or where physical access is not possible and can reduce field assessments to a minimum, e.g. to confirm whether changes occurred between the date of the image acquisition and the date of the assessment.

The occupancy category is considered to be a more dynamic category and departs from the 'checklist of vulnerable groups' and rather considers vulnerable situations that people move into and out of at any given time (Wisner et al., 2003). This category is also therefore the most subjective in terms of scoring and being more strongly linked to the hazard exposure, and captures the relationship between the physical impacts of coastal inundation (water depth) and fragility of the exposed population (Birkmann et al., 2006; Polsky et al., 2007; Cutter et al., 2009 cited in Cho and Chang, 2017). The complexity and subjectivity of this indicator is therefore that the actual vulnerability will only be revealed when an inundation event is experienced by the population that is present at the time of the event.

### **6.1.2 Framework application on study sites**

The so developed framework was applied to the two study sites in 2017. In a preliminary desktop exercise, the study sites were examined using Google Maps Streetview which had imagery dated 2017 and allowed observation of the areas and navigation along formal roads. Subsequent site visits were conducted at each study site in order to validate the preliminary desktop scores derived from the Google Streetview imagery and confirm they still reflect the current status quo. Building occupancy was initially inferred from the building ground usage indicator and using Google Maps Streetview, but required on site verification, which was subsequently undertaken. Further information for the scoring was derived from additional available (spatial) data, such as CCT zoning scheme (.shp), CCT flood prone areas (.shp) and Statistics South Africa Census 2011 small area level population data (.shp).

Each building located in the hazard exposed area was scored individually. The resulting vulnerability indicator scores were captured in individual attribute fields the attribute table of the buildings.shp polygon and were used to calculate the final vulnerability score per building in ArcGIS using the following formula:

$$\text{Vulnerability Score} = ((P1 + P2 + P3 + P4 + P5) * 0.6) + ((O1 + O2 + O3) * 0.4)$$

Equation 6.1 Vulnerability Score

The minimum and maximum score values that can technically be achieved, based on the scoring provided in Table 6.1 and Equation 6.1, are:

- Minimum vulnerability score value = 4.2
- Maximum vulnerability score value = 12.6

Subsequently, building vulnerability score maps were produced using ArcGIS.

## 6.2 RESULTS AND DISCUSSION

The results of the building vulnerability assessments for both sites are summarise in Table 6.2. The maximum building vulnerability score for Fish Hoek was 8.6 and 9.8 for Strand (out of a maximum achievable score of 12.6). Fish Hoek has a minimum vulnerability score of 7.2, which is higher than that of Strand which achieved 5.2. The average vulnerability score for both sites is 7.5.

For the purpose of displaying the results of this assessment in a meaningful way in a GIS map, the vulnerability scores were divided into 3 equal interval classes, based on the respective data ranges per site (Figure 6.3 and Figure 6.5). Thus, this approach does not allow for immediate across-site comparison. However, having the minimum and maximum values per site (Table 6.2) allows for easy reclassification.

Table 6.2 Summary of building vulnerability results

	Strand	Fish Hoek
Total number of buildings assessed	716	206
Minimum vulnerability score	5.2	7.2
Maximum vulnerability score	9.8	8.6
Average vulnerability score	7.5	7.5
Vulnerability score range	4.6	1.4

In addition, results for the physical building vulnerability indicators, which carry the highest weight in the vulnerability assessment, are presented as graphs for Fish Hoek (Figure 6.2) and Strand (Figure 6.4). This provides insight in terms of the physical vulnerability building profile for each study site.

### 6.2.1 Fish Hoek

In Fish Hoek all 206 buildings within the study site were assessed. Based on indicators and scores achieved (Figure 6.2), Fish Hoek's overall building vulnerability can be described as follows:

- Physical vulnerability: Most buildings are single storey (highly vulnerable) with the ground floor at ground level (moderately vulnerable) and are orientated away from the coast (slightly vulnerable). All buildings are constructed from reinforced concrete (slightly vulnerable) and do not have solid boundary walls (highly vulnerable); and
- Occupancy: Most buildings have low density usage on the ground floor (moderate vulnerability) and are primarily occupied at night (high vulnerability) by a mixed age population (low vulnerability).

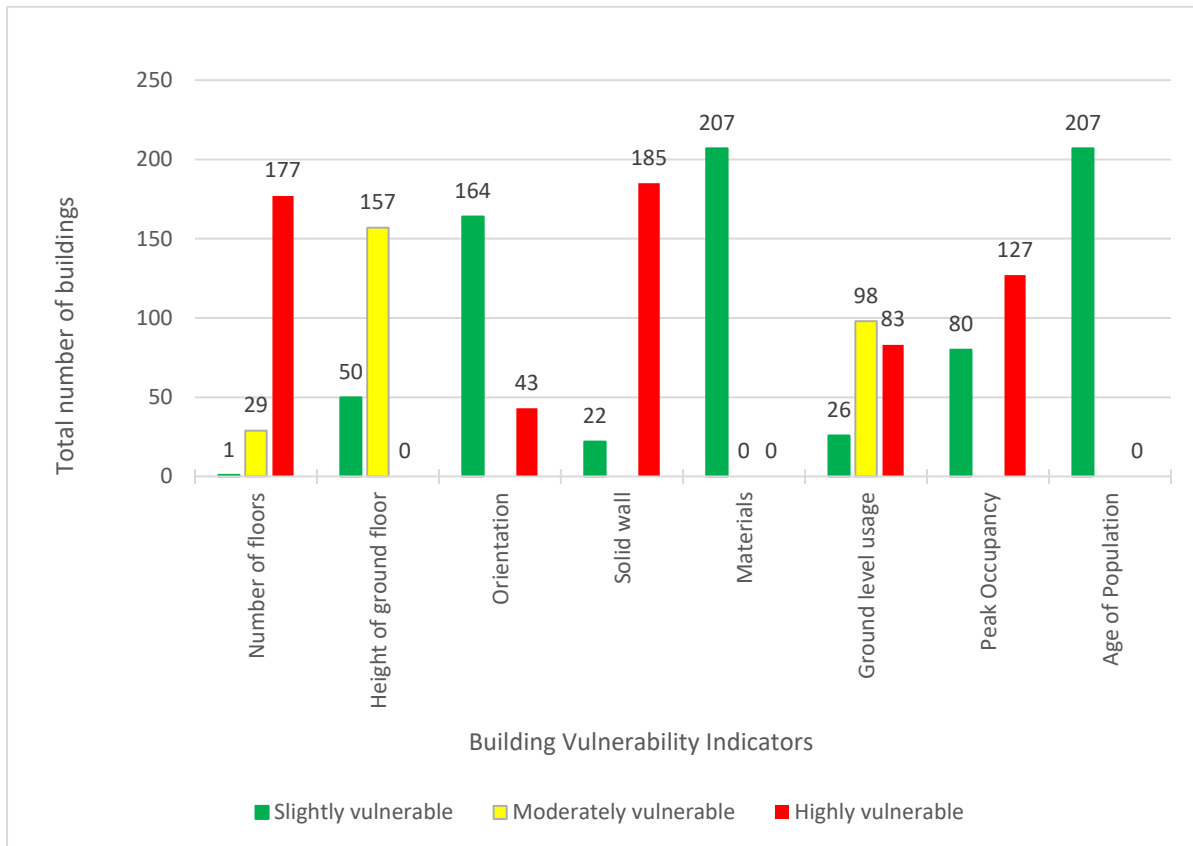


Figure 6.2 Summary of physical building vulnerability indicator scores for Fish Hoek. Zero values are true scores. Data gaps: no data available.

As for the spatial distribution of the final score of the buildings in Fish Hoek (Figure 6.3), all buildings at the Seaside Cottages development have moderate to high vulnerability scores which is primarily due to the physical vulnerability weightings. The development comprises of single storey buildings, built at ground level and without any walls or barriers. The restaurant on the southern end of the beach is also indicated as highly vulnerable, which can be attributed to the lack of protective structures, being a single storey building built at ground level. Unlike the Seaside Cottages development, the restaurant is orientated towards the coast. North of the restaurant, the lifeguard facility buildings have a moderate vulnerability score. These buildings are all situated on the landward side of the sea wall and revetments. During the on-site assessment, the ground floor usage of the biggest building was observed to be primarily for storage and parking of lifesaving vehicles, while human activity occurs



on the 1<sup>st</sup> floor above ground level. The buildings located landward of the railway line primarily have low or moderate vulnerability scores, with the exception of two highly vulnerable buildings, regardless all these buildings are well set back from the coast.

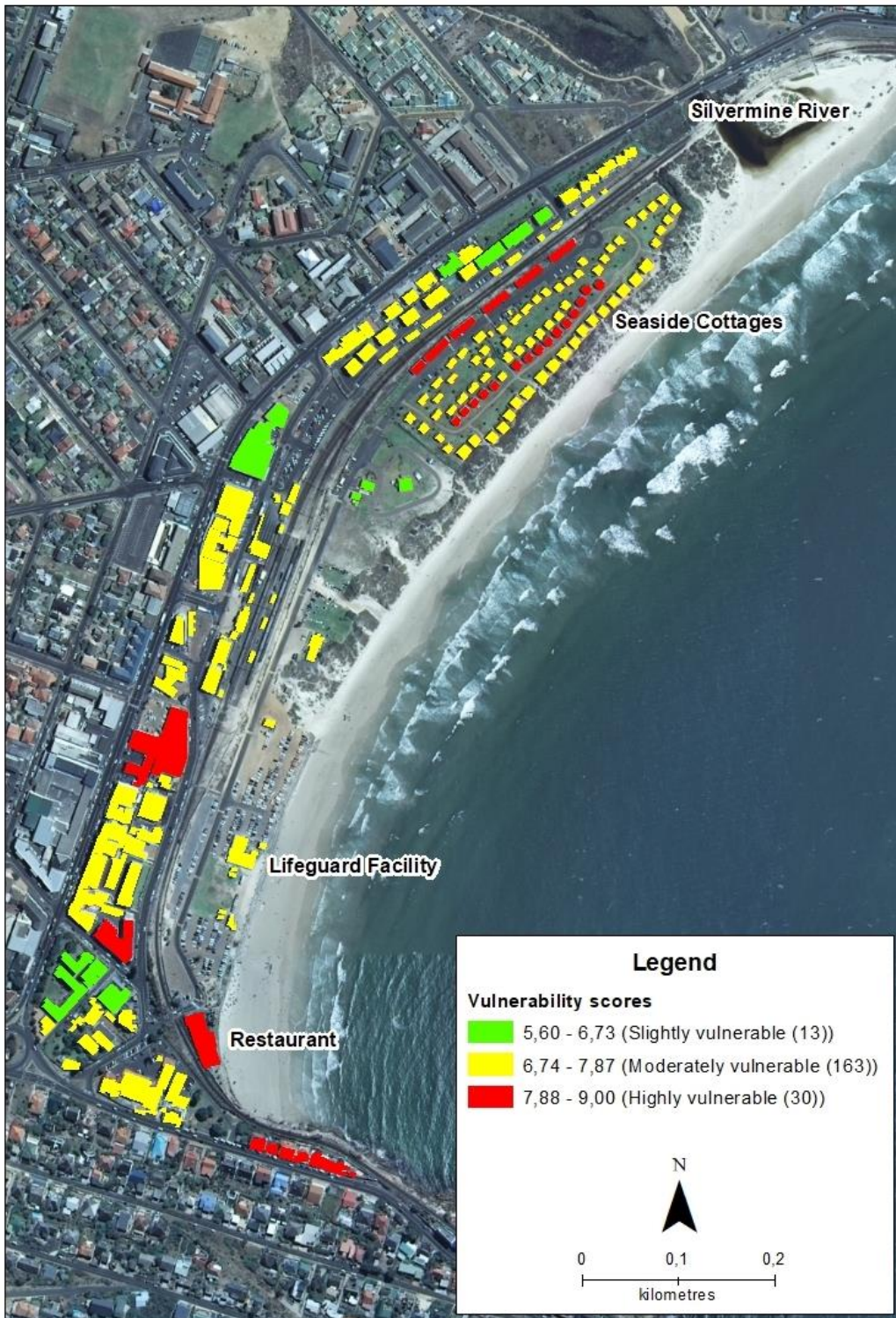


Figure 6.3 Fish Hoek vulnerability per building



## 6.2.2 Strand

In Strand, 716 buildings were assessed. Figure 6.4 shows the overall building vulnerability profile based on the indicators and actual scored values. The situation in Strand can be summarised as follows:

- **Physical:** Most buildings are single storey (highly vulnerable) with the ground floor at ground level (moderately vulnerable) and are orientated towards the coast (highly vulnerable). All buildings are constructed from reinforced concrete (slightly vulnerable) and have solid boundary walls (slightly vulnerable); and
- **Occupancy:** Most buildings have low density ground level usage (moderately vulnerable) and are predominantly occupied at night (highly vulnerable) by a mixed age population group (low vulnerability).

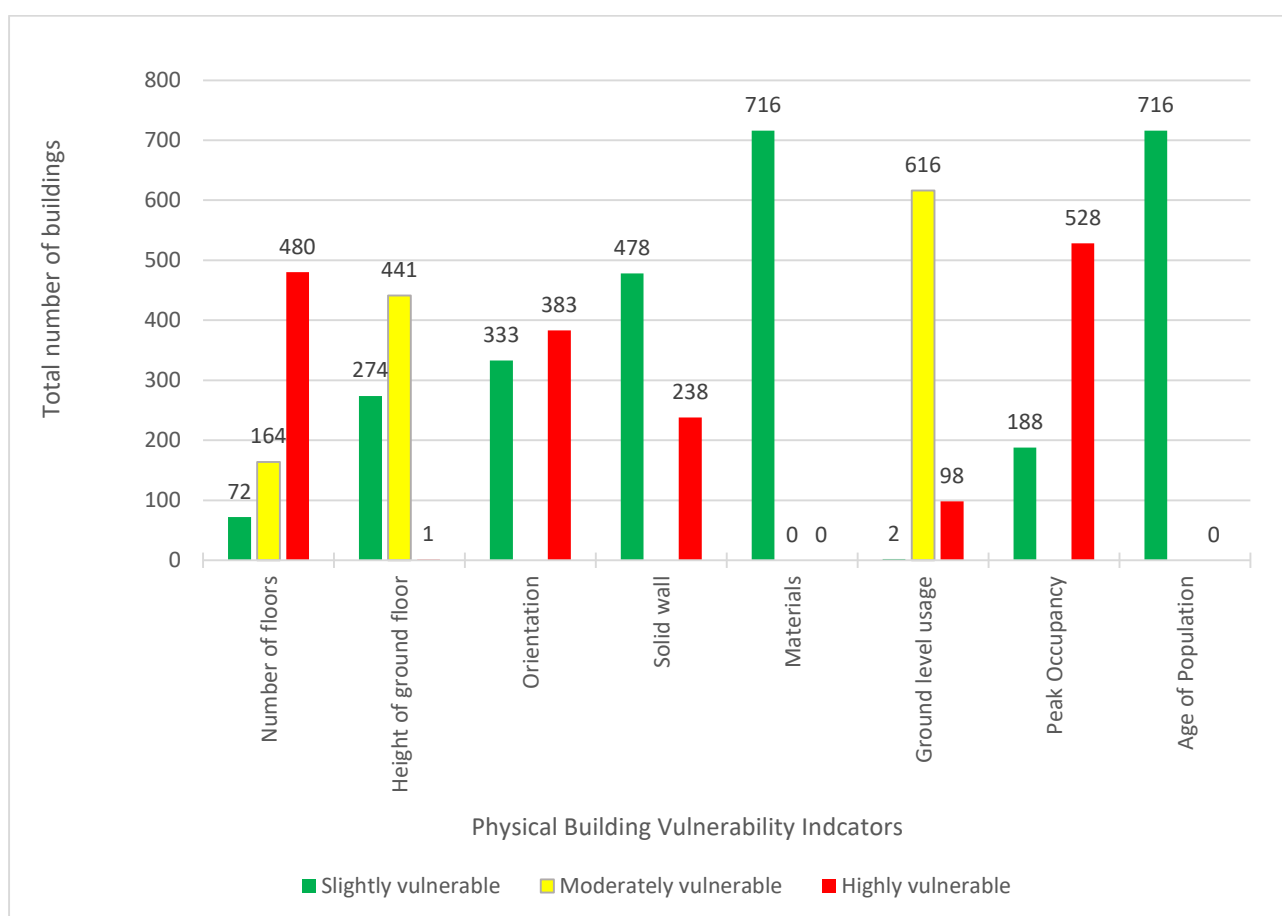


Figure 6.4 Summary of physical building vulnerability indicator scores for Strand. Zero values are true scores. Data gaps: no data available.

Figure 6.5 shows that in Strand 254 buildings are slightly vulnerable, 354 are moderately vulnerable and 108 are highly vulnerable. The northern area of the study site predominantly shows buildings that are slightly and moderately vulnerable. Moderately vulnerable buildings are seemingly interspersed throughout the study site, while highly vulnerable buildings are primarily located in the central and southern areas.

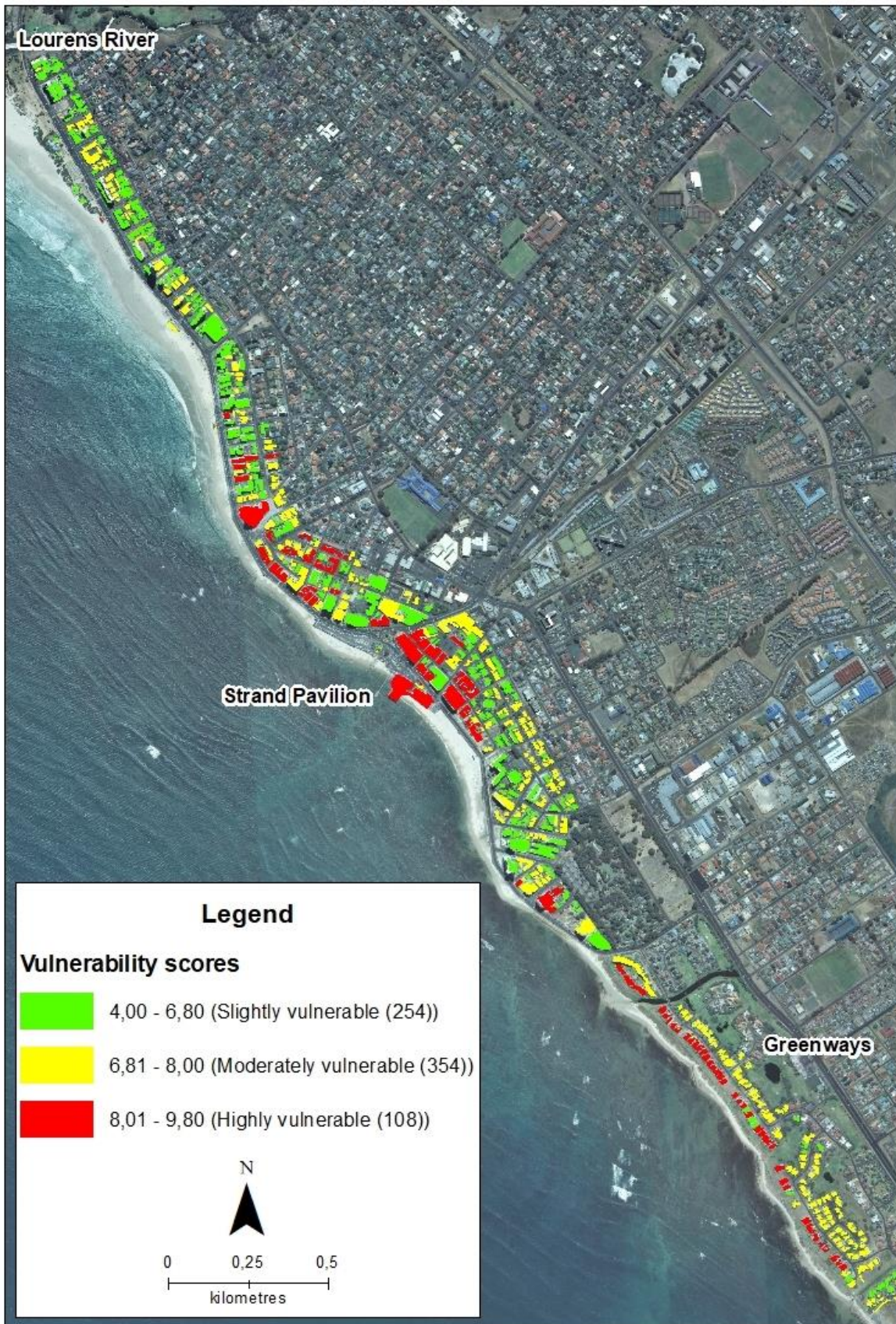


Figure 6.5 Strand: vulnerability per building

### 6.3 SUB-CONCLUSION

In this section, a framework for a building vulnerability assessment was developed and applied to all buildings in the determined hazard exposure zones in Stand and Fish Hoek. The results were presented in the form of statistical vulnerability profiles and geospatial maps. This dual representation allowed for the identification of spatially most prevalent factors contributing to building and occupancy vulnerability and to identify the buildings which are most vulnerable (Villagrán de León 2006).

The building vulnerability indicators are intended as a rapid assessment method that can be utilised by anyone without specialised inputs in order to determine a vulnerability score for individual buildings. The weightings used in this study were obtained via expert consultation, due to data scarcity and can be considered to be subjective, however statistical methods such as the analytical hierarchy process (AHP) can also be applied to generate weightings where sufficient data are available (Dang, Babel & Luong 2011; Ouma & Tateishi 2014). The derived results can be used to inform decision makers as to where resources are required to reduce vulnerability and further support mitigation and planning at a local level. In the broader disaster risk management context such maps, using baseline indicators, and applying weightings can be used to inform other aspects such as preparedness, mitigation, response and relief efforts.

Utilising the Building Vulnerability Framework developed in this study means that the building vulnerability indicator scores will only change under the following conditions:

- if the construction/nature/use of the building changes or there are external measures put in place which would result in the indicator score changing e.g. construction of a solid boundary wall put in place that either increases or decreases the building's vulnerability;
- the indicators themselves are changed e.g. indicators are added, removed or altered;
- the scoring mechanism is changed; and/or
- the indicator weightings are changed.

Overall, this component of the study achieved its objective of developing a locally relevant building vulnerability assessment framework that can be utilised:

- by non-specialists; and
- in a rapid assessment context.

This section, combined with Section 5.2 concludes the response to the second research question i.e. *How can buildings be categorised according to their exposure and vulnerability to coastal inundation hazard?*



## CHAPTER 7: DEVELOPING A SPATIAL RISK PROFILE FOR BUILDINGS IN THE COASTAL ZONE

The final aim of this research was the development of a spatial risk profile in terms of the physical vulnerability of buildings to coastal inundation hazard. The spatial risk profile represents idiosyncratic risk<sup>21</sup> of buildings to coastal inundation hazard.

In the previous sections the inundation **hazard** was identified through the development and application of the enhanced Bathtub Model eBTM (Chapter 4 and Section 5.1). The **hazard exposure** of coastal buildings was assessed in Section 5.2, and the **vulnerability** of the buildings of the area of the buildings in the inundation exposed coastal area was assessed in Chapter 6. In this section all these components will now be combined to calculate the building inundation **risk**. Figure 7.1 gives a schematic overview of this process, which is described in detail in the following sections.

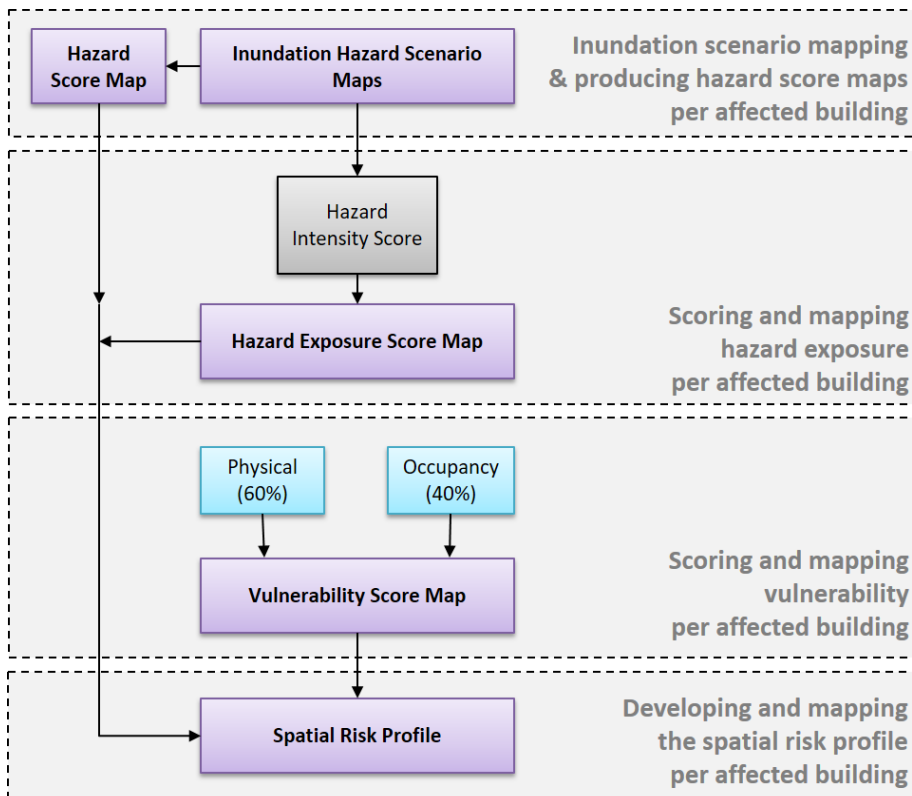


Figure 7.1 Spatial risk profile framework

<sup>21</sup> One building's experience is unrelated to another (Christoplos 2010)



## 7.1 DEVELOPMENT OF A BUILDING INUNDATION RISK FRAMEWORK

In order to assess the total risk, the rankings and classes developed in the previous sections for inundation hazard, hazard exposure and the vulnerability of the buildings, needed to be combined in a meaningful way. Two processes were undertaken, namely scaling and weighting. Scaling involves presenting data according to a particular scale (in the context of this thesis: dividing a continuous data range into discrete classes) while weighting introduces an adjustment to the weight of individual input data and is applied to accommodate specific circumstances.

### 7.1.1 Scaling

This process required the recoding of the original classes and scores of the three previous processes, in order to align the respective output formats. The target classes were ‘low’, ‘moderate’ and ‘high’ inundation risk to reflect risk qualitatively. This avoids ‘over categorisation’ and creating artificial divides in the data e.g. a building categorised as ‘high risk’ would effectively receive the same attention as a building categorised as ‘extreme risk’, because they both require more immediate attention/intervention (Els 2019, Pers com). The ruleset applied for this recoding is presented in Table 7.1 below.

Table 7.1 Rescaled risk component classes and definitions

Target risk class	Hazard probability	Hazard exposure	Building vulnerability score range
No risk (0)	Not affected by any of the modelled scenarios	Water depth = 0 m	Not applicable as all buildings have predisposed vulnerability
Low (1)	Affected by modelled scenario three	Water depth between 0.01 m and 0.3 m	Fish Hoek: 5.6 to 6.73 Strand: 4 to 6.8
Moderate (2)	Affected by modelled scenarios two and three	Water depth between 0.31 m and 0.6 m	Fish Hoek: 6.74 to 7.87 Strand: 6.81 to 8
High (3)	Affected by modelled scenarios one, two and three	Water depth $\geq$ 0.61 m	Fish Hoek: 7.88 to 9 Strand score range: 8.01 to 9.8

Armenakis et al. (2017) state that if there is no hazard, there is no risk, therefore all buildings that are located outside of inundated areas were assigned a risk score of 0. While this component of the analysis follows this principle, the statement is not entirely true as the predisposed vulnerability of buildings exists with or without the hazard e.g. structural fatigue that may cause collapse (Davidson 1997; Mamuji & Etkin 2019). The vulnerability of buildings within each study site is presented in Figure 6.3 and Figure 6.5. The buildings that are not exposed to the defined hazard scenarios were then excluded from further analysis. The risk components of the remaining buildings were rescaled, ranging from 1 – 3, based on Table 7.1.

### 7.1.2 Weighting

Different weighting factors were applied to the hazard, hazard exposure and vulnerability components to enhance the validity of the score (Papathoma-Köhle et al. 2019). These weightings are presented below:

- $w_H = 1$
- $w_{HE} = 0.75$
- $w_V = 2$

The motivation for these weightings is as follows:

**Hazard** ( $w_H$ ) was not weighted as it presents the baseline inundation information against which the hazard exposure and vulnerability are weighted.

**Hazard exposure** ( $w_{HE}$ ): The main reason for giving this factor less weight than the others was that the calculation of the inundation extent in this project did not include several factors that might influence actual flooding. For instance, as previously stated, drainage systems could not be accommodated in the eBTM as well as the porosity of the surface and soil saturation as well as potential wind push impact. Through consultation with experts therefore a factor of 0.75 was applied to the hazard exposure scores.

**Vulnerability** ( $w_V$ ): Vulnerability is a defining component of risk (UNDDR 2015). This is the ‘vulnerability state’ inherent to the building whether inundation hazard is present or not. In the context of this study it presents the predisposition of a building and was therefore assigned a weighting of 2 in the risk assessment, based on expert agreement.

Based on the above weightings, the maximum risk score that can be achieved is 3.75 and the minimum is 1.17.

### 7.1.3 Calculating final building inundation risk scores

As shown in Table 2.1, there are different methodologies for expressing disaster risk. Following Armenakis et al. (2017), the conventional equation proposed by Dilley et al. (2005) and van Westen & Greiving (2017) i.e.  $R = H * HE * V$ , is contextualised in terms of spatial risk whereby:

- Risk = Spatial risk
- Hazard = Coastal inundation hazard
- Hazard Exposure = Building exposure

- $\underline{Vulnerability} = \text{Building vulnerability}$

Considering the scaling and weighting parameters included in the preceding sections, the final equation used to calculate the building risk scores is presented in Equation 7.1.

$$Risk = w_H H * w_{HE} HE * w_V V$$

Equation 7.1 Calculating final building inundation risk

According to this framework, the coastal inundation risk for all 196 buildings in Strand and 4 buildings in Fish Hoek located in an area exposed to any flood hazard was assessed.

## 7.2 RESULTS AND DISCUSSION

The hypothetically minimum and maximum achievable risk scores based on Equation 7.1 are 1.5 and 54 respectively. Buildings achieving a low risk score are considered to be less prone to coastal inundation hazard, either due to lower hazard exposure and/or lower vulnerability. Conversely, buildings achieving a higher risk score are more likely to either be more exposed, more vulnerable or a combination of both.

The results of the inundation risk assessment were ranging between 1.5 and 40.5 in Strand and between 3 and 27 in Fish Hoek, see Table 7.2 below. This means that the total absolute building risk in Strand was higher than in Fish Hoek. This will be unpacked in detail below.

Table 7.2 Data summary for mapping risk in Strand and Fish Hoek

	Strand	Fish Hoek
Buildings assessed	196	4
Minimum risk score	1.5	3
Maximum risk score	40.5	27
Average risk score	9.16	9
Risk score Range	39	24
Author defined number of intervals	3	3
Class width	13	8
Score class ranges		
Low risk class	1.5 - 9 (131 buildings)	3 - 11 (3 buildings)
Moderate risk class	9.01 - 18 (37 buildings)	11.1 - 19 (0 buildings)
High risk class	18.1 – 40.5 (24 buildings)	19.1 - 27 (1 building)

In order to allow a meaningful display of the results in GIS maps, the respective risk score ranges were divided into three equally wide classes, using the equal interval classification method. This resulted in three site-specific risk classes ‘low’, ‘moderate’ and ‘high’ (Table 7.2).

The resulting spatial risk profiles for the buildings in the coastal zone in Fish Hoek and Strand are presented in Figure 7.2 and Figure 7.3 respectively.

In Fish Hoek, out of the 206 buildings assessed, one was classified “high risk”, three as “low risk” and 202 as “no risk” (Figure 7.2). The low risk buildings in Fish Hoek, even while partly scoring higher vulnerabilities are clearly benefitting from the protection afforded by the revetment and sea wall, while the restaurant is a high risk building in a high inundation risk location and does not have protective structures. It was initially expected that more buildings would be at risk, specifically the Seaside Cottages development being located in an area declared unfit for development (CCT 2012a). However, the established dune shows to provide natural protection from coastal inundation as well as inundation that may emanate from the river.

In Strand, 524 out of the total of 716 assessed buildings were classified as “no risk”, 131 as “low risk”, 37 as “moderate risk” and 24 as “high risk” (Figure 7.3). Similar to Fish Hoek, despite many buildings being located close to the shore, relatively few are at high risk. The high risk buildings are primarily present in the central area where vulnerable buildings are located where the inundation hazard risk is high because the beach is very narrow and no dunes are present. This allows focussed attention to the few ‘hotspots’ for intervention.





Figure 7.2 Spatial Risk Profile of buildings at risk to coastal inundation in Fish Hoek. Numbers in brackets: No. of buildings per class



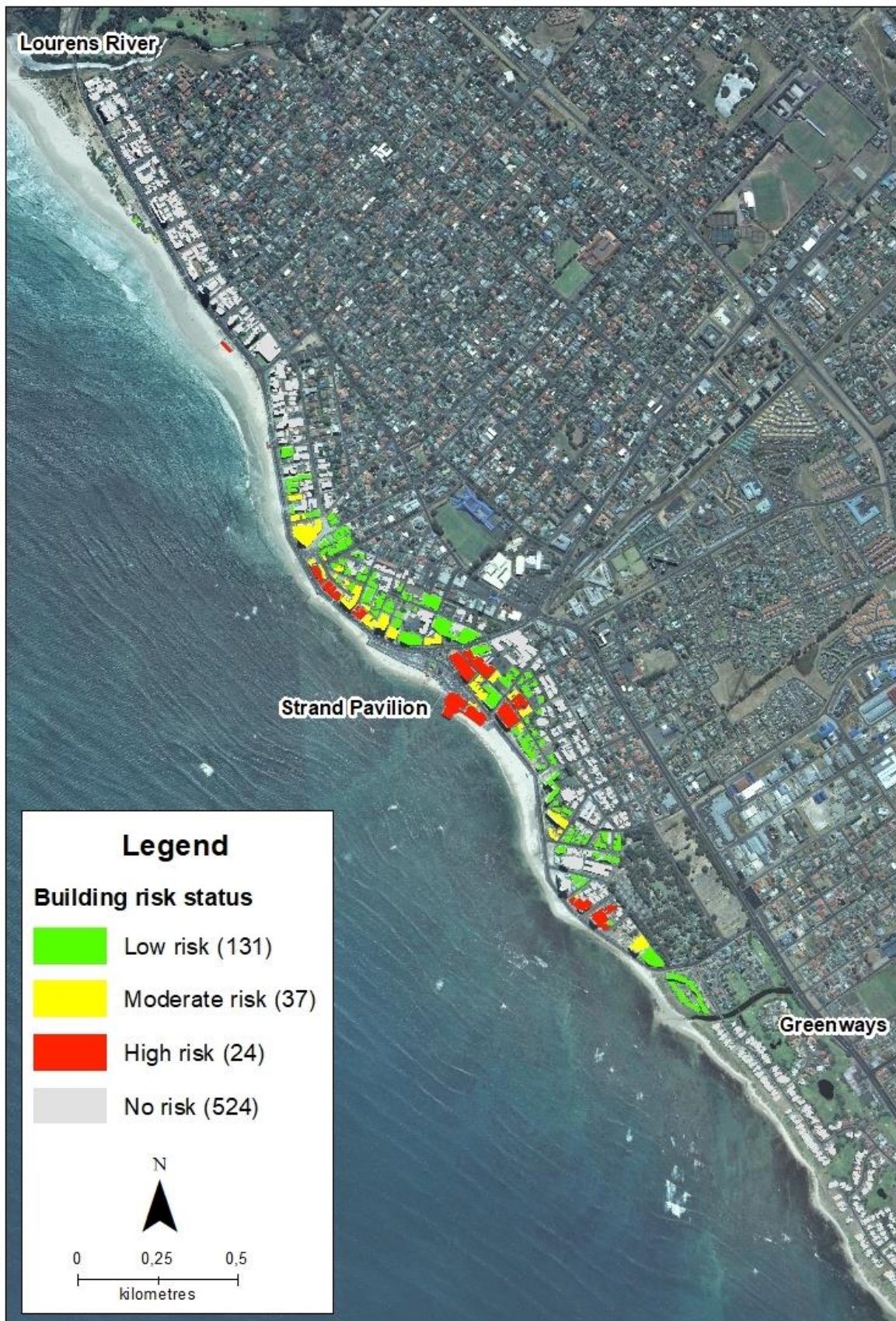


Figure 7.3 Spatial Risk Profile for buildings at risk to coastal inundation in Strand. Numbers in brackets: No. of buildings per class

Currently and internationally, building risk profiles are not being developed in relation to individual buildings and specific hazards. However in hazard prone areas e.g. regions subjected to earthquakes, countries are implementing building codes to reduce structural loss (and subsequent loss of life) during these natural events. Other approaches just conduct the delineation of risk zones. The cumulative methods presented in this research, culminating in a building specific risk profile, presents a novel approach that can inform focused and proactive management.

The limitation of this approach is that the weighting of the hazard exposure was uniformly applied, whereas in reality e.g. the degree of functionality of the drainage systems might vary spatially. There are also factors (surface processes) that may increase the hazard exposure such as wind-push resulting in large surface waves that are negated through the reduced weighting. These processes have the potential to increase both the inundation hazard limits and hazard exposure, however this can only be determined when the hazard manifests or through predictive modelling (e.g. weather forecasts) (Shmueli, 2010). Weightings were applied in this thesis to reduce the influence of the risk components with known limitations which could not be catered for.

### **7.3 SUB-CONCLUSION**

While previous sections discussed the methods used to achieve hazard (Section 5.1), hazard exposure (Section 5.2) and vulnerability scores (Chapter 6), in this section these individual scores were used to determine a final risk score for each building. Rules and weightings were applied so that the final risk maps reflected the interaction between hazard, hazard exposure and vulnerability.

The building risk status presented here (Figure 7.2 and Figure 7.3) shows all buildings, including those not at risk (i.e. 'no risk' category), that formed part of the hazard exposure (Section 5.2) and vulnerability assessments (Chapter 6). The reasoning is that buildings that are not exposed to the presented scenarios, still have known elements of vulnerability that may manifest under other scenarios. It is useful for disaster management practitioners to know where data pertaining to hazard and vulnerability exist even where buildings are not impacted or where the hazard is negligible (Minnie 2019, Pers com).

This section concludes the response to the third research question i.e. *How can, based on i and ii, a spatial risk profile relating to coastal inundation and building vulnerability be developed using GIS?*



## **CHAPTER 8: CONCLUSIONS**

This chapter revisits the research problem, the aims and objectives and how the research questions of this research were answered. Thereafter it discusses the limitations encountered and provides recommendations on improving the eBTM and coastal disaster risk assessment process as a whole, and concludes with the overall value and contribution this research has made to science and spatial development and disaster management in coastal zones in South Africa and beyond.

### **8.1 RESEARCH PROBLEM**

The coast is a dynamic space where atmospheric, oceanographic and terrestrial processes converge. It is also subject to intense development. More than 60% of the world's population resides in coastal areas as they have a wealth of natural resources and attractive and diverse economic activities and opportunities. Coastal buildings and infrastructure are thus at the interface of natural and dynamic anthropogenic processes, often being directly impacted during extreme events. In light of climate change and compounding localised hazard impacts, there is a need for improved methods for determining risk to existing coastal buildings and infrastructure.

This research established and confirmed through stakeholder interaction that currently there is very little capacity to develop and run specialised (GIS and/or HDm based) coastal inundation models within disaster and government entities in South Africa and that the data which these models require are often technologically inaccessible, expensive to acquire or do not exist. In addition, the current disaster risk assessments conducted in South Africa are undertaken at scales that are inappropriate, which include statistics that are provided at the local municipality level and are not spatially explicit. Coastal hazards are often 'lost' within these assessments as they are only prevalent along localised areas of the coastline and are therefore perceived to have less impact. Therefore, spatial risk profiles focussing on coastal hazards and the receiving environment (such as buildings) do not currently exist.

In this context, a new approach specifically focussed on capturing the effect of coastal hazards and assessing vulnerability at the local level was needed to provide a baseline for future assessments. This was achieved through the development of a locally relevant and technologically accessible GIS based eBTM for determining the potential coastal inundation hazard, packaged into a user-friendly ArcGIS GUI tool, the assessment of the exposure to the inundation hazard, the vulnerability of buildings and subsequently the generation of a spatial risk profile.

## 8.2 AIMS AND OBJECTIVES REVISITED

This study aimed to develop and test a methodology for developing a spatial risk profile for physical building vulnerability to three extreme coastal inundation scenarios for two test sites in False Bay, Cape Town, South Africa. The spatial risk profile was to be derived from a GIS based hazard modelling component and physical building vulnerability assessment. In order to achieve this aim, eight objectives were set for this thesis and were successfully achieved. Table 8.1 lists the objectives and indicates the sections of this thesis where they were dealt with.

Table 8.1 Revisiting the Objectives

Obj. No.	Objective	Objectives addressed and achieved in sections
1	Review of literature on GIS and hydrodynamic modelling based inundation models, building vulnerability assessments and risk quantification to inform the study based on international best practice	Chapter 2
2	Selecting appropriate study sites, based on data availability and accessibility	Chapter 3
3	Data collation	Chapter 4 & 6
4	Develop an inundation model to determine the areas within the selected study sites that will be affected by coastal inundation scenarios	Chapter 4
5	Test the coastal inundation model's response to changes in the input parameters and demonstrate the model's appropriateness for determining coastal inundation	Chapter 4
6	Determine the vulnerability of buildings potentially exposed to the coastal inundation hazard through the analysis of available data, spatial analysis techniques and field studies	Chapter 5
7	Quantify the coastal inundation hazard, hazard exposure and building vulnerability	Chapter 5 & 6
8	Develop a spatial risk profile illustrating a risk gradient of individual buildings to coastal inundation hazard	Chapter 7

## 8.3 RESEARCH QUESTIONS REVISITED

As indicated above, the aims and objectives of this research were successfully achieved, thereby resolving the three research questions presented in Section 1.3, namely:

*Research Question 1: How can a GIS based coastal inundation model be developed that is more accurate than the existing sBTM, but simpler and quicker to apply than HDm to assess coastal inundation hazard on a local level?*

This question was answered through the review of literature on existing coastal inundation assessment approaches elsewhere, and stakeholder engagement on technical and data requirements and constraints in the South African context, which informed the development of the GIS-based eBTM model, which produces a layer of inundation extent and depth in shapefile format (Chapter 4). The eBTM was packaged into an ArcGIS Toolbox called 'ArcCoastTools' that can be added to the existing ArcGIS suite of tools (Williams, 2019). The packaging in the ArcGIS Toolbox, i.e. a GUI,

significantly simplifies the use of the eBTM and thus enables its use by non-domain experts. The model run-time was tested, and while it depends on the spatial resolution and spatial extent of the input DEM, it was still in a range acceptable for operational (near-real time) use and did not require expensive high spec computers.

*Research Question 2: How can buildings be categorized according to their exposure and vulnerability to coastal inundation?*

The building exposure was determined using the water depths produced by the eBTM to assign a hazard exposure score (Section 5.2). Guided by experts, a building vulnerability framework was developed, consisting of vulnerability indicators and weightings for buildings (Chapter 6). These indicators were used to score each building within the study sites to determine their vulnerability scores.

*Research Question 3: How can, based on i and ii, a spatial risk profile relating to coastal inundation and building vulnerability be developed using GIS?*

The final spatial risk profile was developed, based on the risk equation  $Risk = Hazard * Hazard Exposure * Vulnerability$  (Chapter 7). This risk profile built on the results achieved in the previous section of this thesis, namely the inundation hazard extent maps for three inundation scenarios (Section 5.1), the inundation hazard exposure scoring of buildings (Section 5.2) and the building vulnerability assessment (Chapter 6). The final outputs are spatial risk profile maps for building vulnerability to coastal inundation hazard in the two study sites in Strand and Fish Hoek in False Bay.

## **8.4 RESEARCH LIMITATIONS**

### **8.4.1 Dependency on high resolution DEMs**

An important aspect of ‘data-driven’ assessments such as this, is that the results are largely dependent on the quality of the input data. This is particularly relevant for the hazard (Section 5.1) and hazard exposure scores (Section 5.2) which were directly based on the modelled outputs. The eBTM developed in Chapter 4 does not require many different datasets as input data, but rather relies extensively on a high resolution DSM from which other datasets e.g. coastline and beach slope are derived. Literature has shown that there is a preference towards high resolution DEMs as it improves on the quality of the results (e.g. Mark and Bates, 2000; Gesch, 2009, and Neumann and Ahrendt, 2013; Parker, 2013; amongst others). As demonstrated in Section 4.4.3, the resolution of the DSM directly influenced the eBTM results, and for the purpose of coastal inundation it was recommended



that a 1 m resolution LiDAR derived DSM is used. Therefore the applicability of the eBTM in other areas where LiDAR data are not available can be limited if no high resolution DSM data are available.

#### **8.4.2 Outdated data**

Model outputs are only as relevant as the used input data. Given the current cost constraints to acquire LiDAR for creating high-resolution DEMs, the only LiDAR available for this study was from 2014. Hence, topography for the study sites based on these data was representative for the conditions in 2014. However, between 2015 – 2017, i.e. during the course of this study, a sea wall was constructed in the central region of Strand, northwards from the Strand Pavilion and therefore the overall results achieved here do not reflect the current situation on the ground as more recent LiDAR is not yet available.

Obviously, the same limitations are valid for the acquisition date of population and building usage data relating to the building vulnerability assessment. However, this may be addressed through ground-truthing.

#### **8.4.3 Hydrological & hydrodynamic processes not accounted for**

While the eBTM was designed to incorporate physical conditions that may impede water flow, such as beach slope and a RC, the eBTM only considers a single representative roughness coefficient for each study site, while a spatially more differentiated roughness surface might be more realistic. Furthermore, the eBTM does not take surface drainage structures into account e.g. stormwater systems. This would require more advanced tools and assessment techniques that were beyond the scope of this study. Consequently, the omission of drainage factors has a direct impact on the hazard and hazard exposure scores. The omission of other factors impacting on inundation distribution, such as wind pressure and wave runup and the potential contribution of inland flooding to water levels, especially in estuarine or riverine areas etc. might further bias the reliability of the results.

#### **8.4.4 Risk category classes**

Arguably, representing risk in qualitative categories (i.e. low, moderate and high) simplifies the results. While this format is useful for communicating risk, practitioners who are more engaged with disaster management can make use of the original continuous numerical results.

Continuous risk scores also allow for the comparison of risk over large areas (in this case, across two study sites). However, this research used site specific score ranges based on the “equal interval classification”, subsequently creating the three risk classes for display purposes. The site specific

score ranges leads to the same continuous risk scores on both sites now potentially being classified differently, e.g. on one site as ‘moderate’ and on the other site as ‘high’. This is a circumstance which must clearly be made clear to the user.

#### **8.4.5 Dependence on licenced software**

The ArcGIS software used to develop the eBTM provides an array of tools to the user such as the Spatial Analyst extension. ArcGIS is however, proprietary software that comes at a significant license fee. As the targeted audience for the eBTM, i.e. government, academic and private institutions in South Africa make use of ArcGIS software, the decision was made to build the eBTM model using ArcGIS. This may however somewhat limit the use of the tool by other users without ArcGIS access. Furthermore, while the eBTM is presented as a user-friendly tool, people still need to have basic GIS application skills in order to make use of the tool.

### **8.5 RECOMMENDATIONS**

Stemming from the identified limitations, this section presents recommendations that may further contribute to improving analyses in the disaster risk context.

#### **8.5.1 Recommendations for improving the eBTM**

As previously stated, the eBTM was developed using ArcGIS, and while it is considered to be accessible by many users, it would be beneficial to have the tool available for open source applications e.g. QGIS as well. In this context, the arcpy script has also been made available when downloading the eBTM model (Williams 2019b) and can be converted to the preferred application format by the user. In addition, the detailed model development process has also been published (Williams & Lück-Vogel 2020), allowing users to reconstruct and improve on the model.

The eBTM currently requires the user to input a single value RC, which would be representative of the study site. However, natural coasts typically have spatially heterogeneous surfaces with varying roughness. This can be accounted for by modifying the model to incorporate a ‘roughness raster’ whereby surface roughness is represented as a raster dataset. The resolution of the raster should ideally be that of the input DSM or DTM. While it may be an intensive exercise, the raster will provide a variable surface for the water to negotiate and therefore may produce different inundation outputs.

As technology advances and solutions become more accessible, it would be useful to investigate how surface drainage systems may influence the model outputs i.e. possibly resulting in lesser inundation extent. More broadly, the eBTM model is packaged such that it can be edited and customised as/when

needed to improve on the existing model. Furthermore, the eBTM can serve as a complimentary tool to be used in conjunction with HDm, particularly where inundation hazard is perceived to threaten human life and/or property. It can be used as an initial approach to identify inundation points of entry and potential water pathways, where after the user can consider further modelling efforts to inform the mitigation or interventions required.

Further, given the highly dynamic nature of the coast, it is important to note that the coast has the potential to undergo extreme physical changes in a relatively short period of time e.g. erosion, accretion, inundation etc., but also due to coastal development (Balica, Wright & van der Meulen 2012; Doukakis 2005). Updated and multi-temporal high resolution topographic data such as LiDAR are therefore imperative for models that will assist planners, coastal practitioners, disaster management etc. in decision making processes. In the context of this study, the coastline for Strand had changed due to the construction of a sea wall between 2015 – 2017, whereas the LiDAR data used in this study was acquired in 2014. Therefore the inundation results presented here are likely to be outdated. However, with the development of the eBTM tool, the inundation hazard assessment can easily be repeated when new data become available. It would therefore be of interest to see how the introduction of the sea wall affects the eBTM results.

### **8.5.2 Recommendations for improving the coastal disaster risk assessment process**

This study introduced a localised approach to coastal disaster risk assessments which can serve as a baseline for future studies.

However, during the process it turned out that for making the approach faster and more efficient, better availability of the required input data would be desirable. For instance, there needs to be more effective use and sharing of data, particularly in the context of LiDAR data which are expensive to acquire. The work undertaken to capture the building roofprints from aerial imagery preceded this study as a manual GIS digitising exercise, however through the proper use of technology, the building roofprints could be extracted from LiDAR more effectively. This would aid to produce updated building layers (.shp) which can then serve as a common baseline for e.g. land use management, development planning processes and disaster management, which will be beneficial as all practitioners would have access to the same baseline data. From a (coastal) disaster management perspective, information pertaining to building heights and building construction material is important, as tall buildings constructed from robust materials such as reinforced concrete that have the potential to withstand the inundation impact can be identified to serve as vertical evacuation structures and places of safety. This would contribute to better resilience planning.

In addition, mechanisms are required that record damage experienced and costs incurred due to the impact of coastal inundation hazard. Damage can be recorded per building (or infrastructure asset), which could then build a damage profile for areas, again informing the mitigation responses required. In this context, collaborations between local authorities and the insurance industry would be beneficial.

Overall, this study demonstrates the importance of scale, given that localised (coastal) hazards have the potential to cause major disruptions and damage to infrastructure. There needs to be a distinction made in the way in which hazards are assessed and more flexibility in the current risk assessment techniques. A suggestion in this regard would be that hazards themselves be assessed as either regional (e.g. drought) or localised (e.g. coastal inundation) and this would in turn inform the relevant disaster risk assessment approach and more accurately depict the way in which the hazard manifests itself at a local level. Furthermore, the frameworks presented here can be used as a baseline for future studies and customised to address the local context.

## **8.6 RESEARCH VALUE AND CONTRIBUTIONS**

Broadly, this study has contributed to knowledge in the GIS application, disaster management and coastal management fields.

### **8.6.1 Improved GIS based coastal inundation approach**

As mentioned above, currently available approaches for reliably modelling coastal inundation are either too simplistic (sBTM) or technologically too sophisticated to be applied by a wide range of managers and over wide regions. This is problematic, as coastal spaces are getting increasingly crowded by expanding developments and the predicted effects of climate change on the coast, the combination of which will put an increasing amount of infrastructure, assets and people at risk. This makes it essential to identify and mitigate hazards, hazard exposure and vulnerability – preferably during the spatial planning phase of new developments.

The development of the eBTM in this thesis aimed at closing this gap, as it advanced existing inundation models and combines some physical input parameters (roughness and slope) with GIS technology that is accessible.

### **8.6.2 Framework for building vulnerability developed**

The building vulnerability assessment framework developed in this thesis presented a set of indicators that are transferable between areas and are locally relevant, where no previous framework existed.



The indicators are also simplistic enough to be utilised by non-specialists and in a rapid assessment context.

### **8.6.3 Cross-disciplinary vulnerability and risk assessment**

The cross disciplinary approach presented in this study combines GIS, disaster management and coastal management to address coastal inundation hazard. Combining two aspects which are not usually assessed together, namely physical building vulnerability and physical coastal inundation hazard as presented in this study, provides a framework to enhance the South African approach for localised disaster risk assessments. This is the first step towards a true inter- and transdisciplinary assessment of risk and vulnerability, which are currently usually either assessed from a purely physical, social or economic perspective. These silo approaches usually miss important risk and vulnerability components which hinders effective risk management. Further, the risk maps produced in this thesis (or produced in the future using the approach developed here) can be used beyond the scope of disaster management and applied to disciplines such as town planning, as a substitute for building codes that promote resilience to localised hazards, which currently do not exist.

### **8.6.4 Providing a method for generating geospatial risk information at levels relevant for local management**

Currently, South Africa consistently undertakes first and second pass approaches (presented in Sharples, Attwater & Carley 2008), where disaster risk assessments and the review/updating of assessments are conducted at regional scale i.e. local municipality level, without sufficient consideration for the localised, site specific context (e.g. Province of the Western Cape 2012b). The regional mapping scale presents a further challenge in terms of visual interpretation as localised (coastal) hazards are often lost amongst more widespread hazards. This study puts forward an assessment mechanism that allows the risk components (i.e. hazard, hazard exposure and vulnerability) each to be assessed individually, at a locally relevant scale and through their individual assessment frameworks. Assessing risk components individually is important as it allows for more transversal application e.g. this study assessed physical building vulnerability in relation to coastal inundation hazard, but likewise the socio-economic response to coastal inundation hazard can also be assessed using the same inundation scenarios. The vulnerability framework that was developed is also transferable to other regions.

In the previous risk assessments undertaken in South Africa, GIS was not being used to its full potential. In the disaster management context spatially explicit data are very useful and can dramatically support and enhance decision making processes. The localised spatial risk profiles for

both study sites immediately provide the user with an indication of where vulnerable buildings at the highest risk of experiencing coastal inundation are located. This information can be used to inform management interventions to reduce vulnerability and/or improve on resilience and mitigation efforts. The user of the spatial risk profile products must however be cognisant of the fact that **classification methods can be subjective** and based on the user's discretion and it would be advisable to have consensus from the user group or decision making parties on the classification to be used to represent risk e.g. what risk score would constitute 'high risk'?

The flexibility of the framework also allows for additional indicators to be developed and included in the GIS database, which then also has the function of performing calculations on the data as well as having the tools to undertake spatial analysis. The development of such data is also gaining international traction for improved analysis and reporting (Aitsi-Selmi et al. 2016; UNISDR 2016).

For all the assessments thus far, i.e. hazard, hazard exposure and vulnerability, all the individual building scores were captured in GIS. Recording the vulnerability indicators individually and scoring each building individually in GIS allows the user to query buildings individually and access all information pertaining to that individual building at one glance (example provided in Figure 8.1).

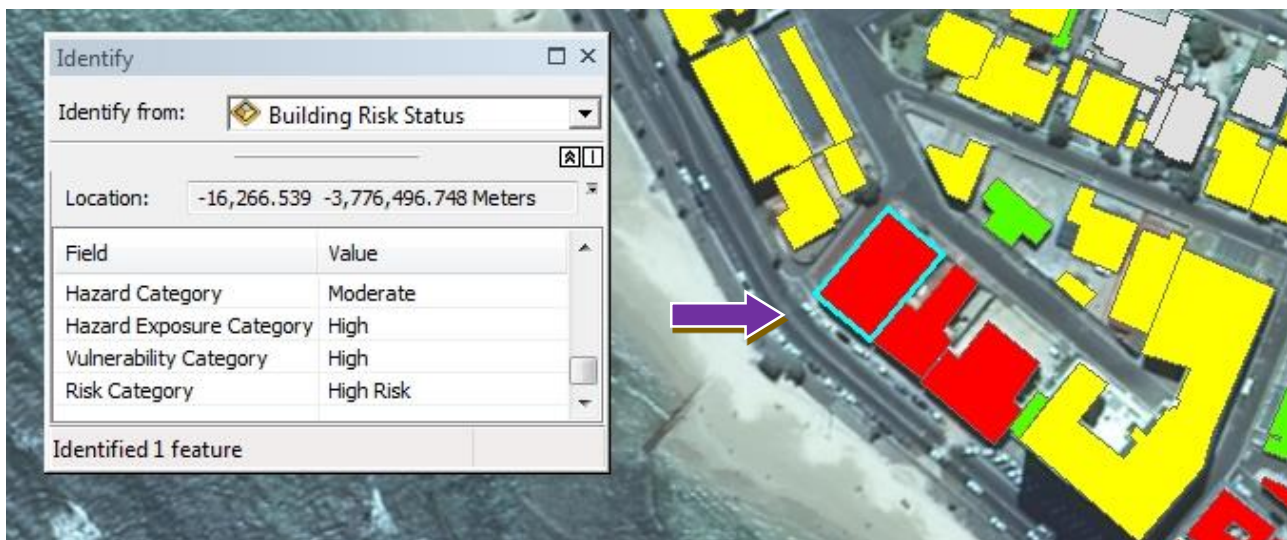


Figure 8.1 Example of querying risk and vulnerability scores for individual buildings

A spatial representation of individual buildings at risk and the ability to consider the hazard, hazard exposure and vulnerability in their individual spatial contexts provides a valuable way forward for disaster risk assessments.

### 8.6.5 Tool to empower local municipalities to conduct local inundation assessments

Packaging the eBTM model in a GUI tool empowers coastal municipalities, disaster management and coastal practitioners to determine coastal inundation relevant to their own study sites and based on their own scenarios. Specifically, the developed and freely accessible ArcGIS Toolbox GUI interface tool:

- Allows practitioners to engage with a user-friendly front-end tool to construct inundation scenarios, without being exposed to the back-end model architecture;
- Is computationally inexpensive to run i.e. does not require sophisticated technologies or high performance computing; and
- Only requires a high resolution DEM as GIS data input.

## **8.7 CONCLUDING REMARKS**

The concepts and methodologies devised in this research demonstrated a successful approach for developing a spatial risk profile at a local level by considering coastal inundation hazard, building hazard exposure and building vulnerability as independent components. Different technologies were explored and expert advice was sought, resulting in the tools and techniques developed here that can be customised and applied to other areas. The eBTM tool developed here thus presents a user-friendly, standardised model and tool for GIS based coastal inundation assessments that is now available to practitioners, where previously only the sBTM existed. Furthermore the tool benefits from having been validated against actual data from a previous storm event and further tested.

The hazard, hazard exposure and vulnerability indicators were developed through a consultative process with experts, with the intention that using the indicators for physical building assessments can be undertaken as a rapid assessment by non-specialists to acquire baseline data. The indicator and weighting frameworks developed through the vulnerability assessment provide guidance for localised and improved (disaster) risk assessments to be undertaken. In this context, the methodology in its current state should be relevant and transferable to other coastal areas.

Overall, this study highlights the benefit of undertaking localised risk assessments following methods such as the one developed to assist decision makers in better understanding local hazards and identifying vulnerable elements (e.g. buildings) - thereby improving planning and mitigation processes. Understanding the local context is becoming increasingly relevant and important, particularly in light of climate change and the way in which these effects are experienced on the ground.

## REFERENCES

- Adger WN 2006. Vulnerability. *Global Environmental Change* 16, 3: 268–281. [online]. Available from: <https://doi.org/10.1016%2Fj.gloenvcha.2006.02.006> [Accessed 19 November 2015].
- Ahmad N, Hussain M, Riaz N, Subhani F, Haider S, Alamgir KS & Shinwari F 2013. Flood prediction and disaster risk analysis using GIS based wireless sensor networks, a review. *Journal of Basic and Applied Scientific Research* 3, 8: 632–643. [online]. Available from: <https://www.semanticscholar.org/paper/Flood-Prediction-and-Disaster-Risk-Analysis-using-A-Ahmad-Hussain/3c6906eb4da7cb37b3a02e2ba4fad255ac1af316> [Accessed 13 September 2019].
- Aitsi-Selmi A, Murray V, Wannous C, Dickinson C, Johnston D, Kawasaki A, Stevance AS & Yeung T 2016. Reflections on a Science and Technology Agenda for 21st Century Disaster Risk Reduction: Based on the Scientific Content of the 2016 UNISDR Science and Technology Conference on the Implementation of the Sendai Framework for Disaster Risk Reduction 2015–20. *International Journal of Disaster Risk Science* 7, 1: 1–29.
- Ajai NS 2012. *Coastal zones of India*. Ahmedabad: Space Applications Centre, ISRO. [online]. Available from: [http://envfor.nic.in/sites/default/files/Coastal\\_Zones\\_of\\_India.pdf](http://envfor.nic.in/sites/default/files/Coastal_Zones_of_India.pdf) [Accessed 9 October 2015].
- Alexander D 2000. *Confronting catastrophe: New perspectives on natural disasters*. New York: Oxford University Press.
- Alexander DE 2012. Models of Social Vulnerability to Disasters. *RCCS Annual Review* , 4. [online]. Available from: <http://journals.openedition.org/rccsar/412> [Accessed 8 June 2020].
- Appelquist L, Balstrøm T & Kirsten H 2016. *The Coastal Hazard Wheel decision-support system: Main Manual*. Nairobi: UNEP. [online]. Available from: <https://www.coastalhazardwheel.org/> [Accessed 11 May 2020].
- Armaş I & Gavriş A 2013. Social vulnerability assessment using spatial multi-criteria analysis (SEVI) and the Social Vulnerability Index (SoVI): A case study for Bucharest, Romania. *Natural Hazards and Earth System Sciences* 13, 6: 1481–1499. [online]. Available from: <https://doi.org/10.5194%2Fnhess-13-1481-2013> [Accessed 4 September 2015].

- Armenakis C, Du E, Natesan S, Persad R & Zhang Y 2017. Flood risk assessment in urban areas based on spatial analytics and social factors. *Geosciences* 7, 4: 1–15. [online]. Available from: <https://doi.org/10.3390%2Fgeosciences7040123> [Accessed 13 August 2019].
- Balakrishnan Nair TM, Sirisha P, Sandhya KG, Srinivas K, Sanil Kumar V, Sabique L, Nherakkol A, Krishna Prasad B, Kumari R, Jeyakumar C, Kaviyazhahu K, Ramesh Kumar M, Harikumar R, Shenoi SSC & Nayak S 2013. Performance of the ocean state forecast system at Indian National Centre for Ocean Information Services. *Current Science* 105, 2: 175–181. [online]. Available from: <https://www.jstor.org/stable/24092636> [Accessed 11 October 2019].
- Balica SF, Wright NG & van der Meulen F 2012. A flood vulnerability index for coastal cities and its use in assessing climate change impacts. *Natural Hazards* 64, 1: 73–105. [online]. Available from: <http://link.springer.com/10.1007/s11069-012-0234-1> [Accessed 9 September 2015].
- Bates PD, Dawson RJ, Hall JW, Horritt MS, Nicholls RJ, Wicks J & Mohamed AAMH 2005. Simplified two-dimensional numerical modelling of coastal flooding and example applications. *Coastal Engineering* 52, 9: 793–810. [online]. Available from: <https://linkinghub.elsevier.com/retrieve/pii/S037838390500075X> [Accessed 6 July 2018].
- Birkmann J 2007. Risk and vulnerability indicators at different scales: Applicability, usefulness and policy implications. *Environmental Hazards* 7, 1: 20–31. [online]. Available from: <http://www.tandfonline.com/doi/abs/10.1016/j.envhaz.2007.04.002> [Accessed 6 December 2019].
- Birkmann J, Fernando N, Hettige S, Amarasinghe S, Jayasingam T, Ravi M, Paranagama D, Nandana M, Nassel M, Voight S & Wolferts J 2006. *Summary UNU-EHS vulnerability study: Measuring revealed vulnerability in Sri Lanka at the local level*. Bonn: United Nations University. [online]. Available from: [https://www.preventionweb.net/files/2182\\_VL323144.pdf](https://www.preventionweb.net/files/2182_VL323144.pdf) [Accessed 22 March 2016].
- Boateng I 2010. *Spatial planning in coastal regions: Facing the impact of climate change*. Copenhagen: International Federation of Surveyors (FIG). [online]. Available from: <https://www.fig.net/pub/figpub/pub55/figpub55.pdf> [Accessed 20 April 2015].
- Boon JD 2012. Evidence of sea level acceleration at U.S. and Canadian tide stations, Atlantic Coast, North America. *Journal of Coastal Research* 28, 6: 1437–1445. [online]. Available from: <http://www.bioone.org/doi/abs/10.2112/JCOASTRES-D-12-00102.1>



- Borrero JC, Sieh K, Chlieh M & Synolakis CE 2006. Tsunami inundation modeling for western Sumatra. *Proceedings of the National Academy of Sciences* 103, 52: 19673–19677. [online]. Available from: <http://www.pnas.org/cgi/doi/10.1073/pnas.0604069103>
- Brock J & Purkis SJ 2009. The emerging role of LiDAR remote sensing in coastal research and resource management. *Journal of Coastal Research* 10053: 1–5. [online]. Available from: <http://www.bioone.org/doi/abs/10.2112/SI53-001.1> [Accessed 16 October 2015].
- Brundrit G 2009. *Global climate change and adaptation : City of Cape Town sea- level rise risk assessment. Phase 5*. Cape Town: City of Cape Town. [online]. Available from: [https://resource.capetown.gov.za/documentcentre/Documents/City\\_research\\_reports\\_and\\_review/Phase 5 - SLRRA Full assessment+vulnerability Section\\_1\\_2\\_combined.pdf](https://resource.capetown.gov.za/documentcentre/Documents/City_research_reports_and_review/Phase_5_-_SLRRA_Full_assessment+vulnerability_Section_1_2_combined.pdf) [Accessed 4 April 2016].
- Burbidge D, Cummins PR, Mleczko R & Thio HK 2008. A probabilistic tsunami hazard assessment for Western Australia. In Cummins PR Satake K & Kong L (eds) *Tsunami Science Four Years after the 2004 Indian Ocean Tsunami*, 2059–2088. Basel: Birkhäuser Basel. [online]. Available from: [http://link.springer.com/10.1007/978-3-0346-0057-6\\_6](http://link.springer.com/10.1007/978-3-0346-0057-6_6)
- Cannon T 2008. *Reducing people's vulnerability to natural hazards: Communities and resilience*. Research Paper 2008/034. Helsinki: UNU-WIDER. [online]. Available from: <https://www.wider.unu.edu/publication/reducing-people's-vulnerability-natural-hazards> [Accessed 6 December 2019].
- Cartwright A 2011. *Coastal vulnerability in the context of climate change: A South African perspective*. Cape Town: Centre for Criminology. [online]. Available from: [https://www.academia.edu/7977816/COASTAL\\_VULNERABILITY\\_IN\\_THE\\_CONTEXT\\_OF\\_CLIMATE\\_CHANGE\\_A\\_SOUTH\\_AFRICAN\\_PERSPECTIVE](https://www.academia.edu/7977816/COASTAL_VULNERABILITY_IN_THE_CONTEXT_OF_CLIMATE_CHANGE_A_SOUTH_AFRICAN_PERSPECTIVE) [Accessed 9 September 2015].
- Cartwright A, Brundrit G & Fairhurst L 2008a. *Global climate change and adaptation – A sea-Level rise risk assessment. Phase four: Final report sea-level rise adaptation and risk mitigation measures for the City of Cape Town*. Cape Town: Ci.
- Cartwright A, Brundrit G & Fairhurst L 2008b. *Global climate change and adaptation – A sea-level rise risk assessment*. Cape Town: City of Cape Town. [online]. Available from: [https://www.ipcc.ch/apps/nj-lite/ar5wg2/nj-lite\\_download2.php?id=8350](https://www.ipcc.ch/apps/nj-lite/ar5wg2/nj-lite_download2.php?id=8350) [Accessed 4 April 2016].

- CCT (City of Cape Town) 2012a. *Helderberg district plan 2012*. [online]. Available from: [http://resource.capetown.gov.za/documentcentre/Documents/City\\_research\\_reports\\_and\\_review/Helderberg\\_District\\_Plan\\_Technical\\_Report.pdf](http://resource.capetown.gov.za/documentcentre/Documents/City_research_reports_and_review/Helderberg_District_Plan_Technical_Report.pdf) [Accessed 24 October 2016].
- CCT (City of Cape Town) 2012b. *Southern district plan 2012*. [online]. Available from: [http://resource.capetown.gov.za/documentcentre/Documents/City\\_research\\_reports\\_and\\_review/Southern\\_District\\_Plan\\_Technical\\_Report.pdf](http://resource.capetown.gov.za/documentcentre/Documents/City_research_reports_and_review/Southern_District_Plan_Technical_Report.pdf) [Accessed 24 October 2016].
- CD:NGI (National Geospatial Information) 2013. *GeoID and Vertical Reference Frame*. Cape Town: CD: NGI. [online]. Available from: <http://www.ngi.gov.za/index.php/technical-information/geodesy-and-gps/geoid-and-vertical-reference-frame> [Accessed 27 July 2019].
- Cho SY & Chang H 2017. Recent research approaches to urban flood vulnerability, 2006–2016. *Natural Hazards* 88, 1: 633–649. [online]. Available from: <http://link.springer.com/10.1007/s11069-017-2869-4> [Accessed 16 April 2018].
- Christoplos I 2010. *The Multiplicity of Climate and Rural Risk*. Copenhagen: Danish Institute for International Studies. [online]. Available from: [https://www.diis.dk/files/media/publications/import/extra/wp2010-08\\_multiplicity\\_climate\\_rural\\_risk\\_3.pdf](https://www.diis.dk/files/media/publications/import/extra/wp2010-08_multiplicity_climate_rural_risk_3.pdf) [Accessed 27 May 2020].
- Church JA, Clark PU, Cazenave A, Gregory JM, Jevrejeva S, Levermann A, Merrifield MA, Milne GA, Nerem RS, Nunn PD, Payne AJ, Pfeffer WT, Stammer D & Unnikrishnan AS 2013. Sea level change. In Intergovernmental Panel on Climate Change (ed) *Climate change 2013 - The physical science basis*, 1137–1216. Cambridge: Cambridge University Press. [online]. Available from: [https://www.cambridge.org/core/product/identifier/CBO9781107415324A034/type/book\\_part](https://www.cambridge.org/core/product/identifier/CBO9781107415324A034/type/book_part)
- Cooper HM, Chen Q, Fletcher CH & Barbee MM 2013. Assessing vulnerability due to sea-level rise in Maui, Hawai‘i using LiDAR remote sensing and GIS. *Climatic Change* 116, 3–4: 547–563. [online]. Available from: <http://link.springer.com/10.1007/s10584-012-0510-9> [Accessed 10 December 2018].
- Corbella S & Stretch DD 2012. Multivariate return periods of sea storms for coastal erosion risk assessment. *Natural Hazards and Earth System Sciences* 12, 8: 2699–2708. [online]. Available from: <https://www.nat-hazards-earth-syst-sci.net/12/2699/2012/> [Accessed 10 December 2018].

- Cowell PJ, Thom BG, Jones RA, Everts CH & Simanovic D 2006. Management of Uncertainty in Predicting Climate-Change Impacts on Beaches. *Journal of Coastal Research* 221: 232–245. [online]. Available from: <http://www.bioone.org/doi/abs/10.2112/05A-0018.1> [Accessed 24 October 2018].
- CSIR (Council for Scientific and Industrial Research) 2018. *National coastal assessment (Draft)*. Stellenbosch: CSIR.
- Cutter SL & Gall M 2015. Sendai targets at risk. *Nature Climate Change* 5, 8: 707–709.
- Cutter SL, Barnes L, Berry M, Burton C, Evans E, Tate E & Webb J 2008. A place-based model for understanding community resilience to natural disasters. *Global Environmental Change* 18, 4: 598–606. [online]. Available from: <https://linkinghub.elsevier.com/retrieve/pii/S0959378008000666>
- Dall’Osso F, Dominey-Howes D, Tarbotton C, Summerhayes S & Withycombe G 2016. Revision and improvement of the PTVA-3 model for assessing tsunami building vulnerability using “international expert judgment”: Introducing the PTVA-4 model. *Natural Hazards* 83, 2: 1229–1256. [online]. Available from: <http://link.springer.com/10.1007/s11069-016-2387-9> [Accessed 27 November 2015].
- Dang NM, Babel MS & Luong HT 2011. Evaluation of food risk parameters in the Day River Flood Diversion Area, Red River Delta, Vietnam. *Natural Hazards* 56, 1: 169–194. [online]. Available from: <http://link.springer.com/10.1007/s11069-010-9558-x> [Accessed 13 August 2019].
- Davidson R 1997. EERI Annual Student Paper Award a Multidisciplinary Urban Earthquake Disaster Risk Index. *Earthquake Spectra* 13, 2: 211–223. [online]. Available from: [https://stacks.stanford.edu/file/druid:zy159jm6182/TR121\\_Davidson.pdf](https://stacks.stanford.edu/file/druid:zy159jm6182/TR121_Davidson.pdf) [Accessed 27 May 2020].
- Desai PS, Narain A, Nayak S, Manikiam B, Adiga S & Nath AN 1991. IRS-1A applications for coastal and marine resources. *Current Science* 61, 3&4: 204–210. [online]. Available from: [http://www.currentscience.ac.in/Downloads/article\\_id\\_061\\_03-04\\_0204\\_0208\\_0.pdf](http://www.currentscience.ac.in/Downloads/article_id_061_03-04_0204_0208_0.pdf) [Accessed 11 October 2019].
- Dias P, Dissanayake R & Chandratilake R 2006. Lessons learned from tsunami damage in Sri Lanka. *Proceedings of the Institution of Civil Engineers - Civil Engineering* 159, 2: 74–81. [online]. Available from: <http://www.icevirtuallibrary.com/doi/10.1680/cien.2006.159.2.74>

- Dias WPS, Yapa HD & Peiris LMN 2009. Tsunami vulnerability functions from field surveys and Monte Carlo simulation. *Civil Engineering and Environmental Systems* 26, 2: 181–194. [online]. Available from: <http://www.tandfonline.com/doi/abs/10.1080/10286600802435918>
- Didier D, Bernatchez P, Boucher-Brossard G, Lambert A, Fraser C, Barnett R & Van-Wierts S 2015. Coastal flood assessment based on field debris measurements and wave runup empirical model. *Journal of Marine Science and Engineering* 3, 3: 560–590. [online]. Available from: <http://www.mdpi.com/2077-1312/3/3/560> [Accessed 19 May 2017].
- Dilley M, Chen RS, Deichmann U, Lerner-Lam AL & Arnold M 2005. *Natural disaster hotspots: A global risk analysis*. Washington: The World Bank. [online]. Available from: <http://documents.worldbank.org/curated/en/621711468175150317/Natural-disaster-hotspots-A-global-risk-analysis> [Accessed 4 March 2017].
- Douben K 2006. Characteristics of river floods and flooding: a global overview, 1985–2003. *Irrigation and Drainage* 55, S1: 9–21. [online]. Available from: <http://doi.wiley.com/10.1002/ird.239> [Accessed 16 April 2017].
- Doukakis E 2005. Coastal vulnerability and risk parameters. *European Water* 11/12: 3–7. [online]. Available from: [www.ewra.net/ew/pdf/EW\\_2005\\_11-12\\_01.pdf](http://www.ewra.net/ew/pdf/EW_2005_11-12_01.pdf) [Accessed 9 September 2015].
- Eckert S, Jelinek R, Zeug G & Krausmann E 2012. Remote sensing-based assessment of tsunami vulnerability and risk in Alexandria, Egypt. *Applied Geography* 32, 2: 714–723. [online]. Available from: <https://linkinghub.elsevier.com/retrieve/pii/S0143622811001548> [Accessed 16 April 2017].
- Elrick C & Travers A 2009. *Mandurah coastal zone climate change risk assessment and adaptation plan: risk assessment methods*. Mandurah: City of Mandurah. [online]. Available from: [www.mandurah.wa.gov.au/HBItem\\_79617.pdf](http://www.mandurah.wa.gov.au/HBItem_79617.pdf) [Accessed 1 December 2015].
- Els Z 2011. Data availability and requirements for flood hazard mapping in South Africa. Master's thesis. Stellenbosch: Stellenbosch University, Department of Geography and Environmental Studies. [online]. Available from: <https://scholar.sun.ac.za/handle/10019.1/17803> [Accessed 28 October 2019].
- ESRI (Environmental Systems Research Institute) 2016. *ArcGIS online user guide: Resample*. Redlands: ESRI. [online]. Available from: <http://desktop.arcgis.com/en/arcmap/10.3/tools/data-management-toolbox/resample.htm> [Accessed 16 October 2019].

- ESRI (Environmental Systems Research Institute) 2018. *Water Resources*. Redlands: ESRI. [online]. Available from: <https://www.esri.com/en-us/industries/water/segments/water-resources> [Accessed 16 October 2019].
- Eurostat 2018. *Energy, transport and environment indicators. 2018 edition*. Luxembourg: Publications Office of the European Union. [online]. Available from: <http://dx.doi.org/10.2785/94549> [Accessed 12 May 2020].
- FEMA (Federal Emergency Management Agency) 2007. *Guidance for coastal flooding analyses and mapping*. Washington: FEMA. [online]. Available from: <https://www.fema.gov/media-library/assets/documents/13948> [Accessed 4 December 2018].
- FEMA (Federal Emergency Management Agency) 2016. *Guidance for flood risk analysis and mapping elevation guidance*. Washington: FEMA. [online]. Available from: [www.fema.gov/guidelines-and-standards-flood-risk-analysis-and-mapping](http://www.fema.gov/guidelines-and-standards-flood-risk-analysis-and-mapping) [Accessed 21 December 2017].
- Feng Q, Gong J, Liu J & Li Y 2015. Flood mapping based on multiple endmember spectral mixture analysis and random forest classifier—The case of Yuyao, China. *Remote Sensing* 7, 9: 12539–12562. [online]. Available from: <http://www.mdpi.com/2072-4292/7/9/12539> [Accessed 16 April 2017].
- Fish Hoek Centenary 2018. *Fish Hoek centenary*. Cape Town: Fish Hoek Centenary. [online]. Available from: <http://www.fishhoekcentenary.co.za/> [Accessed 16 February 2018].
- Fitchett JM, Grant B & Hoogendoorn G 2016. Climate change threats to two low-lying South African coastal towns: Risks and perceptions. *South African Journal of Science* Volume 112, Number 5/6: 1–9. [online]. Available from: <http://sajs.co.za/article/view/4084> [Accessed 7 August 2016].
- Frazier TG, Wood N, Yarnal B & Bauer DH 2010. Influence of potential sea level rise on societal vulnerability to hurricane storm-surge hazards, Sarasota County, Florida. *Applied Geography* 30, 4: 490–505. [online]. Available from: <https://linkinghub.elsevier.com/retrieve/pii/S0143622810000573>
- Füssel HM 2007. Vulnerability: A generally applicable conceptual framework for climate change research. *Global Environmental Change* 17, 2: 155–167. [online]. Available from: <https://linkinghub.elsevier.com/retrieve/pii/S0959378006000525> [Accessed 20 May 2016].



- Füssel HM 2005. *Vulnerability in climate change research: A comprehensive conceptual framework*. Berkley: University of California, International and Area Studies. [online]. Available from: <https://escholarship.org/uc/item/8993z6nm> [Accessed 20 May 2016].
- Gallien TW, Sanders BF & Flick RE 2014. Urban coastal flood prediction: Integrating wave overtopping, flood defenses and drainage. *Coastal Engineering* 91: 18–28. [online]. Available from: <https://linkinghub.elsevier.com/retrieve/pii/S0378383914000775> [Accessed 14 June 2017].
- Gesch DB 2009. Analysis of LiDAR elevation data for improved identification and delineation of lands vulnerable to sea-level rise. (Special Issue). *Journal of Coastal Research* 53: 49–58. [online]. Available from: <http://www.bioone.org/doi/abs/10.2112/SI53-006.1> [Accessed 16 October 2015].
- Goshen W 2011. *Coping with sea-level rise and storm surges*. Pretoria: SAEON. [online]. Available from: <http://www.saeon.ac.za/enewsletter/archives/2011/april2011/doc08> [Accessed 25 May 2016].
- Graham SR, Carlton C, Gaede D & Jamison B 2011. Student column : The benefits of using Geographic Information Systems as a community assessment tool. *Public Health Reports* 126, 2: 298–303. [online]. Available from: <http://journals.sagepub.com/doi/10.1177/0033354911112600224> [Accessed 8 September 2016].
- Greeff M 2007. Information collection: Interviewing. In Vos AS De Strydom H Fouché CB & Delpont CSL (eds) *Research at grass roots: For the social sciences and human service professions*, 341–375. Pretoria: Van Schaik.
- Guha-Sapir D, Hoyois P & Below R 2015. *Annual disaster statistical review 2015: The numbers and trends*. Brussels: Université catholique de Louvain. [online]. Available from: [http://www.cred.be/sites/default/files/ADSR\\_2015.pdf](http://www.cred.be/sites/default/files/ADSR_2015.pdf) [Accessed 8 September 2016].
- Hahn H, Villagrán de León J. & Hidajat R 2003. *Indicators and other instruments for local risk management for communities and local governments*. Washington: Deutsche Gesellschaft für Technische Zusammenarbeit (GTZ) GmbH International Services. [online]. Available from: <https://publications.iadb.org/en/comprehensive-risk-management-communities-and-local-governments-component-iii-indicators-and-other> [Accessed 16 March 2017].

- Hammar-Klose ES & Thieler ER 2001. *Coastal vulnerability to sea-level rise: a preliminary database for the U.S. Atlantic, Pacific, and Gulf of Mexico coasts*. Woods Hole: United States Geological Survey. [online]. Available from: <https://pubs.usgs.gov/dds/dds68/> [Accessed 7 September 2015].
- Hansen JE 2007. Scientific reticence and sea level rise. *Environmental Research Letters* 2, 024002: 6pp. [online]. Available from: <http://stacks.iop.org/1748-9326/2/i=2/a=024002?key=crossref.6221ce73ab13dc9c12bcd28f69db6e89> [Accessed 19 February 2016].
- Haq M, Akhtar M, Muhammad S, Paras S & Rahmatullah J 2012. Techniques of remote sensing and GIS for flood monitoring and damage assessment: A case study of Sindh Province, Pakistan. *The Egyptian Journal of Remote Sensing and Space Science* 15, 2: 135–141. [online]. Available from: <https://doi.org/10.1016%2Fj.ejrs.2012.07.002> [Accessed 19 February 2016].
- Hejazi K, Ghavami A & Aslani A 2017. Numerical modeling of breaking solitary wave run up in the surf zone using incompressible smoothed particle hydrodynamics. *Coastal Engineering Proceedings* 1, 35: p.waves.31. [online]. Available from: <https://icce-ojs-tamu.tdl.org/icce/index.php/icce/article/view/8269> [Accessed 4 December 2018].
- Helmer O & Rescher N 1959. On the epistemology of the inexact sciences. *Management Science* 6, 1: 25–52. [online]. Available from: <http://pubsonline.informs.org/doi/abs/10.1287/mnsc.6.1.25>
- Henman J & Poulter B 2008. Inundation of freshwater peatlands by sea level rise: Uncertainty and potential carbon cycle feedbacks. *Journal of Geophysical Research: Biogeosciences* 113, G1: n/a-n/a. [online]. Available from: <http://doi.wiley.com/10.1029/2006JG000395>
- Hettiarachchi SSL, Samarawickrama S, Wijeratne N, Ratnasooriya AHR & Samarasekera RSM 2015. *Risk assessment and mitigation within a tsunami forecasting and early warning framework case study-Port City of Galle*. Port City of Galle: University of Moratuwa, Department of Civil Engineering.

- Hettiarachchi SSL, Samarawickrama S, Wijeratne N & Villagrán de León J. 2008. *Tsunami risk assessment for coastal cities of Sri Lanka: Case study for the Port City of Galle, Galle Bay and Headland comprising the Dutch Fort*. Mahe: Paper delivered at IOC UNESCO on Coastal Hazards, Mahe. [online]. Available from: [https://idrc.info/fileadmin/user\\_upload/idrc/former\\_conferences/idrc2008/presentations2008/Hettiarachchi\\_Samantha\\_Coastal\\_Vulnerability\\_and\\_Risk\\_Assessment\\_Vietnam.pdf](https://idrc.info/fileadmin/user_upload/idrc/former_conferences/idrc2008/presentations2008/Hettiarachchi_Samantha_Coastal_Vulnerability_and_Risk_Assessment_Vietnam.pdf) [Accessed 2 July 2018].
- Hsu T-W, Shih D-S, Li C-Y, Lan Y-J & Lin Y-C 2017. A study on coastal flooding and risk assessment under climate change in the Mid-Western Coast of Taiwan. *Water* 9, 390: 13pp. [online]. Available from: <http://www.mdpi.com/2073-4441/9/6/390> [Accessed 7 March 2018].
- Hughes P 1992. The impacts of sea level rise on the South African coastal environment. Doctoral dissertation. Cape Town: University of Cape Town, Department of Oceanography. [online]. Available from: [https://open.uct.ac.za/bitstream/item/27169/Hughes\\_impacts\\_sea\\_level\\_1992\\_1.pdf?sequence=1](https://open.uct.ac.za/bitstream/item/27169/Hughes_impacts_sea_level_1992_1.pdf?sequence=1) [Accessed 15 June 2017].
- IPCC (Intergovernmental Panel on Climate Change) 2019. Chapter 4: Sea Level Rise and Implications for Low Lying Islands, Coasts and Communities. IPCC SR Ocean and Cryosphere. *IPCC Special Report on the Ocean and Cryosphere in a Changing Climate* [H.- O. Pörtner, D.C. Roberts, V. Masson-Delmotte, P. Zhai, M. Tignor, E. Poloczanska, K. Mintenbeck, M. Nicolai, A. Okem, J. Petzold, B. Rama, N. Weyer (eds.)]. *In press.*: 1–169. [online]. Available from: <https://www.ipcc.ch/srocc/chapter/chapter-4-sea-level-rise-and-implications-for-low-lying-islands-coasts-and-communities/>
- IPCC (Intergovernmental Panel on Climate Change) 2007. *Climate change 2007: Synthesis report. Contribution of working groups I, II and III to the Fourth Assessment Report of the Intergovernmental Panel on Climate Change*. Pachauri RK & Reisinger A (eds). Geneva: IPCC, Geneva, Switzerland. [online]. Available from: <https://www.ipcc.ch/report/ar4/syr/> [Accessed 22 July 2015].
- IPCC (Intergovernmental Panel on Climate Change) 2014. *Climate change 2014: Synthesis report. Contribution of working groups I, II and III to the Fifth Assessment Report of the Intergovernmental Panel on Climate Change*. Pachauri RK & Meyer LA (eds). Geneva: IPCC, Geneva, Switzerland. [online]. Available from: <https://www.ipcc.ch/report/ar5/syr/> [Accessed 1 February 2018].

- Izquierdo T, Fritis E & Abad M 2018. Analysis and validation of the PTVA tsunami building vulnerability model using the 2015 Chile post-tsunami damage data in Coquimbo and la Serena cities. *Natural Hazards and Earth System Sciences* 18, 6: 1703–1716.
- Jones JL 2004. *Mapping a flood...before it happens*. Tacoma: United States Geological Survey. [online]. Available from: <https://doi.org/10.3133/2Ffs20043060> [Accessed 20 June 2016].
- Jongman B, Ward PJ & Aerts JCJH 2012. Global exposure to river and coastal flooding: Long term trends and changes. *Global Environmental Change* 22, 4: 823–835. [online]. Available from: <https://linkinghub.elsevier.com/retrieve/pii/S0959378012000830> [Accessed 12 September 2017].
- Joubert JL & van Niekerk JR 2013. *South African Wave Energy Resource Data*. Stellenbosch: Stellenbosch University, Centre for Renewable and Sustainable Energy Studies. [online]. Available from: [http://www.crses.sun.ac.za/files/research/publications/technical-reports/SANEDI\(WaveEnergyResource\)\\_edited\\_v2.pdf](http://www.crses.sun.ac.za/files/research/publications/technical-reports/SANEDI(WaveEnergyResource)_edited_v2.pdf) [Accessed 6 October 2016].
- Kia MB, Pirasteh S, Pradhan B, Mahmud AR, Sulaiman WNA & Moradi A 2012. An artificial neural network model for flood simulation using GIS: Johor River Basin, Malaysia. *Environmental Earth Sciences* 67, 1: 251–264. [online]. Available from: <http://link.springer.com/10.1007/s12665-011-1504-z> [Accessed 16 September 2016].
- Kim S, Arrowsmith CA & Handmer J 2004. Assessment of socioeconomic vulnerability of coastal areas from an indicator based approach. *10th International Conference on Geo-Computation, UNSW, Sydney, 2009*: 6. [online]. Available from: <https://pdfs.semanticscholar.org/9e71/32ca81d81a0d3b25bbfdb79e07e23753575f.pdf> [Accessed 6 October 2016].
- Klein RJT & Nicholls RJ 1999. Assessment of coastal vulnerability to climate change. *Ambio* 28, 2: 182–187. [online]. Available from: <https://www.jstor.org/stable/4314873> [Accessed 11 October 2019].
- Kleinosky LR, Yarnal B & Fisher A 2007. Vulnerability of Hampton Roads, Virginia to storm-surge flooding and sea-level rise. *Natural Hazards* 40, 1: 43–70. [online]. Available from: <http://link.springer.com/10.1007/s11069-006-0004-z> [Accessed 16 September 2016].

- Krabill W 2004. Greenland Ice Sheet: Increased coastal thinning. *Geophysical Research Letters* 31, 24: L24402. [online]. Available from: <http://doi.wiley.com/10.1029/2004GL021533> [Accessed 19 October 2017].
- Kretzmann S 2019. Rising sea levels are causing problems for Cape Town [online]. Available from: <https://www.timeslive.co.za/news/south-africa/2019-08-30-rising-sea-levels-are-causing-problems-for-cape-town/> [Accessed 5 June 2020].
- Kron W 2013. Coasts: The high-risk areas of the world. *Natural Hazards* 66, 3: 1363–1382. [online]. Available from: <http://link.springer.com/10.1007/s11069-012-0215-4> [Accessed 21 May 2014].
- Lal PN, Mitchell T, Aldunce P, Auld H, Mechler R, Miyan A, Romano LE, Zakaria S, Dlugolecki A, Masumoto T, Ash N, Hochrainer S, Hodgson R, Islam TU, Mc Cormick S, Neri C, Pulwarty R, Rahman A, Ramalingam B, Sudmeier-Reiux K, Tompkins E, Twigg J & Wilby R 2012. *National systems for managing the risks from climate extremes and disasters*.
- Lewis J 2019. The fluidity of risk: Variable vulnerabilities and uncertainties of behavioural response to natural and technological hazards. *Disaster Prevention and Management: An International Journal* 28, 5: 636–648.
- Li X, Grady CJ & Peterson AT 2014. Delineating sea level rise inundation using a graph traversal algorithm. *Marine Geodesy* 37, 2: 267–281. [online]. Available from: <http://www.tandfonline.com/doi/abs/10.1080/01490419.2014.902884> [Accessed 29 October 2018].
- Lück-Vogel M, Macon C & Williams LL 2018. Guidelines for coastal LiDAR. *PositionIT*, April/May 2018: 17–22. [online]. Available from: <https://www.ee.co.za/article/guidelines-for-coastal-lidar.html> [Accessed 2 August 2019].
- Lui H, Sherman D & Gu S 2007. Automated extraction of shorelines from airborne light detection and ranging data and accuracy assessment based on Monte Carlo simulation. *Journal of Coastal Research* 23, 6: 1359–1369.
- Mamuji AA & Etkin D 2019. Disaster Risk Analysis Part 2: The Systemic Underestimation of Risk. *Journal of Homeland Security and Emergency Management* 16, 1. [online]. Available from: [https://www.researchgate.net/publication/330739905\\_Disaster\\_Risk\\_Analysis\\_Part\\_2\\_The\\_Systemic\\_Underestimation\\_of\\_Risk](https://www.researchgate.net/publication/330739905_Disaster_Risk_Analysis_Part_2_The_Systemic_Underestimation_of_Risk) [Accessed 27 May 2020].



- Marcy D, Brooks W, Draganov K, Hadley B, Haynes C, Herold N, McCombs J, Pendleton M, Ryan S, Schmid K, Sutherland M & Waters K 2011. *New mapping tool and techniques for visualizing sea level rise and coastal flooding impacts*. Proceedings of the Solutions to Coastal Disasters Conference held 25-29 July 2011. Reston. American Society of Civil Engineers.: 474–490. [online]. Available from: <http://ascelibrary.org/doi/10.1061/41185%28417%2942> [Accessed 7 April 2017].
- Marks K & Bates PD 2000. Integration of high-resolution topographic data with floodplain flow models. *Hydrological Processes* 14, 11–12: 2109–2122. [online]. Available from: [https://www.researchgate.net/publication/248017507\\_Integration\\_of\\_High-Resolution\\_Topographic\\_Data\\_With\\_Floodplain\\_Flow\\_Models](https://www.researchgate.net/publication/248017507_Integration_of_High-Resolution_Topographic_Data_With_Floodplain_Flow_Models) [Accessed 14 March 2018].
- Martínez Sánchez J 2015. *Assessment of coastal hazards, vulnerability and risk for the coast of Oman*. Oman: Sultanate of Oman. [online]. Available from: [https://www.jcomm.info/index.php?option=com\\_oe&task=viewDocumentRecord&docID=15550](https://www.jcomm.info/index.php?option=com_oe&task=viewDocumentRecord&docID=15550) [Accessed 5 June 2016].
- Marujo-Silva NRC 2011. Storm surge hydrodynamic modelling. Master's thesis. Universidade Technica de Lisboa, Instituto Superior Tecnico. [online]. Available from: <https://dspace.ist.utl.pt/bitstream/2295/1066510/1/dissertacao.pdf> [Accessed 5 June 2016].
- Mather A 2007. Linear and nonlinear sea-level changes at Durban, South Africa. *South African Journal of Science* 103, 11–12: 509–512.
- Mather A, Garland GG & Stretch DD 2009. Southern African sea levels: corrections, influences and trends. *African Journal of Marine Science* 31, 2: 145–156. [online]. Available from: <http://www.tandfonline.com/doi/full/10.2989/AJMS.2009.31.2.3.875> [Accessed 12 July 2018].
- Mather A, Stretch D & Garland G 2011a. Predicting extreme wave run-up on natural beaches for coastal planning and management. *Coastal Engineering Journal* 53, 2: 87–109. [online]. Available from: <https://www.tandfonline.com/doi/full/10.1142/S0578563411002288> [Accessed 12 July 2018].
- Mather A, Stretch D & Garland G 2011b. Predicting extreme wave run-up on natural beaches for coastal planning and management. *Coastal Engineering Journal* 53, 2: 87–109. [online]. Available from: <https://www.tandfonline.com/doi/full/10.1142/S0578563411002288> [Accessed 12 July 2018].

- McCain N 2017. City sweeps up sand. *People's Post* 7 March [online]. Available from: <https://www.news24.com/SouthAfrica/Local/Peoples-Post/city-sweeps-up-sand-20170306> [Accessed 9 February 2018].
- Miller F, Osbahr H, Boyd E, Thomalla F, Bharwani S, Ziervogel G, Walker B, Birkmann J, van der Leeuw S, Rockström J, Hinkel J, Downing T, Folke C & Nelson D 2010. Resilience and vulnerability: Complementary or conflicting concepts? *Ecology and Society* 15, 3: art11. [online]. Available from: <http://www.ecologyandsociety.org/vol15/iss3/art11/> [Accessed 3 July 2019].
- Nanayakkara KIU & Dias WPS 2016. Fragility curves for structures under tsunami loading. *Natural Hazards* 80, 1: 471–486. [online]. Available from: <http://link.springer.com/10.1007/s11069-015-1978-1> [Accessed 18 October 2017].
- Nandi A, Mandal A, Wilson M & Smith D 2016. Flood hazard mapping in Jamaica using principal component analysis and logistic regression. *Environmental Earth Sciences* 75, 6: 465. [online]. Available from: <http://link.springer.com/10.1007/s12665-016-5323-0> [Accessed 4 October 2019].
- Navalgund RR, Nayak SR, Thakker PS, Rajawat AS, Chauhan HB, Ray SS, Chaudhary KN, Bhanumurthy V, Singh TP & Mehta RL 1998. *An assessment of the Gujarat cyclone damage through IRS-1C/1D data*. Ahmedabad: ISRO.
- Nayak SR 1996. Monitoring the coastal environment of India using satellite data. *Science, Technology and Development* 14, 2: 100–120.
- Nayak SR, Sarangai RK & Rajawat AS 2001. Application of IRS-P4 OCM data to study the impact of cyclone on coastal environment of Orissa. *Current Science* 80, 9: 1209–1213.
- Neumann T & Ahrendt K 2013. *Comparing the “bathtub method” with MIKE 21 HD flow model for modelling storm surge inundation: Case study Kiel Fjord*. RADOST report series, report No. 22. Kiel: University of Kiel, Geographical Institute University of Kiel. [online]. Available from: <http://klimzug-radost.de/en/info/comparing-bathtub-method-mike-21-hd-flow-model-modelling-storm-surge-inundation-case-study-kie> [Accessed 27 May 2016].

- Nicholls RJ, Wong PP, Burkett V, Woodroffe CD & Hay J 2008. Climate change and coastal vulnerability assessment: scenarios for integrated assessment. *Sustainability Science* 3, 1: 89–102. [online]. Available from: <http://link.springer.com/10.1007/s11625-008-0050-4> [Accessed 14 November 2016].
- Nielsen P & Hanslow DJ 1991. Wave runup distributions on natural beaches. *Journal of Coastal Research* 7, 4: 1139–1152. [online]. Available from: <https://www.jstor.org/stable/4297933> [Accessed 14 November 2016].
- NOAA (National Oceanographic and Atmospheric Administration) 2012. *Mapping coastal inundation primer*. Charleston: NOAA. [online]. Available from: <https://coast.noaa.gov/data/digitalcoast/pdf/coastal-inundation-guidebook.pdf> [Accessed 17 July 2015].
- Nock AH 2014. The integration of coastal flooding into an ArcFLOOD data model. Doctoral dissertation. Plymouth: Plymouth University. [online]. Available from: <http://hdl.handle.net/10026.1/3199> [Accessed 29 October 2018].
- O’Keefe P, Westgate K & Wisner B 1976. Taking the naturalness out of natural disasters. *Nature* 260, 5552: 566–567. [online]. Available from: <http://www.nature.com/articles/260566a0> [Accessed 18 September 2016].
- Ouma Y & Tateishi R 2014. Urban flood vulnerability and risk mapping using integrated multi-parametric AHP and GIS: Methodological overview and case study assessment. *Water* 6, 6: 1515–1545. [online]. Available from: <https://doi.org/10.3390%2Fw6061515> [Accessed 8 August 2019].
- Papathoma-Köhle M, Cristofari G, Wenk M & Fuchs S 2019. The importance of indicator weights for vulnerability indices and implications for decision making in disaster management. *International Journal of Disaster Risk Reduction* 36: 101103. [online]. Available from: <https://linkinghub.elsevier.com/retrieve/pii/S2212420918308665> [Accessed 30 July 2019].
- Papathoma-Köhle M, Gems B, Sturm M & Fuchs S 2017. Matrices, curves and indicators: A review of approaches to assess physical vulnerability to debris flows. *Earth-Science Reviews* 171: 272–288. [online]. Available from: <https://linkinghub.elsevier.com/retrieve/pii/S001282521630438X> [Accessed 8 August 2019].

- Papathoma M & Dominey-Howes D 2003. Tsunami vulnerability assessment and its implications for coastal hazard analysis and disaster management planning, Gulf of Corinth, Greece. *Natural Hazards and Earth System Science* 3, 6: 733–747. [online]. Available from: <http://www.nat-hazards-earth-syst-sci.net/3/733/2003/> [Accessed 21 May 2016].
- Perini L, Calabrese L, Salerno G, Ciavola P & Armaroli C 2016. Evaluation of coastal vulnerability to flooding: comparison of two different methodologies adopted by the Emilia-Romagna region (Italy). *Natural Hazards and Earth System Sciences* 16, 1: 181–194. [online]. Available from: <https://www.nat-hazards-earth-syst-sci.net/16/181/2016/> [Accessed 1 June 2018].
- Pfaff MC, Logston RC, Raemaekers SJP, Hermes JC, Blamey LK, Cawthra HC, Colenbrander DR, Crawford RJM, Day E, Du Plessis N, Elwen SH, Fawcett SE, Jury MR, Karenyi N, Kerwath SE, Kock AA, Krug M, Lamberth SJ, Omardien A, Pitcher GC, Rautenbach C, Robinson TB, Rouault M, Ryan PG, Shillington FA, Sowman M, Sparks CC, Turpie JK, Van Niekerk L, Waldron HN, Yeld EM & Kirkman SP 2019. A synthesis of three decades of socio-ecological change in False Bay, South Africa: setting the scene for multidisciplinary research and management. *Elementa Science of the Anthropocene* 7, 1: 32. [online]. Available from: <https://www.elementascience.org/article/10.1525/elementa.367/> [Accessed 15 May 2020].
- Polsky C, Neff R & Yarnal B 2007. Building comparable global change vulnerability assessments: The vulnerability scoping diagram. *Global Environmental Change* 17, 3–4: 472–485. [online]. Available from: <https://linkinghub.elsevier.com/retrieve/pii/S0959378007000210> [Accessed 25 February 2017].
- Poulter B & Halpin PN 2008. Raster modelling of coastal flooding from sea-level rise. *International Journal of Geographical Information Science* 22, 2: 167–182. [online]. Available from: <http://www.tandfonline.com/doi/abs/10.1080/13658810701371858> [Accessed 25 August 2018].
- Pregolato M, Galasso C & Parisi F 2015. *A compendium of existing vulnerability and fragility relationships for flood: Preliminary results*. Proceedings of the 12th International conference on applications of statistics and probability in civil engineering, ICASP12 held 12-15 July 2015. Vancouver. CERRA.
- Province of the Eastern Cape 2010. *Disaster risk assessment for the Nelson Mandela Bay Municipality*. Nelson Mandela Bay: Province of the Eastern Cape. [online]. Available from: [www.nelsonmandelabay.gov.za/datarepository/documents/qqGwV\\_DM\\_Plan.pdf](http://www.nelsonmandelabay.gov.za/datarepository/documents/qqGwV_DM_Plan.pdf) [Accessed 2 July 2018].

- Province of the Western Cape 2013a. *Eden District Municipality disaster risk assessment*. Cape Town: Province of the Western Cape.
- Province of the Western Cape 2010a. *Eden District Municipality sea level rise phase 1 literature review final*. Cape Town: Province of the Western Cape. [online]. Available from: [https://www.westerncape.gov.za/eadp/files/basic-page/downloads/Eden DM SLR Phase 1 Literature Review.pdf](https://www.westerncape.gov.za/eadp/files/basic-page/downloads/Eden_DM_SLR_Phase_1_Literature_Review.pdf) [Accessed 11 July 2017].
- Province of the Western Cape 2010b. *Eden District Municipality sea level rise phase 2 modelling final*. Cape Town: Province of the Western Cape. [online]. Available from: [https://www.westerncape.gov.za/eadp/files/basic-page/downloads/Eden DM SLR Phase 2 Modelling Final.pdf](https://www.westerncape.gov.za/eadp/files/basic-page/downloads/Eden_DM_SLR_Phase_2_Modelling_Final.pdf) [Accessed 11 July 2017].
- Province of the Western Cape 2010c. *Eden District Municipality sea level rise phase 3 risk assessment final*. Cape Town: Province of the Western Cape. [online]. Available from: [https://www.westerncape.gov.za/eadp/files/basic-page/downloads/Eden DM SLR Phase 3 Risk Assessment.pdf](https://www.westerncape.gov.za/eadp/files/basic-page/downloads/Eden_DM_SLR_Phase_3_Risk_Assessment.pdf) [Accessed 11 July 2017].
- Province of the Western Cape 2013b. *Overberg District Municipality disaster risk assessment*. Cape Town: Province of the Western Cape.
- Province of the Western Cape 2012a. *Proposed comprehensive disaster risk assessment standardised methodology*.
- Province of the Western Cape 2012b. *West Coast District Municipality disaster risk assessment*. Cape Town: Province of the Western Cape.
- RADAR (Research Alliance for Disaster and Risk Reduction) 2010. *Risk and development annual review*. Cape Town: PeriPeri Publications. [online]. Available from: [https://www.preventionweb.net/files/16151\\_16151radar2010english1.pdf](https://www.preventionweb.net/files/16151_16151radar2010english1.pdf) [Accessed 9 January 2017].
- Rajawat AS, Gupta M, Pradhan Y, Thomaskutty AV & Nayak SR 2005. Coastal processes along the Indian coast – case studies based on synergistic use of IRS-P4 OCM and IRS-1C/1D data. *Indian Journal of Marine Sciences* 34, 4: 459–472.



- Rajawat AS & Nayak S 2000. Remote sensing applications in coastal zone hazards. In *Natural Disasters and their Mitigations, Remote Sensing and Geographic Information System Perspectives*, 58–174. Dehradun: Indiana Institute of Remote Sensing (NRSA).
- Rajawat AS & Nayak SR 2004. *Applications of satellite survey in coastal disasters*. Valdiya KS (ed). Proceedings of the Coping with Natural Hazards Symposium held 5-6 October 2001. Allahabad. The National Academy of Sciences.
- Rautenbach C, Daniels T, de Vos M & Barnes MA 2020. *A coupled wave, tide and storm surge operational forecasting system for South Africa: validation and physical description*. Springer Netherlands. [online]. Available from: <https://doi.org/10.1007/s11069-020-04042-4>
- Rignot E 2006. Changes in the velocity structure of the Greenland ice sheet. *Science* 311, 5763: 986–990. [online]. Available from: <http://www.sciencemag.org/cgi/doi/10.1126/science.1121381> [Accessed 15 May 2018].
- Rodriguez A 2010. *Mexican Gulf of Mexico Regional Introduction and Sea Level Rise Analysis of the Carmen Island, Campeche, Mexico Region*. Austin: University of Texas. [online]. Available from: <http://www.geo.utexas.edu/courses/371c/project/2010S/Projects/Rodriguez.pdf> [Accessed 2 November 2017].
- Rollason V, Fisk G & Haines P 2010. *Applying the ISO 31000 risk assessment framework to coastal zone management*. Proceedings of the NSW Coastal Conference held 10-12 November 2010. Batemans Bay. East Coast Conferences.: 1–16. [online]. Available from: [https://www.coastalconference.com/2010/papers2010/Verity Rollason full paper 2.pdf](https://www.coastalconference.com/2010/papers2010/Verity%20Rollason%20full%20paper%202.pdf) [Accessed 26 November 2015].
- Rossouw M, Stander J, Farre R & Brundrit G 2012. *Real time observations and forecasts in the South African coastal ocean*. Working paper. Stellenbosch: CSIR.
- Rozos D, Bathrellos GD & Skillodimou HD 2011. Comparison of the implementation of rock engineering system and analytic hierarchy process methods, upon landslide susceptibility mapping, using GIS: a case study from the Eastern Achaia County of Peloponnesus, Greece. *Environmental Earth Sciences* 63, 1: 49–63. [online]. Available from: <http://link.springer.com/10.1007/s12665-010-0687-z> [Accessed 16 March 2018].

- Salecker D, Gruhn A, Schlamkow C & Fröhle P 2011. Statistical analysis of hydrodynamic impacts for risk assessment of coastal areas. (Special Issue). *Journal of Coastal Research* , 64: 1906–1910. [online]. Available from: <https://www.jstor.org/stable/26482508> [Accessed 11 October 2019].
- Samarasinghea SMJS, Nandalalb HK, Weliwitiyac DP, Fowzed JSM, Hazarikad MK & Samarakoond L 2010. *Application of remote sensing and GIS for flood risk analysis : A case study at Kalu- Ganga River, Sri Lanka*. International Archives of the Photogrammetry, Remote Sensing and Spatial Information Science. Kyoto. ISPRS.: 110–115. [online]. Available from: [https://www.researchgate.net/publication/289840047\\_Application\\_of\\_remote\\_sensing\\_and\\_gis\\_for\\_flood\\_risk\\_analysis\\_A\\_case\\_study\\_at\\_Kalu-Ganga\\_River\\_Sri\\_Lanka](https://www.researchgate.net/publication/289840047_Application_of_remote_sensing_and_gis_for_flood_risk_analysis_A_case_study_at_Kalu-Ganga_River_Sri_Lanka) [Accessed 21 December 2017].
- Satake K 2014. Advances in earthquake and tsunami sciences and disaster risk reduction since the 2004 Indian Ocean Tsunami. *Geoscience Letters* 15: 15. [online]. Available from: <http://www.geoscienceletters.com/content/1/1/15> [Accessed 29 June 2018].
- Schwarz J & Maiwald H 2008. *Damage and loss prediction model based on the vulnerability of building types*. Proceedings of the 4th International symposium on flood defence held 6-8 May 2008. Toronto. United States Geological Survey. [online]. Available from: [http://gfzpublic.gfz-potsdam.de/pubman/item/escidoc:6057:7/component/escidoc:6058/74\\_Schwarz.pdf](http://gfzpublic.gfz-potsdam.de/pubman/item/escidoc:6057:7/component/escidoc:6058/74_Schwarz.pdf) [Accessed 11 October 2019].
- Sekovski I, Armaroli C, Calabrese L, Mancini F, Stecchi F & Perini L 2015. Coupling scenarios of urban growth and flood hazards along the Emilia-Romagna coast (Italy). *Natural Hazards and Earth System Sciences* 15, 10: 2331–2346. [online]. Available from: <https://www.nat-hazards-earth-syst-sci.net/15/2331/2015/> [Accessed 1 June 2018].
- Sharifi F & Ezam M 2017. A comparison between the results of Hormuz Strait wave simulations using WAVEWATCH-III and satellite altimetry observations. *Oceanography & Fisheries Open access Journal* 1, 5. [online]. Available from: <https://juniperpublishers.com/foaj/OFOAJ.MS.ID.555572.php> [Accessed 1 November 2018].

- Sharifi F, Ezam M & Karami Khaniki A 2012. Evaluating the results of Hormuz Strait wave simulations using WAVEWATCH III and MIKE21-SW. *International Journal of Marine Science and Engineering* 2, 2: 163–170. [online]. Available from: <https://pdfs.semanticscholar.org/c267/af8ec2d06a19404fb323c2381b65410cbaa2.pdf> [Accessed 16 March 2016].
- Sharples C, Attwater C & Carley J 2008. *Three pass approach to coastal risk assessment*. Proceedings of the Coast to coast conference held 18-22 August 2008. Darwin. Australian Coastal Society. [online]. Available from: [https://www.researchgate.net/publication/238100175\\_Three\\_Pass\\_Approach\\_To\\_Coastal\\_Risk\\_Assessment](https://www.researchgate.net/publication/238100175_Three_Pass_Approach_To_Coastal_Risk_Assessment) [Accessed 23 April 2016].
- Shmueli G 2010. To Explain or to Predict? *Statistical Science* 25, 3: 289–310. [online]. Available from: <http://projecteuclid.org/euclid.ss/1294167961> [Accessed 1 November 2018].
- Sieh K, Natawidjaja DH, Meltzner AJ, Shen C-C, Cheng H, Li K-S, Suwargadi BW, Galetzka J, Philiposian B & Edwards RL 2008. Earthquake supercycles inferred from sea-level changes recorded in the corals of West Sumatra. *Science* 322, 5908: 1674–1678. [online]. Available from: <http://www.sciencemag.org/cgi/doi/10.1126/science.1163589>
- Sivakumar B 2001. Rainfall dynamics at different temporal scales: A chaotic perspective. *Hydrology and Earth System Sciences* 5, 4: 645–652. [online]. Available from: <http://www.hydrol-earth-syst-sci.net/5/645/2001/>
- Slatton KC, Carter WE, Shrestha RL & Dietrich W 2007. Airborne laser swath mapping: Achieving the resolution and accuracy required for geosurficial research. *Geophysical Research Letters* 34, 23. [online]. Available from: <http://doi.wiley.com/10.1029/2007GL031939> [Accessed 15 June 2017].
- South Africa (Republic of) 2016. *Conducting comprehensive disaster risk assessments*. Pretoria: Department of Cooperative Governance and Traditional Affairs.
- South Africa (Republic of) 2014. *National coastal management programme of South Africa*. Pretoria: Department of Environmental Affairs. [online]. Available from: [https://www.environment.gov.za/sites/default/files/docs/nationalcoastal\\_managementprogramme.pdf](https://www.environment.gov.za/sites/default/files/docs/nationalcoastal_managementprogramme.pdf) [Accessed 1 February 2014].

- South Africa (Republic of) 2005. *National disaster management framework*. Pretoria: Department of Cooperative Governance and Traditional Affairs. [online]. Available from: <https://www.westerncape.gov.za/text/2013/July/sa-national-disaster-man-framework-2005.pdf> [Accessed 23 February 2015].
- South Africa (Republic of) 2008. *South African Tide Information*. Cape Town: SANHO. [online]. Available from: [http://www.sanho.co.za/tides/tide\\_index.htm](http://www.sanho.co.za/tides/tide_index.htm) [Accessed 4 August 2017].
- South Africa (Republic of) 2009. *South African Tide Tables*. Tokai: Naval Hydrographer, South African Navy Publishing Unit.
- South Africa (Republic of) 2019. State of the Environment South Africa [online]. Available from: <http://soer.environment.gov.za/soer/CMSWebSite/Content.aspx?menuId=4318,3307> [Accessed 19 May 2020].
- Sowman M, Scott D & Sutherland C 2016. *Governance and social justice position paper: Milnerton Beach*. Cape Town: City of Cape Town.
- Spencer T, Naylor L, Lane S, Darby S, Macklin M, Magilligan F & Möller I 2017. Stormy geomorphology: An introduction to the Special Issue. *Earth Surface Processes and Landforms* 42, 1: 238–241. [online]. Available from: <http://doi.wiley.com/10.1002/esp.4065> [Accessed 25 July 2017].
- START 2013. *Cities at risk workshop: Africa*. Durban: START. [online]. Available from: <http://start.org/programs/cities-at-risk/africa-workshop> [Accessed 1 December 2015].
- Stockdon HF, Sallenger AH, Holman RA & Howd PA 2007. A simple model for the spatially-variable coastal response to hurricanes. *Marine Geology* 238, 1–4: 1–20. [online]. Available from: <https://linkinghub.elsevier.com/retrieve/pii/S0025322706003355>
- Strauss D, Mirferendesk H & Tomlinson R 2007. Comparison of two wave models for Gold Coast, Australia. *Journal of Coastal Research* 50, 50: 312–316.
- Strunz G, Post J, Zosseder K, Wegscheider S, Mück M, Riedlinger T, Mehl H, Dech S, Birkmann J, Gebert N, Harjono H, Anwar HZ, Sumaryono S, Khomarudin RM & Muhari A 2011. Tsunami risk assessment in Indonesia. *Natural Hazards and Earth System Science* 11, 1: 67–82. [online]. Available from: <http://www.nat-hazards-earth-syst-sci.net/11/67/2011/>

- Sumaryono S 2010. Assessing building vulnerability to tsunami hazard using integrative remote sensing and GIS approaches. Doctoral dissertaion. Munich: Ludwig-Maximilians-Universität München, Faculty of Geosciences. [online]. Available from: <https://edoc.ub.uni-muenchen.de/12390/> [Accessed 11 October 2017].
- Suppasri A, Goto K, Muhari A, Ranasinghe P, Riyaz M, Affan M, Mas E, Yasuda M & Imamura F 2015. A decade after the 2004 Indian Ocean Tsunami: The progress in disaster preparedness and future challenges in Indonesia, Sri Lanka, Thailand and the Maldives. *Pure and Applied Geophysics* 172, 12: 3313–3341. [online]. Available from: <http://link.springer.com/10.1007/s00024-015-1134-6>
- Tehrany MS, Pradhan B & Jebur MN 2014. Flood susceptibility mapping using a novel ensemble weights-of-evidence and support vector machine models in GIS. *Journal of Hydrology* 512: 332–343. [online]. Available from: <https://linkinghub.elsevier.com/retrieve/pii/S0022169414001826>
- Terry JP & Goff J 2012. *Natural hazards in the Asia-Pacific region: recent advances and emerging concepts*. Terry JP & Goff J (eds). London: Geological Society.
- The State of Queensland 2013. *Coastal hazard technical guide*. Brisbane: The State of Queensland. [online]. Available from: <https://www.ehp.qld.gov.au/coastalplan/pdf/hazards-guideline.pdf> [Accessed 1 August 2016].
- Thomas TJ & Dwarakish GS 2015. Numerical wave modelling – A review. *Aquatic Procedia* 4: 443–448. [online]. Available from: <https://linkinghub.elsevier.com/retrieve/pii/S2214241X15000607> [Accessed 29 June 2018].
- Tol RSJ, Klein RJT & Nicholls RJ 2008. Towards successful adaptation to sea-level rise along Europe’s coasts. *Journal of Coastal Research* 242: 432–442. [online]. Available from: <http://www.bioone.org/doi/abs/10.2112/07A-0016.1> [Accessed 25 August 2017].
- Turpie J & Wilson G 2011. *Cost/benefit assessment of marine and coastal resources in the Western Indian Ocean : Mozambique and South Africa. Office Report*. Pretoria: UNDP.
- UNDDR (United Nations Disaster Risk Reduction) 2015. *Vulnerability*. Geneva: UNDRR. [online]. Available from: <https://www.preventionweb.net/risk/vulnerability> [Accessed 5 September 2019].



- UNISDR (United Nations International Strategy for Disaster Reduction) 2016. *Launching UNISDR science and technology partnership and the science and technology road map to 2030. Short concept note: Work stream 2, working Group 2*. Cambridge: Cambridge University Press. [online]. Available from: [http://www.preventionweb.net/files/45270\\_unisdr-cnws2wg2-vulnerability-and-exposure.pdf](http://www.preventionweb.net/files/45270_unisdr-cnws2wg2-vulnerability-and-exposure.pdf) [Accessed 9 June 2020].
- UNISDR (United Nations International Strategy for Disaster Reduction) 2004. *Living with risk: A global review of disaster reduction initiatives*. Geneva: UNISDR. [online]. Available from: <https://www.unisdr.org/we/inform/publications/657> [Accessed 28 August 2015].
- UNISDR (United Nations International Strategy for Disaster Reduction) 2015. *Sendai framework for disaster risk reduction 2015–2030*. 2. Geneva: UNISDR. [online]. Available from: [http://www.wcdrr.org/uploads/Sendai\\_Framework\\_for\\_Disaster\\_Risk\\_Reduction\\_2015-2030.pdf](http://www.wcdrr.org/uploads/Sendai_Framework_for_Disaster_Risk_Reduction_2015-2030.pdf) [Accessed 4 April 2019].
- UNISDR (United Nations International Strategy for Disaster Reduction) 2017. *Terminology*. Geneva: UNISDR. [online]. Available from: <https://www.unisdr.org/we/inform/terminology#letter-r> [Accessed 5 April 2019].
- UNU-IDHP (United Nations University's International Human Dimensions Programme) 2015. *Coastal zones and urbanization: Summary for decision-makers*. June. Bonn: UNU-IDHP. [online]. Available from: [https://www.researchgate.net/publication/279455992\\_Coastal\\_zones\\_and\\_urbanization](https://www.researchgate.net/publication/279455992_Coastal_zones_and_urbanization) [Accessed 31 August 2015].
- Velicogna I 2006. Measurements of time-variable gravity show mass loss in Antarctica. *Science* 311, 5768: 1754–1756. [online]. Available from: <http://www.sciencemag.org/cgi/doi/10.1126/science.1123785> [Accessed 14 May 2018].
- Viavattene C, Jiménez JA, Ferreira O, Priest S, Owen D & McCall R 2018. Selecting coastal hotspots to storm impacts at the regional scale: A coastal risk assessment framework. *Coastal Engineering* 134, September: 33–47. [online]. Available from: <https://linkinghub.elsevier.com/retrieve/pii/S0378383917300583>
- Viles H & Spencer T 1995. *Coastal Problems: Geomorphology, ecology and society at the coast*. London: Edward Arnold. [online]. Available from: <https://www.taylorfrancis.com/books/9781315832586>

- Villagrán de León J. 2006. *Vulnerability: A conceptual and methodological review*. Bonn: UNU-EHS. [online]. Available from: <https://collections.unu.edu/view/UNU:1871#viewAttachments> [Accessed 31 August 2015].
- Villatoro M, Silva R, Méndez FJ, Zanuttigh B, Pan S, Trifonova E, Losada IJ, Izaguirre C, Simmonds D, Reeve DE, Mendoza E, Martinelli L, Formentin SM, Galiatsatou P & Eftimova P 2014. An approach to assess flooding and erosion risk for open beaches in a changing climate. *Coastal Engineering* 87: 50–76. [online]. Available from: <https://linkinghub.elsevier.com/retrieve/pii/S0378383913001920>
- Voulgaris G & Murayama Y 2014. Tsunami vulnerability assessment in the Southern Boso Peninsula, Japan. *International Journal of Disaster Risk Reduction* 10: 190–200. [online]. Available from: <https://linkinghub.elsevier.com/retrieve/pii/S2212420914000636>
- Wang Z, Lai C, Chen X, Yang B, Zhao S & Bai X 2015. Flood hazard risk assessment model based on random forest. *Journal of Hydrology* 527: 1130–1141. [online]. Available from: <https://doi.org/10.1016%2Fj.jhydrol.2015.06.008>
- Weis SWM, Agostini VN, Roth LM, Gilmer B, Schill SR, Knowles JE & Blyther R 2016. Assessing vulnerability: an integrated approach for mapping adaptive capacity, sensitivity, and exposure. *Climatic Change* 136, 3–4: 615–629. [online]. Available from: <http://link.springer.com/10.1007/s10584-016-1642-0> [Accessed 6 June 2020].
- van Westen CJ 2013. Remote sensing and GIS for natural hazards assessment and disaster risk management. *Treatise on Geomorphology* 3: 259–298. [online]. Available from: [https://www.researchgate.net/publication/285929471\\_Remote\\_Sensing\\_and\\_GIS\\_for\\_Natural\\_Hazards\\_Assessment\\_and\\_Disaster\\_Risk\\_Management](https://www.researchgate.net/publication/285929471_Remote_Sensing_and_GIS_for_Natural_Hazards_Assessment_and_Disaster_Risk_Management) [Accessed 27 November 2015].
- van Westen CJ, Castellanos E & Kuriakose SL 2008. Spatial data for landslide susceptibility, hazard, and vulnerability assessment: An overview. *Engineering Geology* 102, 3–4: 112–131. [online]. Available from: <https://linkinghub.elsevier.com/retrieve/pii/S0013795208001786> [Accessed 27 November 2015].
- van Westen CJ & Greiving S 2017. Multi-hazard risk assessment and decision making. In *Environmental hazards methodologies for risk assessment and management*, 31–94. International Water Association. [online]. Available from: [https://doi.org/10.2166%2F9781780407135\\_0031](https://doi.org/10.2166%2F9781780407135_0031) [Accessed 21 May 2019].

- Williams LL 2019a. *ArcCoastTools*. Cape Town: SAEON. [online]. Available from: <http://www.sasdi.net/metaview.aspx?uuid=23379c9052ee1dfbbd1889ffc010d1e0> [Accessed 4 December 2019].
- Williams LL 2019b. *Coastal Inundation (Enhanced Bathtub Model (eBTM))*. Cape Town: SAEON. [online]. Available from: <http://www.sasdi.net/metaview.aspx?uuid=f99e76fbf27cc57eb90bb11e60d09f82> [Accessed 4 December 2019].
- Williams LL 2013. *Towards a GIS methodology for disaster risk assessments*. Proceedings of the Africa Geospatial Forum held 13-14 August 2013. Cape Town. Africa Geospatial Forum. [online]. Available from: <https://slideplayer.com/slide/5676269/> [Accessed 17 December 2019].
- Williams LL & Lück-Vogel M 2020. Comparative assessment of the GIS based bathtub model and an enhanced bathtub model for coastal inundation. *Journal of Coastal Conservation* 24, 2: 23. [online]. Available from: <http://link.springer.com/10.1007/s11852-020-00735-x>
- Wisner B, Blaikie P, Cannon T & Davis I 2003. *At risk: Natural hazards, people's vulnerability and disasters*. 2nd ed. Routledge.
- Wong PP, Losada IJ, Gattuso JP, Hinkel J, Khattabi A, McInnes KL, Saito Y & Sallenger AH 2014. Coastal systems and low-lying areas. In Field CB Barros VR Dokken DJ Mach KJ Mastrandrea MD Bilir TE Chatterjee M Ebi KL Estrada YO Genova RC Girma B Kissel ES Levy AN MacCracken S Mastrandrea PR & White LL (eds) *Climate change 2014: Impacts, adaptation, and vulnerability. Part A: Global and sectoral aspects. Contribution of working group II to the Fifth Assessment Report of the Intergovernmental Panel on Climate Change.*, 361–409. Cambridge University Press, Cambridge, United Kingdom and New York.
- Woodruff S, Vitro KA & BenDor TK 2018. GIS and coastal vulnerability to climate change. In *Comprehensive geographic information systems*, 236–257. Elsevier. [online]. Available from: <https://doi.org/10.1016%2Fb978-0-12-409548-9.09655-x> [Accessed 13 August 2019].
- Xharde R, Long B & Forbes D 2006. *Accuracy and Limitations of Airborne LiDAR Surveys in Coastal Environments*. Proceedings of the IEEE International Symposium on Geoscience and Remote Sensing held 31 July - 4 August 2006. Denver. IEEE. [online]. Available from: <http://ieeexplore.ieee.org/document/4241773/> [Accessed 13 August 2019].

## **PERSONAL COMMUNICATION**

- Bekko I. 2018. Control Environmental Officer: Coastal Management, Western Cape Government. Cape Town. Interview on 12 October 2018 about the existing approaches to coastal risk management in the Western Cape.
- Els Z. 2019. GIS Specialist, SANTAM. Cape Town. Email on 6 August 2019 about risk mapping.
- Mather A. 2017. Project Executive: Coastal Policy, eThekweni Municipality. Cape Town. Email on 7 December 2017 about sea level rise and local vertical datums.
- Minnie J. 2019. Head: Disaster Operations Centre, City of Cape Town. Cape Town. Email on 4 September 2019 about risk mapping.
- Roux P. 2018. Professional Officer: Coastal Engineering, City of Cape Town. Cape Town. Interview on 19 August 2018 about the existing approaches to coastal risk management in the City of Cape Town.
- Rylands N. 2016. Deputy Director: Disaster Risk Reduction, Western Cape Government. Cape Town. Interview on 18 October 2016 about disaster risk reduction approaches in South Africa.
- Villagrán de León J.C. 2016. Head of Office, United Nations Platform for Space-based Information for Disaster Management and Emergency Response (UN-SPIDER). Mahe, Seychelles. Interview on 8 March 2016 about conceptualising vulnerability.
- Villagrán de León J.C. 2018. Head of Office, United Nations Platform for Space-based Information for Disaster Management and Emergency Response (UN-SPIDER). Cape Town. Email on 10 May 2018 about vulnerability indicators.
- Wijetunge J.J. 2018. Professor of Coastal and Ocean Engineering, University of Peradeniya. Cape Town. Email on 2 July 2018 about coastal hazards and vulnerability.

**APPENDICES**

(On CD attached to the dissertation)

**APPENDIX A: CONTENT RELATED TO THE BODY OF THE DISSERTATION**

<b>A1</b>	Examples of the South African approach to disaster risk assessments
<b>A2</b>	Status quo survey results
<b>A3</b>	Interviews with technical experts
<b>A4</b>	Roughness coefficients for wave runup computations (Source: FEMA 2007)
<b>A5</b>	eBTM ArcPy code

**APPENDIX B: DATA USAGE AGREEMENTS**

<b>B1</b>	City of Cape Town LiDAR data usage agreement
-----------	--

**APPENDIX C: RESEARCH RELATED PUBLICATIONS**

<b>C1</b>	Guideline towards the establishment of coastal management lines. Lauren Lyn Williams Department of Environmental Affairs
<b>C2</b>	Guidelines for coastal LiDAR. Melanie Lück-Vogel, Chris Macon and Lauren Lyn Williams PositionIT Journal. Published 21 May 2017
<b>C3</b>	Comparative assessment of the GIS based Bathtub Model and an Enhanced Bathtub Model for coastal inundation. Lauren Lyn Williams and Melanie Lück-Vogel Journal of Coastal Conservation. Published 7 March 2020
<b>C4</b>	Coastal Inundation (Enhanced Bathtub Model (eBTM)). Lauren Lyn Williams Department of Environment, Forestry and Fisheries. DOI: 10.15493/DEFF.10000002.
<b>C5</b>	ArcCoastTools. Lauren Lyn Williams Department of Environment, Forestry and Fisheries. DOI: 10.15493/DEFF.10000001.